DOE/ER/40681--T1

DOE/ER/40681--T1

DE92 014055

AN EXPERIMENTAL HIGH ENERGY PHYSICS PROGRAM

within the

DEPARTMENT OF PHYSICS
PURDUE UNIVERSITY

West Lafayette, Indiana 47907

Supported by

U.S. DEPARTMENT OF ENERGY

Through

Division of Sponsored Programs
Purdue Research Foundation
West Lafayette, Indiana

Current Grant Number: DE-FG02-91ER40681

TASK D

PROGRESS REPORT
for the period ending
15 May, 1992

Principal Investigators: V. E. Barnes, D. D. Carmony
A. F. Garfinkel and L. J. Gutay.

Spokesperson: L. J. Gutay (317) 494-5047 FTS and Commercial

DISCLAIMER

This report was prepared as an account of work sponsored by an agency of the United States Government. Neither the United States Government nor any agency thereof, nor any of their employees, makes any warranty, express or implied, or assumes any legal liability or responsibility for the accuracy, completeness, or usefulness of any information, apparatus, product, or process disclosed, or represents that its use would not infringe privately owned rights. Reference herein to any specific commercial product, process, or service by trade name, trademark, manufacturer, or otherwise does not necessarily constitute or imply its endorsement, recommendation, or favoring by the United States Government or any agency thereof. The views and opinions of authors expressed herein do not necessarily state or reflect those of the United States Government or any agency thereof.

MASTER

DISTRIBUTION OF THIS DOCUMENT IS UNLIMITED

PROGRESS REPORT

for the period ending

15 May, 1992

TABLE OF CONTENTS

page

I. Introduction..... 3

II. The CDF for $\bar{p}$-p Collisions at FNAL..... 5

III. The L3 Detector for e^+e^- Collisions at CERN..... 14

IV. The SDC Detector for pp Collisions at the SSCL (calorimeters)..... 35

V. The SDC Detector for pp Collisions at the SSCL (muon detector).... 48

VI. The C0 Experiment for $\bar{p}$-p Collisions at FNAL..... 52

VII. Accelerator Physics at Fermilab..... 60

VIII. Publications since 1985..... 65

IX. Ph.D. Theses..... 79

I. Introduction to Progress Report and Task D personnel

This progress report summarizes our research effort for the period January 1991 to May 1992.

The members of task D are Professors Virgil Barnes, Duane Carmony, Arthur Garfinkel, and Laszlo Gutay ; Research Assistant Professor Blair Stringfellow; Project Associates Adam Bujak, Robert De Bonte (shared with Task A), and Alvin Laasanen; Research Associates Timothy McMahon and Mark Shaw; Technicians Ernie Beard and Ian Rickey (both shared with Task A); and graduate students Mark Bailey, Kathy Harkay, Todd Huffman, Bill Riemers, and James Tonnison.

During the current report period:

(1) Bailey, Barnes, Garfinkel, Huffman, Laasanen, Shaw, and Tonnison: Since the Purdue group had joint responsibility for the design and fabrication of the CDF central hadron calorimeters it has maintained an interest in their use in measuring jet properties. The techniques developed, in collaboration with other CDF members, continue to contribute to many of the CDF physics results from measurements of the inclusive jet spectrum to measurements of the W Boson mass and P_t distribution. We are pleased that our recent CDF Ph.D. Steve Kuhlman, now at Argonne, has been named co-convenor of the CDF QCD analysis group. On the hardware front we continue to work closely with the Fermilab CDF staff on a number of projects. These include the VTX replacement for the VTPC vertex time projection chamber and the SVX silicon vertex detector. Both of which are in place, functioning well, and ready for their first use in the 1992 collider run. In the longer run, we are participating in the design and fabrication of an upgraded end-plug calorimeter based on the use of scintillating tiles with wave-length shifting fiber readout. As members of the SDC collaboration for the SSC, we are engaged in the design and construction of the central calorimeters. These calorimeters are rather similar to those being used in the CDF end-plug upgrade and hence there is a considerable degree of synergism between these two efforts. In both effort we are emphasizing the use of radioactive sources in calibration procedures. There has been a considerable effort in the last year in testing prototype calorimeters in the Fermilab testbeam.

(2) Bujak, Carmony, Gutay, Harkay, McMahon, Riemers and Stringfellow: Using the L3 data collected in the first run (1991) at LEP we played an important role in extracting the Z° width, the g_V, g_A coupling constants, B-$\bar{B}$ mixing and in the search for lepton nonconserving reactions in the μ-τ final state. There continues to be worldwide interest in the Quark-Gluon plasma and the effects of gluon jets on our data. Therefore, the analysis of our main data taken at FNAL Experiment E735 continues to be important. We have continued our efforts to study automated wire tension monitors for straw tube manufacture for the L3 Forward-Backward system and the SDC Muon Chamber system. We are in the process of hardware studies of the resolution of both the L3 muon chamber octant and SDC muon chamber or superlayer. The Fermilab-Purdue study of proton bunch instabilities has made a breakthrough. A relationship between transient resonant modes and instability has been established experimentally.

II. The Collider Detector at Fermilab (CDF)

A. Introduction

In the past year, CDF has remained at center stage in high energy physics. With the analysis of nearly the complete 4.4 pb^{-1} data sample for a number of final states, we have published improved limits on the top quark mass, the production cross-sections of the W and Z particles, and B° $\bar{B}^\circ$ mixing, as well as a number of other interesting topics discussed below.

B. History of Purdue Involvement in CDF

Purdue had joint responsibility with the Italian Groups at INFN-Frascati and INFN-Pisa for the fabrication, testing, and calibration of the 50 (thirteen-ton) Central and 50 (seven-ton) End Wall hadron calorimeters. In order to fabricate the steel modules, Purdue HEP set up a special shop in conjunction with the Purdue Central Shop. In it, we made use of a computer controlled thermal machining center which cut steel plate by means of a plasma arc. The system was both highly accurate and cost effective. The finished scintillator was provided by the Frascati-Pisa group. The calorimeters were then assembled and cosmic ray tested at Fermilab. The finished calorimeters were all then calibrated in a Fermilab test beam. We also had responsibility for the fabrication, testing, and calibration of the TDC (time to digital) electronics for these calorimeters. More recently, we have been involved in the electronics for the VTX vertex time projection chamber and fabrication of, as well as electronics for the SVX silicon vertex chamber. Both the VTX and SVX chambers will be operational for the first time in the upcoming run.

C. People Involved

Faculty members working on CDF are Professors Barnes and Garfinkel. Postdoctoral physicists are Drs. A. Laasanen, Project Associate, and Mark Shaw Research Associate. Dr. Qifeng Shen has recently accepted an offer to join in the CDF and SDC calorimeter efforts. Thesis students working on CDF are Mark Bailey, Todd Huffman, and Jim Tonnison. Dr. Shaw and the students are based at FNAL.

D. The 1988-89 CDF Run

CDF ran from August 1988 to June 1990 accumulating 4.4 pb^{-1} of integrated luminosity; with peak luminosity up to 2.0×10^{30} $cm^{-2}sec^{-1}$. The data were primarily taken at a center of mass energy of 1.8 TeV. The experiment was capable of being triggered on transverse energy clusters, electrons, muons, or minimum bias events in addition to specialized triggers. A level III

trigger was implemented which permits limited track reconstruction and sophisticated calorimetry cleanup.

E. Published Results from the 1988-89 Run

1. Top-Quark Search in the Electron + Jets Channel in Proton-Antiproton Collisions at $\sqrt{s}$ = 1.8 TeV.

Using a 4.4 pb^{-1} sample, a search was made for decays of a $\bar{t}t$ pair into an electron, two or more jets, and missing transverse energy. A study of the resulting transverse mass distribution, which was consistent with pure W production, allowed us to exclude top masses between 40 and 77 GeV at 95% confidence level.

2. Measurement of the W Boson P_t Distribution in $\bar{p}p$ Collisions at $\sqrt{s}$ = 1.8 TeV.

The W Boson differential cross section was measured using W -> eν events. A next-to-leading-order QCD calculation agrees well with the data. The cross section for P_t > 50 GeV was measure to be 423 ± 58 ± 108 pb.

3. Measurement of σ B(W->eν) and σ B(Z°->ee) in $p\bar{p}$ Collisions at $\sqrt{s}$ = 1800 GeV.

We obtained σ B(W->eν) = 2.19 ± 0.04 ± 0.21 nb and σ B(Z°->ee) = 0.209 ± .013 ± .017 nb. Theoretical calculations which include a top quark more massive than the W are in good agreement with these measurements.

4. Measurement of QCD Jet Broadening in $p\bar{p}$ Collisions at $\sqrt{s}$ = 1.8 TeV.

A measurement of the QCD Jet-broadening parameter Q_t is described for high-E_t jet data. The data is well described by QCD predictions.

5. Measurement of the e^+e^- Invariant-Mass Distribution in $\bar{p}p$ Collisions at $\sqrt{s}$ = 1.8 TeV.

Additional heavy neutral vector bosons (Z') are excluded for $M_{Z'}$ < 387 GeV/c^2 at 95% confidence level. A lower limit of 2.2 TeV (at 95% c.l.) is placed on the electron-quark compositeness scale parameter Λ associated with an effective contact interaction. The existence of such a term would indicate lepton-quark compositeness.

6. Search for W' → eν and W' → $\mu\nu$ in $\bar{p}p$ Collisions at $\sqrt{s}$ = 1.8 TeV.

A lower limit of 520 GeV/c^2 at 95% confidence level was established for a hypothetical charged vector boson W', assuming standard couplings.

7. Measurement of $B^\circ\bar{B}^\circ$ Mixing at the Fermilab Tevatron Collider.

The $B^\circ\bar{B}^\circ$ average mixing parameter χ was extracted from eμ and ee events. In a sample of 900 eμ events, the like sign to opposite sign charge ratio R is measured to be 0.556 ± .048 +.035/-.042. In the absence of mixing, the

expected value of R is 0.23 ± .06. For 212 ee events, R = 0.573 ± .116 ± .047. Combining these results leads to a value of χ = 0.176 ± .031 ±.032.

8. Measurement of the W-Boson Mass in 1.8 TeV $\bar{p}p$ Collisions.

The W mass was determined to be 79.91±0.39 GeV/c^2 from a study of W->eν and W->$\mu\nu$ events. Fig. II-1 shows the transverse-mass distributions for the electron and muon samples. The CDF W mass measurement was combined with the world average Z mass to determine the Weinberg angle as $\sin^2\theta_W$ = 0.232 ± 0.008. This also implies that the top quark mass must be less than 220 GeV/c^2 at 95% confidence level. Fig. II-2 shows $\sin^2\theta_W$ versus the top quark mass.

9. Determination of $\sin^2\theta_W$ from the Forward-Backward Asymmetry in $p\bar{p} \rightarrow Z^\circ X \rightarrow e^+e^- X$ Interactions at $\sqrt{s}$ = 1.8 TeV,

An analysis of the forward-backward asymmetry in Z° decays yields A_{fb} = [5.2 ± 5.9 ± 0.4]% and $\sin^2\theta_W$ = 0.288 +.017/-.015 ±.002.

10. Measurement of the Z-Boson p_t Distribution in $\bar{p}p$ Collisions at $\sqrt{s}$ = 1.8 TeV.

Using the decay channels Z -> ee and Z -> $\mu\mu$ we were able to measure the p_t dependence of the production differential cross section from 0 < p_t < 160 GeV. The standard model is in good agreement with the data.

11. Lepton Asymmetry in W-Boson Decays from $\bar{p}p$ Collisions at $\sqrt{s}$ = 1.8 TeV.

Since in $\bar{p}p$ collisions most of the W bosons are created by a valence-valence or valence-sea quark anti-quark interaction, a W^+ will be produced primarily by the interaction of a u quark from the proton and a $\bar{d}$ quark from the anti-proton. This causes the W^+ to be boosted in the proton beam direction and the W^- in the anti-proton direction which leads to a charge asymmetry in the decay leptons. The observed asymmetry is well described by most of the available parton distributions.

12. A Lower Limit on the Top Quark Mass from Events with Two Leptons in $p\bar{p}$ Collisions at $\sqrt{s}$ = 1.8 TeV.

Our previous search for eμ +X final states has been extended to ee and $\mu\mu$ + X final states. In addition, we have searched in each event with a high transverse momentum lepton accompanied by hadron jets for a low transverse momentum muon as a tag of a bottom quark. A lower limit on the top quark mass of 91 GeV/c^2 is obtained at the 95% confidence level.

13. Topology of Three-Jet Events in $\bar{p}p$ Collisions at $\sqrt{s}$ = 1.8 TeV.

The distributions of the three-jet angular variables (ψ and $\cos\theta^*$) and of the variables describing the energy sharing between jets (x_3 and x_4) are well described by tree-level QCD calculations.

14. Progress in the Construction of the CDF Silicon Vertex Detector.

This NIM article describes the construction of the SVX detector.

15. Inclusive Jet cross section in $\bar{p}$ Collisions at $\sqrt{s} = 1.8$ TeV.

Next-to-leading-order QCD calculations are in good agreement with the measured cross section. The new lower limit on the quark compositeness parameter Λ_c has been set at 1.4 TeV at 95% confidence level. Fig. II-3 shows the inclusive E_t spectrum for a cone size of 0.7 compared to the predictions of a next-to-leading order QCD calculation .

F. Progress toward the 1992 run by Purdue people.

Postdoc Mark Shaw with students Todd Huffman and Jim Tonnison, based at Fermilab, have worked with members of the Fermilab staff on the VTX time projection chamber which has replaced the VTPC chamber for the next run. Huffman has been concerned with design, production, and testing of readout electronics for the VTX. The readout boards containing new low noise preamplifiers met specifications and are currently fully operational on the detector. Tonnison has been mainly concerned with developing tracking code for the VTX which is progressing very well.

Mark Shaw and student Mark Bailey have been working at Fermilab on the new silicon vertex detector (SVX). Shaw took responsibility for the quality control of the silicon detectors as delivered from the manufacturer. This was a vital part of the process of defining acceptance standards and refining acceptable production techniques. The SVX has recently been installed in the CDF detector in preparation for the upcoming run. It has undergone extensive testing with cosmic rays and is functioning extremely well. Mark Bailey developed diagnostic tests for the SVX data acquisition system in a program called SVX_CONTROL. This program enabled him to automate debugging of the fabricated circuit boards. He and his coworkers have completely tested all elements of the SVX front end electronics using the standard CDF data acquisition program called Run Control. He has been spending a fair fraction of his time recently in dealing with cross talk problems between the SVX and VTX. Various improvements have been made to shielding and timing patterns which seem to have eliminated the problem. Shaw has also been spending a fraction of his time working on track reconstruction and analysis software for the SVX.

G. Progress toward the 1994/5 run by Purdue people.

Barnes, Garfinkel, Laasanen, and Tonnison are working on the end-plug upgrade project in which the gas based calorimeters will be replaced with scintillating tiles with fiber readout; a technique well suited to use at the

SSC, as well as at the higher luminosities and shorter times between bunch crossings planned for future CDF runs. Purdue has been active in the design and Monte Carlo simulation of the optics of these scintillating tiles. Purdue has taken responsibility for the calibration of both the Electromagnetic and the Hadronic compartments of these calorimeters, using a remotely driven moving radioactive sources. We have developed and successfully used this design of source driver in a variety of prototype calorimeters in the past year, and Purdue has built and used such source drivers in ALL scintillator calorimeter prototypes, both CDF and SSC, in the recent Fermilab test beam. The source measurements are important for characterizing the quality and uniformity of construction of the calorimeters, as well as for carrying the results of test beam calibrations through time.

These drivers are also being used in a set of Radiation Hardness-testing small EM calorimeter modules ("Personal Calorimeters") which have been built jointly by Purdue and Fermilab and shipped to Beijing, Saclay, and KEK, and possibly will be shipped to one or two sites in the USSR for irradiation to high levels in ~1 GeV electron beams. The moving sources access every tile in the calorimeter and are our primary way of assessing the progressive degradation of the tiles as a function of dose.

H. Ongoing physics analysis by Purdue people.

Ongoing physics analyses using the 1988-89 data include a search for stable charged particles which has been written up as a CDF internal memo and a paper is going through the CDF internal referee process. We have succeeded in ruling out the existence of unit-charged color triplets with masses between 50 and 139 GeV/c^2 @95% c.l., with similar limits for particles of charge 2/3 or 4/3. For unit-charged color sextets, octets, and decuplets we exclude @ 95% c.l. masses between 50 GeV/c^2 and 197, 199, and 255 GeV/c^2 respectively. Another analysis involves a test of QCD scaling violatio in a comparison of the inclusive jet cross sections at 540 and 1800 GeV. The data analysis has been completed and is being written up. Fig. II-4 shows the ratio of the preliminary CDF measured dimensionless cross sections at 546 and 1800 GeV as a function of the scaling variable $x_t = 2E_t/\sqrt{s}$. Comparisons to leading order and next-to-leading order QCD calculations have been made. Comparisons to a QCD motivated monte-carlo HERWIG are underway. A third analysis involving b quark production, as measured by the inclusive muon spectrum, is making very good progress. We are also getting ready to analyse data from the upcoming run with emphasis on top and b physics.

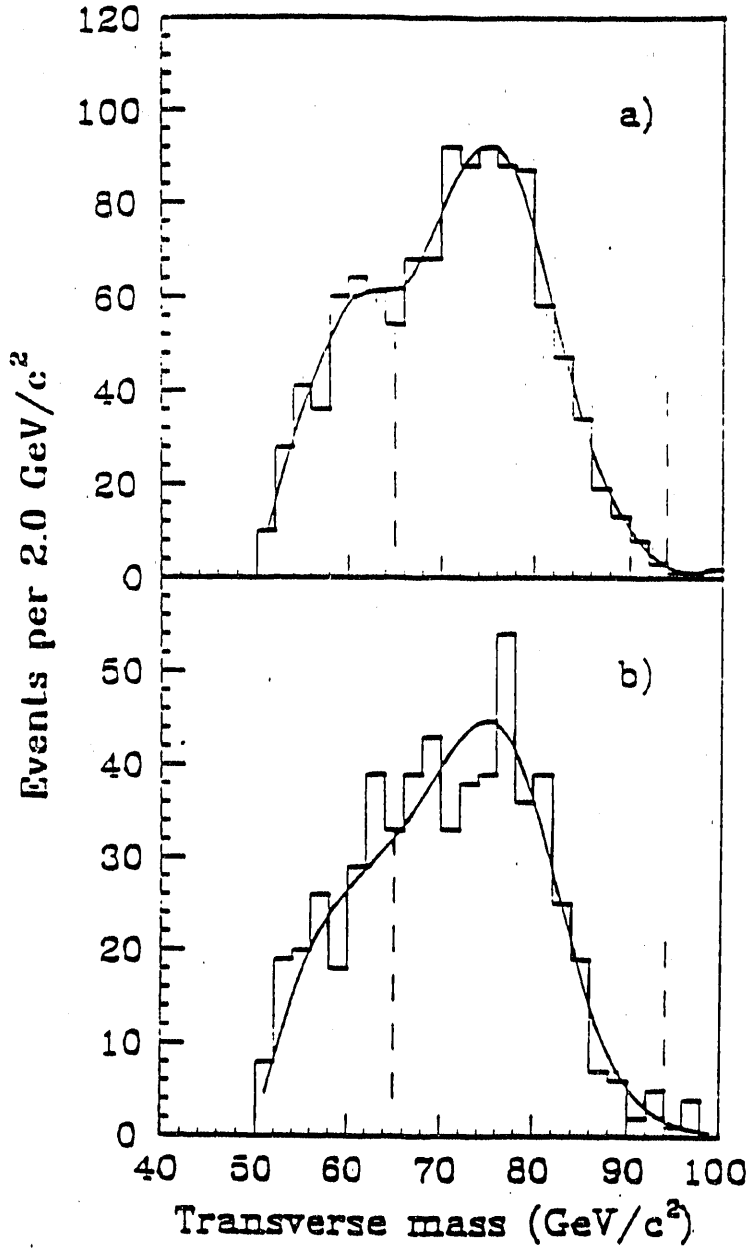

Fig. II-1 a)The transverse mass distribution for W → e ν candidates. Overlaid is the best fit to the data. The range of transverse masses used in the fit is indicated with dashes . b) The transverse mass distribution for W → μν candidates.

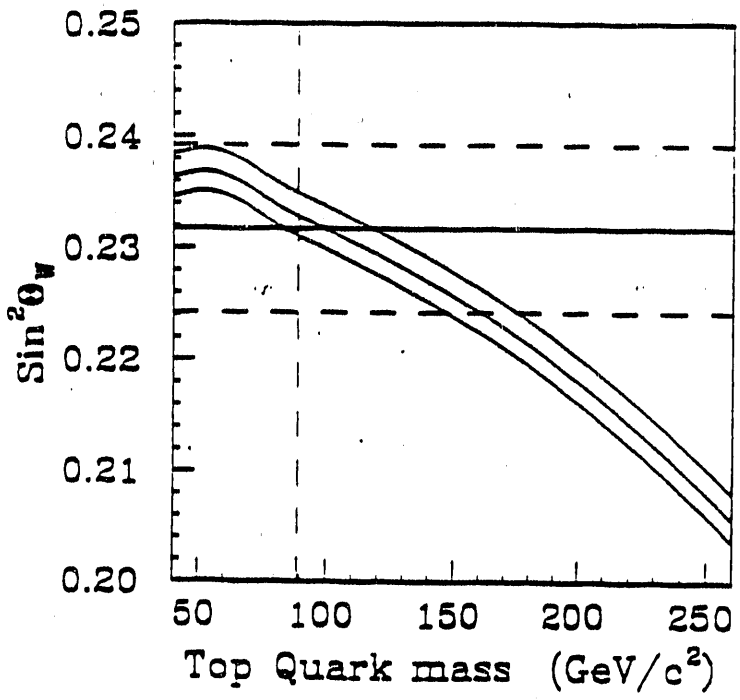

Fig. II-2 The relationship between the top quark mass and $\sin^2\theta_W$ with the Z mass constrained to 91.161 GeV/c^2. The curves[22], from top to bottom, correspond to Higgs masses of 1000, 250 and 50 GeV/c^2. The horizontal dotted lines correspond to the 1 σ uncertainties. The vertical dotted line at 89 Gev/c^2 corresponds to the CDF top mass limit[23].

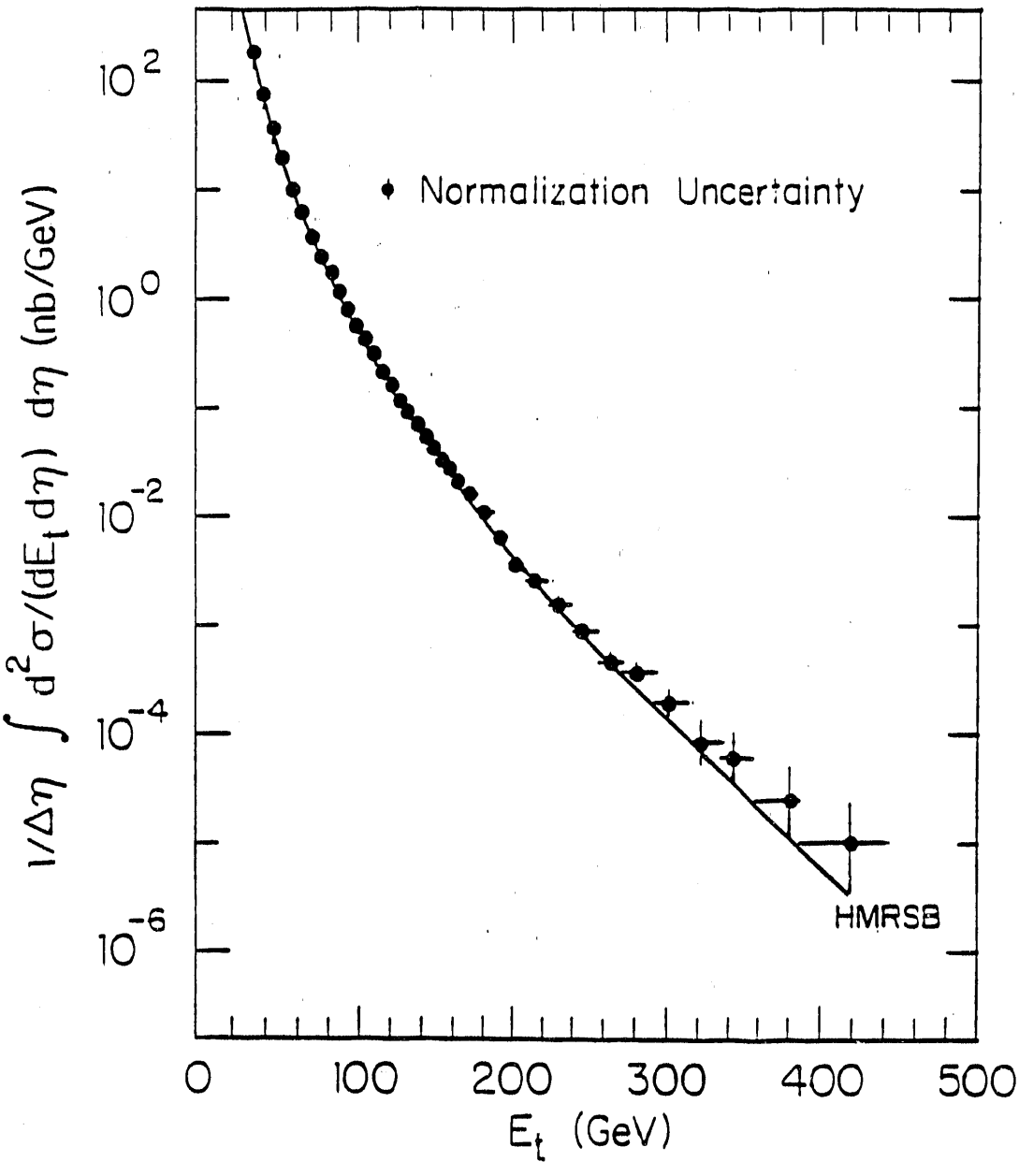

Fig. II-3: Inclusive E_t spectrum for a cone size of $R = 0.7$. The curve represents the predictions of a next-to-leading order QCD calculation by S. Ellis *et al* [3]. The error bars on the data represent statistical and E_t dependent systematic errors. An overall normalization uncertainty is also indicated.

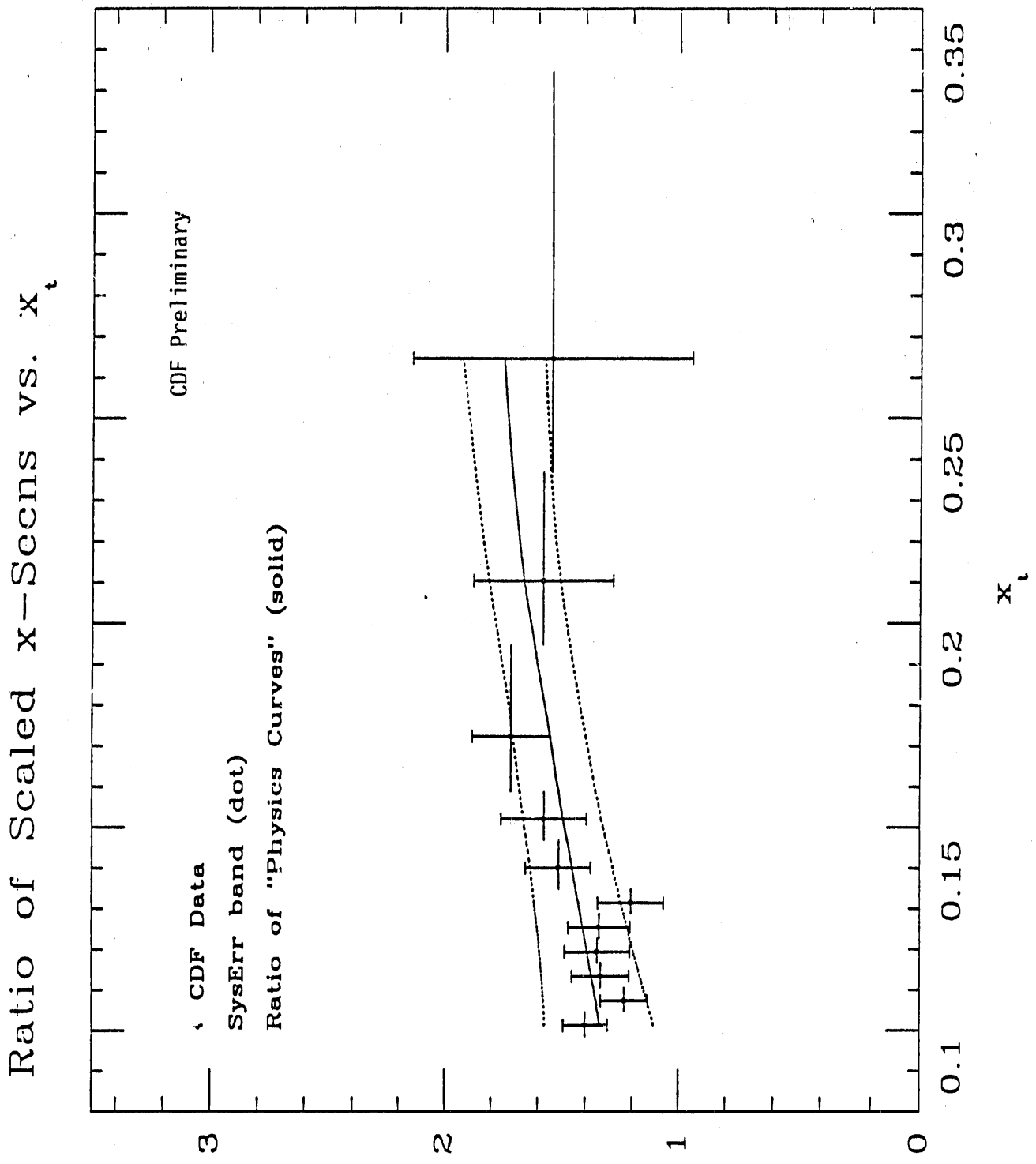

Fig. II-4 Ratio of dimensionless, central, inclusive jet cross sections at 546 and 1800 GeV as a function of x_t.

III. The L3 Detector for e^+e^- Collisions at CERN

3.1 Muon Chamber Resolution Improvement Project

The L3 muon detector is constructed in octants, with each octant consisting of an inner, middle and outer chamber module. The whole detector consists of two barrels, each of which is made of 8 octants. A 17th octant was built which is located outside the tunnel and is available for detailed resolution studies. Our goal is to improve the tracking resolution by a factor of two. Since the L3 muon chamber has achieved the highest momentum resolution in the world, any improvement is difficult to achieve.

As the first project, we chose to study the properties of the pulse shape and pulse interference. The muon chambers are built from 16 (inner and outer) and 24 (middle) sense wire cells, where the sense wires are 10 mm from each other. Because of the cell geometry, we expected possible interference between adjacent pulses due to the proximity of the sense wires (crosstalk and induced signal). Since the sense wires are read out by TDC's when the pulse height reaches a prefixed value, an interference effect causes time jitter and thus degrades time resolution. We found such effects in our Fermilab chambers in E-735.

To study the above effects, we designed a Flash ADC readout system using components of our FNAL E-735. The trigger came from a coincidence of scintillator arrays located above and below the octant. Since the FADC system digitizes the pulse-height distribution every 10 ns, it is ideal to study interference effect. The system is described next.

The FADC Crate

The basic building block of the system is a Flash ADC unit. One unit digitizes the pulseheight distribution of the amplified pulse that propagates down to one end of a wire. The digitization takes place every 10 ns for 2.6 μs. Four FADC units are mounted on a slide in module. Any FADC crate can accommodate 24 modules, thus can digitize 96 wires. Our system consists of 12 FADC crates.

The VME Crate

The VME crate is a gateway between the FADC units which contain the digitized information and the outside world. The 20 modules that are inserted into this crate perform 2 major functions:

1. Read the FADC and CAMAC data, reduce it and write it on tape.
2. Monitoring of the data collected by providing various online displays (both event by event and cumulative).

All the modules communicate with each other via the VME bus. The schematic diagram of the system is shown in Fig. III-1. Specifically, the VME crate contains 15 microcomputer modules, twelve of which are Front-End-Processor (FEP) boards. Each FEP communicates with one FADC crate through the DL307/VME on-board interface. All FEPs are independent from each other and operate in parallel.

The heart of the data acquisition is a SUPERVISOR (SUP) microcomputer which synchronizes the action of all DAQ components by means of elaborate interrupt scheme and services Camac interrupts in parallel to FEPs action.

Two remaining CPU boards play an auxiliary function:

- The BASU Master-Processor-Unit (MPU) is used for software maintenance and development, software down-loading from its hard disk and execution of setup procedures. During a run it is also able to intercept events for on-line display. The monitoring CPU (MON) is running asynchronously to DAQ. It is used for "slow" monitoring of various system parameters.

All microcomputers are BASU/Microsys CPU07 modules based on MC68000 chip and each have 256 kBytes of onboard DRAM dual port memory.

The CBD 8210 Camac driver is used to read Camac data from branch of up to 7 crates. In case of necessity another branch can be added to the system. The STR302 DMA input/output module is used for rapid internal transfer of data from FEP memories to 2 Megabyte event buffer maintained in MM-6200 dynamic memory. The TAPEMASTER 300 board (shown in Fig. III-1) used to interface the VME system to the STC 2925 tape drive. It will be replaced with the MVME327A board interfacing the 8200 EXABYTE 8 mm tape drive.

VME Data Acquisition Software

Performance tests made during system design showed, that operating systems like OS9 introduced unacceptable overhead to overall data acquisition throughput. Because of that the DAQ was implemented as stand alone system, which runs without support of any operating system. Obviously, the ease of programming was sacrificed.

The CP/M operating system was used exclusively for program development (editing, compiling etc.). Most of the software was written in Real-Time-Fortran (RTF68K) compiler from CERN, while the AS68K assembler was used for implementing certain time-critical routines.

The DAQ is loaded to VME memory from hard disk by MPU processor. After the software is loaded the SUP takes over. It's first responsibility is the system initialization. The SUP tailors the system logic to a specific

hardware configuration by executing commands passed to it from MPU, which at this point becomes a system console.

After the logical structure of DAQ is defined all system hardware is initialized based on information supplied to the system during MPU-SUP dialog. FEPs and MON initialize themselves after receiving a packet of necessary information followed by an interrupt from SUP.

The initialization of FADC crates performed by Front-End-Processors is quite elaborate. The most important is the pedestal ("baseline") adjustment and setup of every FADC channel. This adjustment compensates for small variations of electrical parameters in different FADC modules (see "Scanner Module" documentation). Another is programming of the Scanner modules for Common-Start/Common-Stop modes of operation.

After general initialization the system is ready to accept Run-Start command, which basically enables various interrupts within the system. The registering of an event begins with the interrupt signals introduced into each FADC crate. The timing of these signals is determined by external trigger logic (in Common-Stop mode a delay relative to event trigger should be introduced). The input (chamber) information is then digitized in parallel in each FADC channel each 10 nsec for 2.56 microseconds (slower sampling frequency can be requested during setup). The trigger logic can discard the event by issuing fast clear to FADC crates. If an event was accepted the SUP is interrupted by signal sent to the CBD 8210 interrupt input. The SUP then starts the FADC reading routine in each of the FEP.

The FEP can instruct the Scanner module to look for the beginning and the end of hits on pairs of FADC channels (the system was designed for charge division on wires connected to pairs of FADCs - when channels are independent from each other this is a minor complication). The beginning of the hit is defined as at least two consecutive digitizations above a setable threshold on either channel of the pair. After the scanner finds the beginning of the hit the FEP may instruct it to find the end of the hit (two consecutive channels below threshold on both channels). In parallel to Scanner action the FEP in cycle stealing mode copies data from FADC crate to its local memory using pointers previously returned by the Scanner. All the action is controlled by readout routine, which easily can be tailored to specific needs. Number of optional hit processing algorithms are implemented (each requested at setup time). The result of FEP action are packages (buffers) of various information (raw data, preprocessed data, histograms etc.). When all the information associated with a given package has been processed by the

FEP, the pointer to the buffer in FEP memory and its size are written into appropriate package-table in SUP memory and a "package-ready" flag is set. During the readout of FADC crates by the FEPs the SUP reads the Camac data (at this point the SUP formally acts as another FEP) and then polls the status of semaphore flags associated with all packages defined in the system.

The package meant for magnetic tape is usually ready first (the other are monitoring ones). The SUP programs the STR302 module for chained DMA transfer to VME expansion memory using the package-table already constructed by FEPs. The STR302 holds the VME bus, so the transfer is ~ 2 Mbytes/sec, and is limited only by memory speed. During DMA the SUP performs all bookkeeping calculations, prepares itself for transfer of remaining packages (e.g. monitoring data for MON or event for display on MPU) and waits for "DMA complete" interrupt. The other packages are transferred sequentially in the same DMA mode to MON and/or MPU if the SUP sees pending requests from them. After the last transfer, or immediately if there were no requests, the SUP sends the READY signal to trigger electronics through the CBD 8210 module, thus indicating that the DAQ is ready to accept another trigger. At this point the SUP checks if the tape drive controller is ready. If it is, the DMA transfer from buffer in expansion memory to the tape is activated.

By this time the next trigger may already have occurred and the FADC crates have finished the digitization process. The readout for this trigger will then be written to tape.

In Fig III-2 the three layered octant is shown with the trigger hodoscope and a track in two views. The examples of various pictures as seen on the on-line display for the event recorded during the LEP/L3 cosmic ray octant test run are shown on Fig. III-2 to Fig. III-6. The test run was done in December 1991. After analyzing the December data, we will return for more data taking in April/May, 1992. An attempt will be made then to double the time resolution of the FADC's.

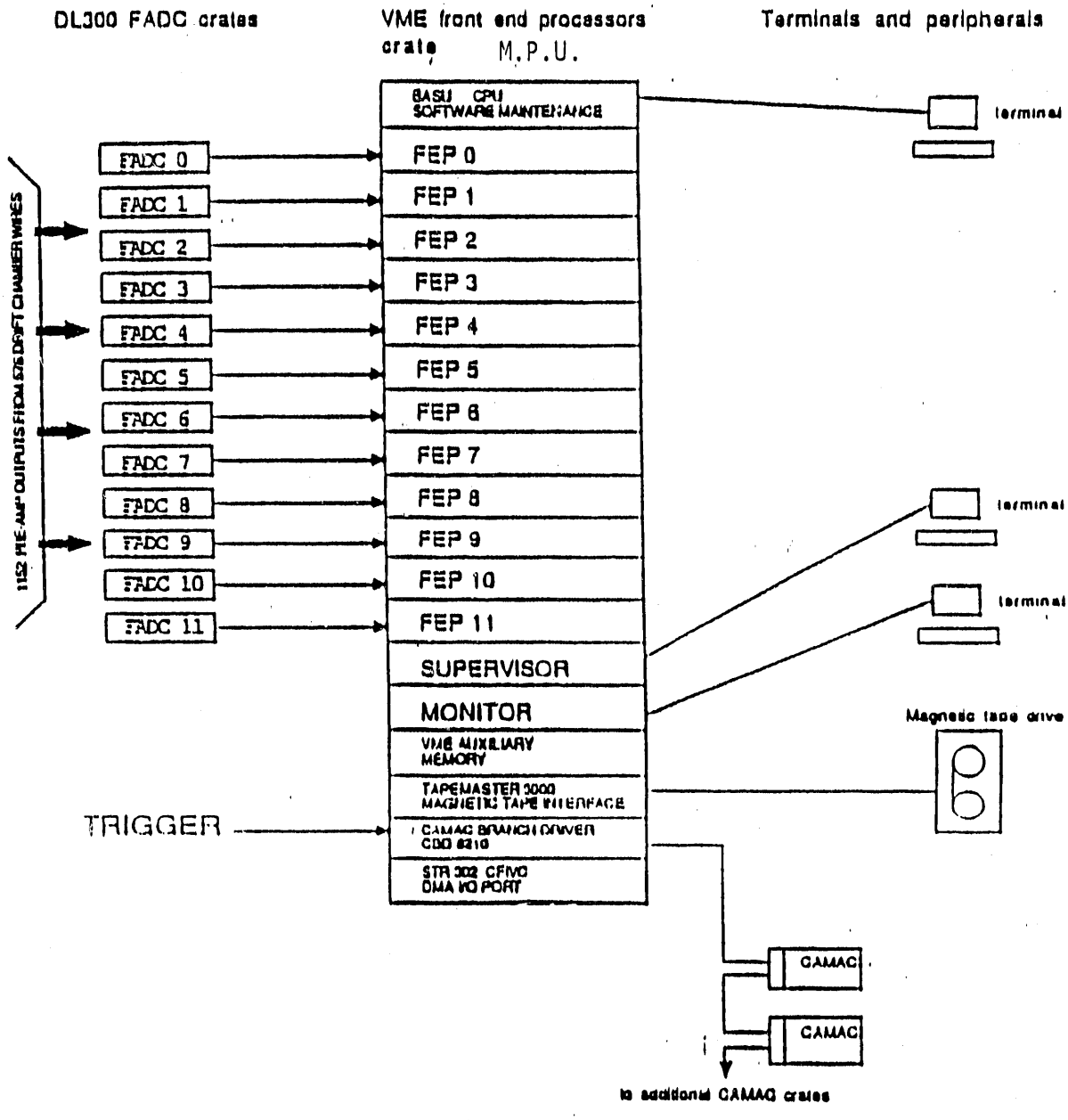
DL300 FADC crates
VME front end processors crate
M.P.U.
Terminals and peripherals
BASU CPU
SOFTWARE MAINTENANCE
FADC 0
FADC 1
FADC 2
FADC 3
FADC 4
FADC 5
FADC 6
FADC 7
FADC 8
FADC 9
FADC 10
FADC 11
FEP 0
FEP 1
FEP 2
FEP 3
FEP 4
FEP 5
FEP 6
FEP 7
FEP 8
FEP 9
FEP 10
FEP 11
SUPERVISOR
MONITOR
VME AUXILIARY MEMORY
TAPEMASTER 3000
MAGNETIC TAPE INTERFACE
CAMAC BRANCH DRIVER
CDC 8210
STR 302 CFIVO
DMA I/O PORT
TRIGGER
terminal
terminal
terminal
Magnetic tape drive
CAMAC
CAMAC
to additional CAMAC crates

Fig. III-1

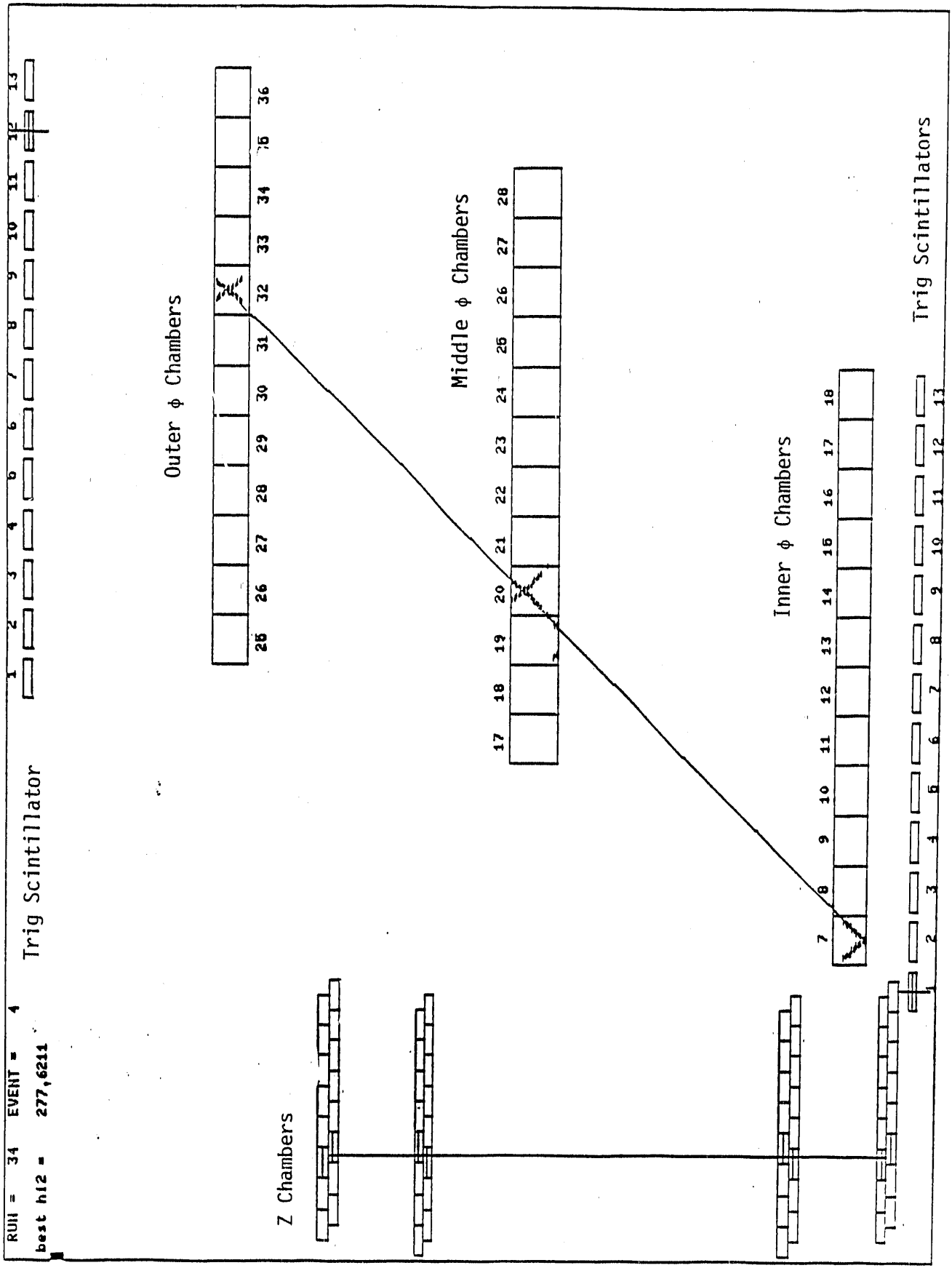
RUN = 34 EVENT = 4
best h12 = 277,6211
Trig Scintillator
Outer φ Chambers
Middle φ Chambers
Inner φ Chambers
Trig Scintillators
Z Chambers

Fig. III-2

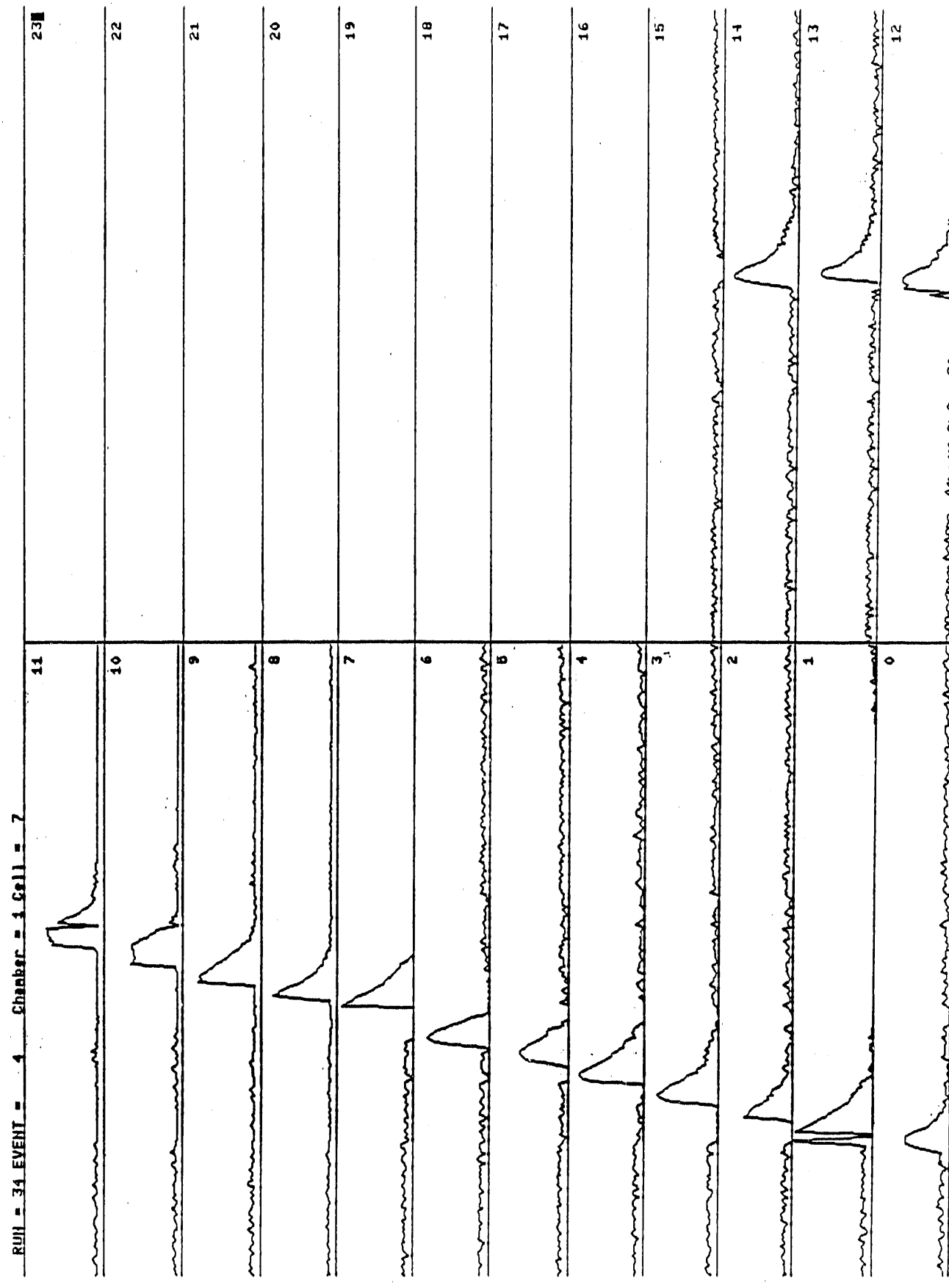
RUN = 34 EVENT = 4 Chamber = 1 Cell = 7
11
10
9
8
7
6
5
4
3
2
1
0
12
13
14
15
16
17
18
19
20
21
22
23

Fig. III-3

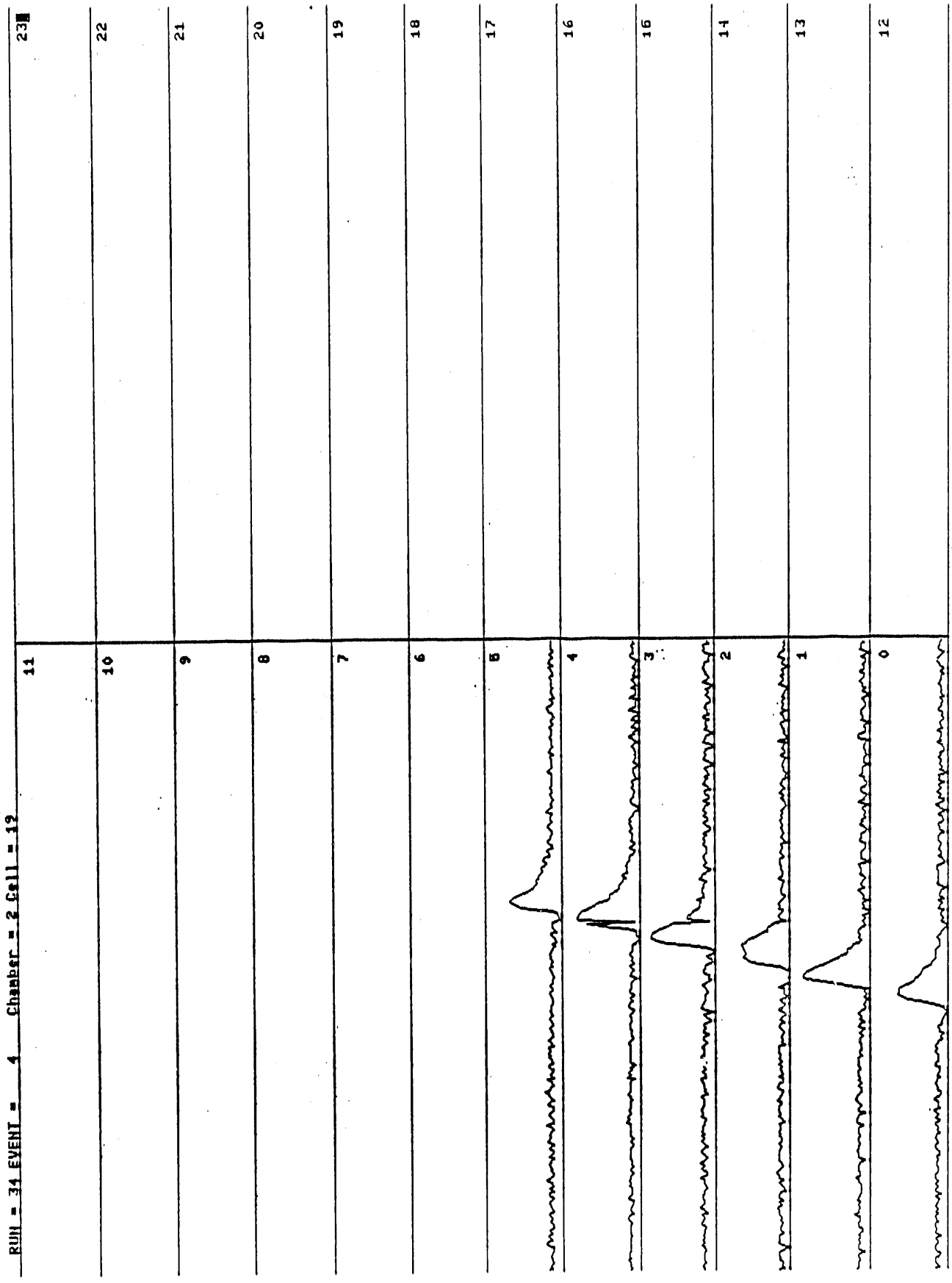
RUN = 34 EVENT = 4 Chamber = 2 Cell = 12
11
10
9
8
7
6
5
4
3
2
1
0
23
22
21
20
19
18
17
16
16
14
13
12

Fig. III-4

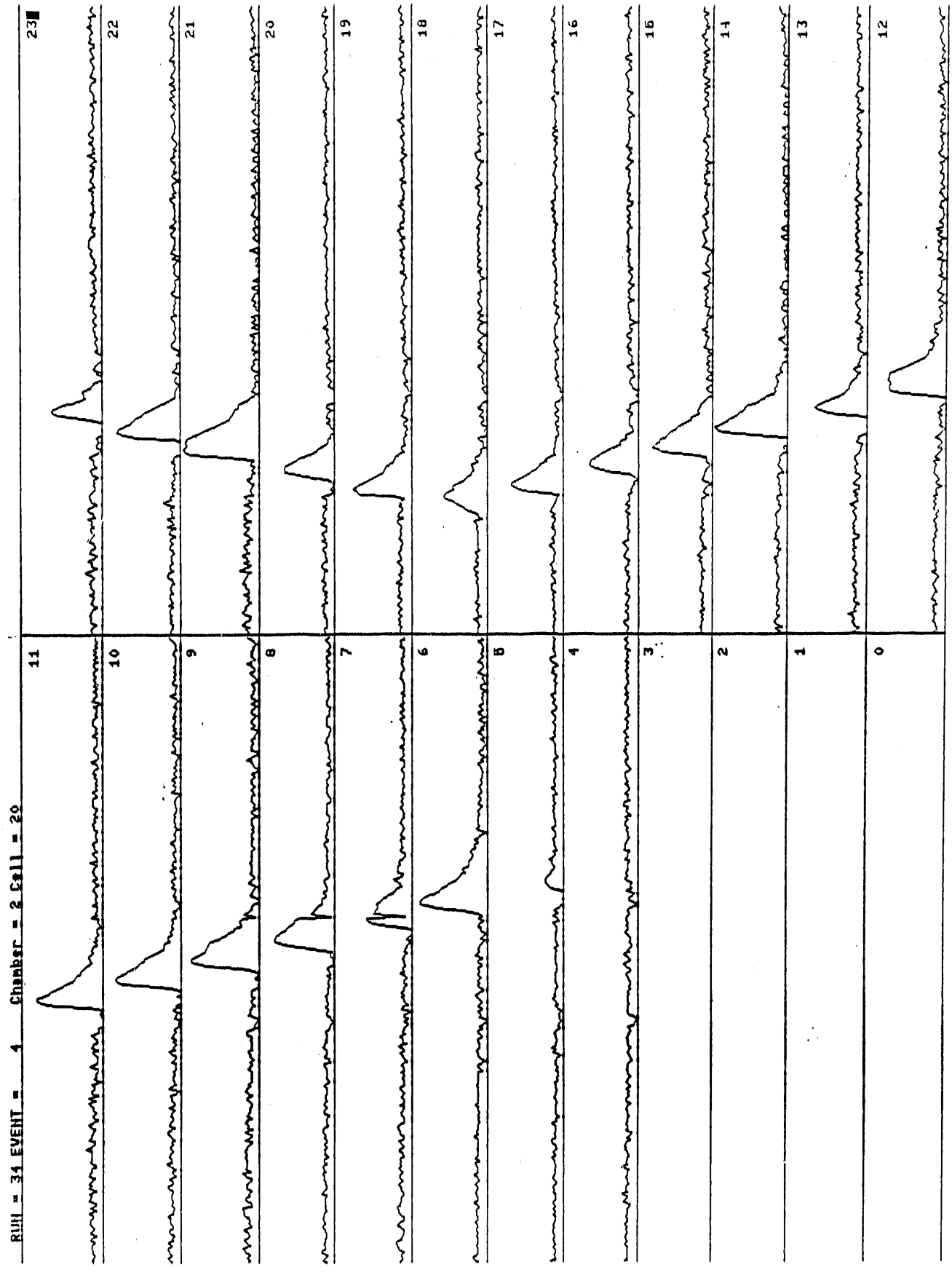
RUN = 34 EVENT = 4 Chamber = 2 Cell = 20
11
10
9
8
7
6
5
4
3
2
1
0
23
22
21
20
19
18
17
16
15
14
13
12

Fig. III-5

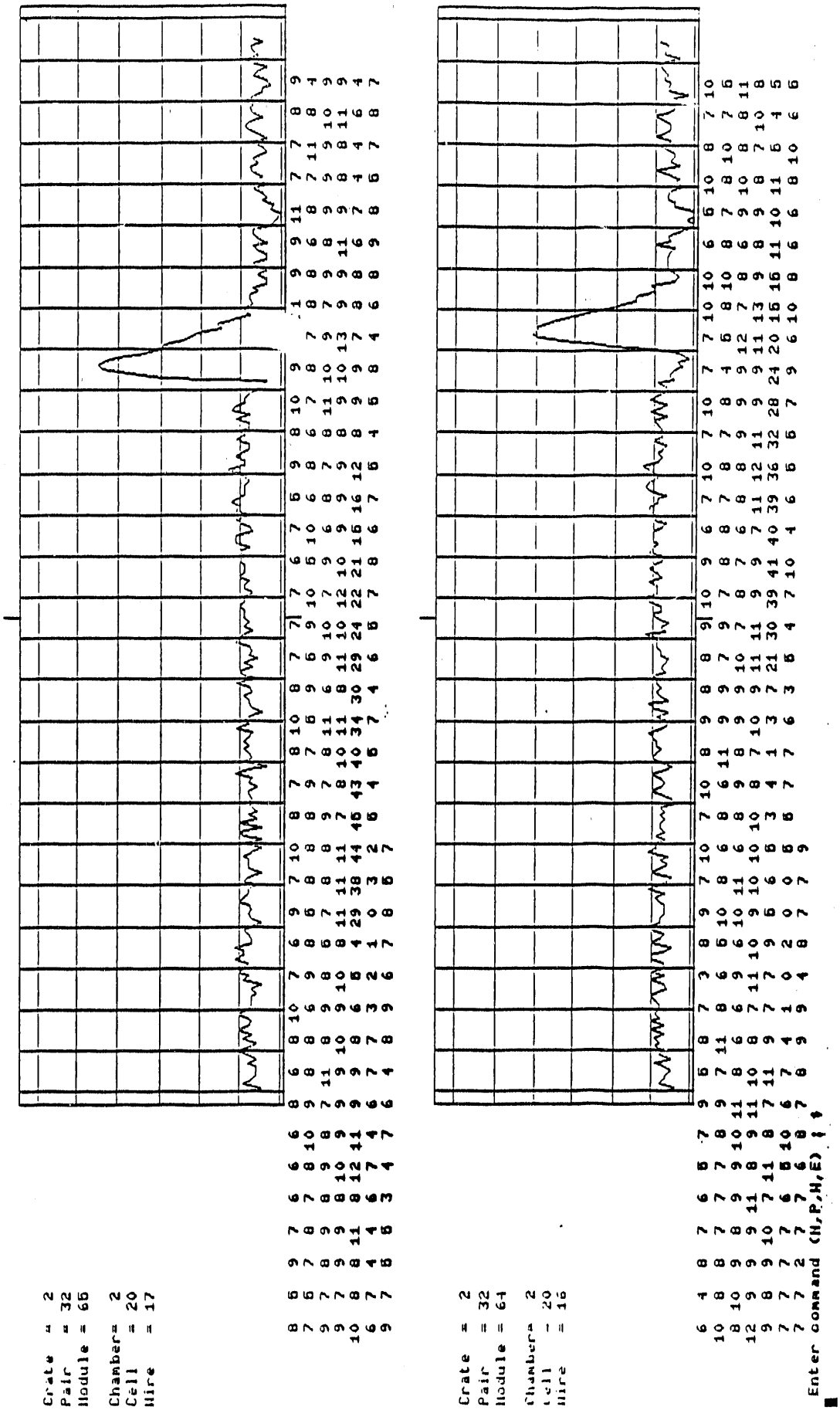
Enter command (N,P,H,E) ↑↓
P
Crate = 2
Pair = 32
Module = 65
Chamber= 2
Cell = 20
Wire = 17
Crate = 2
Pair = 32
Module = 64
Chamber= 2
Cell = 20
Wire = 16
Enter command (N,P,H,E) ↑↓

Fig. III-6

3.2 Improving Resolution and Acceptance of Muon Tracks Passing Near Wires which are Disconnected or are at Subnominal Voltages.

We had the responsibility to produce condensed data tapes for the muon analysis groups and provide the modification for the Monte Carlo programs which take into consideration the wires which were disconnected and wires which operated at subnominal voltages. In order to maintain good muon momentum resolution bad cells and neighboring cells (cells with reduced HV) had to be left out of the muon momentum analysis. These rejected tracks, however, became substantial in number with time. Thus another approach had to be tried, which, instead of rejecting a cell, studied the first order variation of the electric field in a drift cell as a function of wire voltages inside the cell and the effects of wire voltage variations in the neighboring cells.

The cell structure from which the three layers of muon chambers are built is shown in Fig. III-7. The definition, nominal values and subnominal values of the wire voltages are given below and in Table III-1.

V_1 potential of sense wires in the proximity of the track

V_2 potential of field wires in the proximity of the track

V_3 potential of mesh wires in the proximity of the track

V_4 potential of mesh wires which are separated from the track by a sense plane.

V_5 potential of sense wires which are separated from the track by a mesh plane.

V_6 potential of field wires which are separated from the track by a mesh plane.

V_7 potential of guard wires which are separated from the track by a mesh plane.

E^o The nominal field when all values of V_i are at nominal values.

The possible subnominal voltage settings of the V_i voltages are given in Table II.

Table II

Type	Nominal in Volts	Subnominal Voltages in Volts
V_1	4181	2000, 2500, 3000, 3200, 3400, 3600, 4000
V_2	2560	2000, 2500, 2560
V_3	-3070	-600, -1500, -2400, -2500, -3000, -3070
V_4	-3070	-600, -1500, -2400, -2500, -3000, -3070
V_5	4181	2000, 2500, 3000, 3200, 3400, 3600, 4000
V_6	2560	2000, 2500
V_7	4005	-4005 (disconnected), 4005
E^0	1100.1 V/cm	

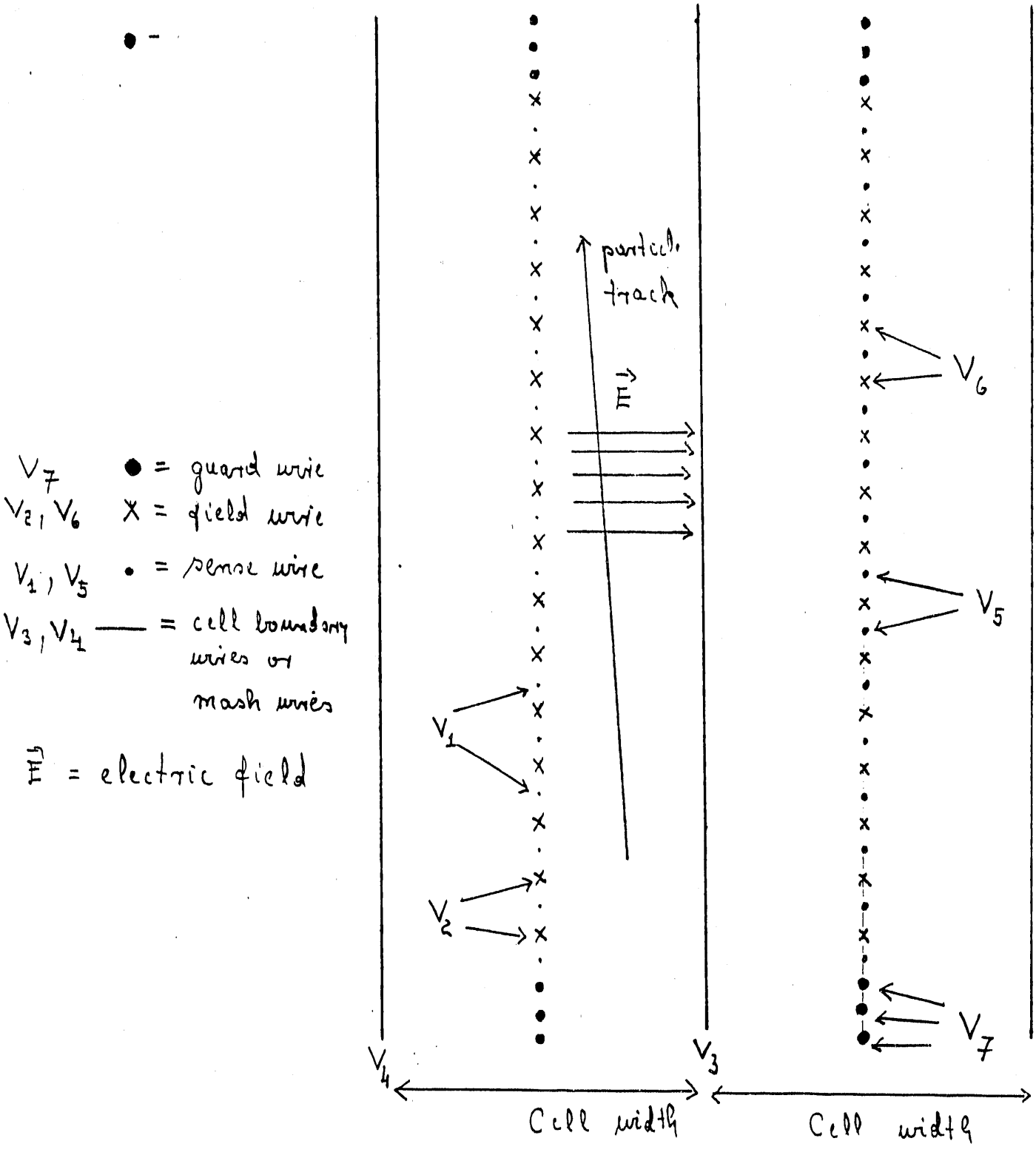
V_7 ● = guard wire
V_2, V_6 X = field wire
V_1, V_5 • = sense wire
V_3, V_4 —— = cell boundary wires or mash wires
$\vec{E}$ = electric field
particle track
$\vec{E}$
V_6
V_5
V_1
V_2
V_7
V_4
V_3
Cell width
Cell width

Fig. III-7

By parametrizing the electric field in terms of V_i, it is reasonable to assume that to the first order approximation the deviation of the electric field from the nominal value varies linearly with the deviation of the voltages from their nominal values that is:

$$E = E^0 - E^0 \sum_{i=1}^{7} a_i (V_i^0 - V_i)$$

or in differential form

$$\Delta E = E^0 \sum_{i=1}^{7} a_i \Delta V_i$$

Using 276 different voltage settings from Table II as inputs to the program Wircha, 276 values of E_j were calculated. To obtain a linear parametrization of Wircha's result, a linear least squares minimization was performed for the expression

$$d(a_1, a_2, a_3, a_4, a_5, a_6, a_7) = \sum_{j=1}^{276} (E^0 \sum_{i=1}^{7} \Delta V_{ji} a_i - \Delta E_j)^2$$

The least square minimalization condition

$$\frac{\delta d}{\delta a_k} = 0$$

for k = 1,2,3,4,5,6,7

gives 7 equations

$$\sum_{j=1}^{276} \Delta V_{jk} (E^0 \sum_{i=1}^{7} \Delta V_{ji} a_i - \Delta E_j) = 0$$

Let us introduce

$$B_{ki} = E^0 \sum_{j=1}^{276} \Delta V_{jk} \Delta V_{ji}$$

$$C_k = \sum_{j=1}^{276} \Delta V_{jk} \Delta E_j$$

and solve the matrix equation

$$B \cdot a = C$$

The solution for a is

$a_1 = 72717 \times 10^{-9}$

$a_2 = 88413 \times 10^{-9}$

$a_3 = -166368.7 \times 10^{-9}$

$a_4 = 7201.9 \times 10^{-9}$

$a_5 = -1494.0 \times 10^{-9}$

$a_6 = -1490.2 \times 10^{-9}$

$a_7 = 127.7 \times 10^{-9}$

By inputing potentials for which we have electric field values from WIRCHA or setting all $V_i = 0$, we find that E_j^{-5} deviate from the known values by about 0.95%. With this accuracy we have $a_5 = a_6$ and $a_7 = 0$. Thus, we can represent E_j as a function of five parameters only.

With the help of the above parametrization, proper electric field thus drift velocity corrections can be made. As a result of these corrections a 30% increase of the analyzable muon sample was achieved with good momentum resolution.

3.3 Ongoing Physics Analysis by the Purdue Group at LEP-3

The Purdue group has continued to analyze b-physics related topics from L3 data taken from the recently completed 1991 LEP run. Our analysis now consists of data taken from both the 1990 and 1991 data runs of LEP and together comprise ~ 415,000 $Z^\circ \to q\bar{q}$ events. This sample is a nearly four-fold increase in statistics over the sample used for our previously published papers. Currently, we are preparing 5 papers covering b-physics topics with our new sample for publication.

We have used our inclusive muon and electron sample from $Z^\circ \to q\bar{q}$ events to measure the mixing in the $B^\circ\bar{B}^\circ$ system. Mixing is parameterized by,

$$\chi_B = \frac{\mathrm{Br}(b\bar{B}^0 B^0 \ell^+ + X)}{\mathrm{Br}(bB\ell^\pm + X)}$$

The high abundance of B_s in the sample (B_s/B_d ~.4) makes the measurement of interest since mixing in the B_s system is expected to be maximal in the Standard Model. Figure III-8 shows the final selected sample of dilepton events where the leptons occupy opposite hemispheres in the event. Fig. III-8 and III-8(b) compares the data with a JETSET monte carlo sample with mixing equal to 0, $\chi_B = 0$. Fig. III-8(c) and III-8(d) shows the results after fitting with mixing introduced to the monte carlo. Our preliminary measurement gives $\chi_B = .118 \pm .02(\text{stat.}) \pm .015(\text{sys.})$. We can infer a value for B_s mixing by using the CLEO/ARGUS value for B_d of $\chi_d = .16$ giving with our preliminary measurement $\chi_s = .39 \pm .15$. This value is consistent with having maximal mixing in the B_s system of $\chi = .5$.

Since our last progress report we have published a paper on the lifetime of B-hadrons using inclusive lepton data from the 1990 running period. Using an impact parameter method to fit the data the lifetime of B-hadrons produced in decays of the Z° was found to be $\tau_B = 1.32 \pm 0.08(\text{stat.}) \pm 0.09(\text{sys.})$ picosec. Using our previously measured valued of the semi-leptonic branching ratio of $\mathrm{Br}(B \to l + X) = 0.119$ we determine then the CKM matrix element $|V_{cb}|$ to be $0.046 \pm 0.002(\text{exp.}) \pm 0.004(\text{theory})$.

Other papers in preparation cover forward-backward asymmetry of $Z^\circ \to b\bar{b}$, b semi-leptonic decays, partial decay width of Z° to b quarks and b quark fragmentation. With our recent data sample the asymmetry measurement will allow us to measure the effective weak mixing angle $\sin^2\bar{\theta}_W$ (= .233 theory)

with a precision of $\pm$ .004. This will provide another alternate indirect measurement of the top quark mass.

With our inclusive muon and electron sample we measure the branching ratio of $Z^\circ \rightarrow J/\psi + X$ and obtain $4.1 \pm 0.6 \times 10^{-3}$ (very preliminary). The data allows an upper limit on J/ψ production from colour forbidden gluon decay to be made. Both of these results are to be reported in a forthcoming paper.

The Purdue group is also involved in searching for lepton flavour violating decays of the Z°. Such decays are forbidden in the Standard Model, however, theoretical extensions provide for branching ratios for $Z^\circ \rightarrow \mu\tau$ as high as 10^{-4}. Figure 8(e) shows the muon energy from data and the solid curve from a $Z^\circ \rightarrow \mu\tau$ signal. The necessity of good muon resolution can be seen from the curves. From analysis of our 1990 and partial 1991 sample we extract a 95% CL limit of 4.8×10^{-5} for the process of $Z^\circ \rightarrow \mu\tau$.

Analysis and data processing stream software packages have been introduced and maintained by the Purdue group for the b-physics analysis group of L3. The LXDSU inclusive muon and electron format software has been maintained and upgraded and is now in use by the L3 analysis group. We have continued to study and improve the muon chamber data for selecting inclusive muons.

During the past year we worked in the initial stages of the design work for the L3 forward-backward muon chamber upgrade. Electrostatic studies were done for drift cell prototype designs to determine optimal voltage settings and wire spacing geometries. By obtaining uniform drift time for all sense wires in the drift cell we were able to optimize overall hit position resolution. Mechanical tolerances for wire positioning for achieving desired resolution were also determined.

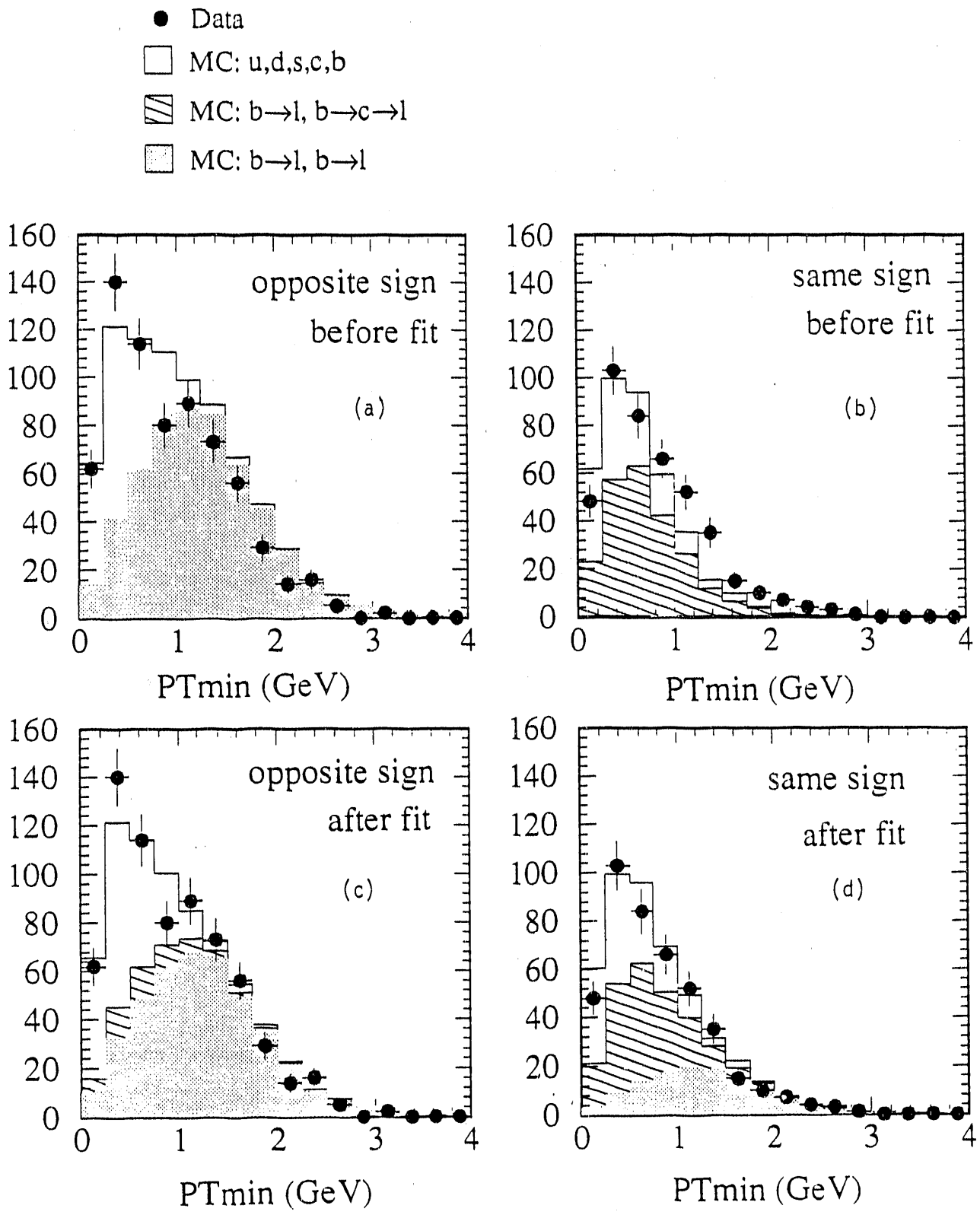
Data
MC: u,d,s,c,b
MC: b→l, b→c→l
MC: b→l, b→l
opposite sign
before fit
(a)
same sign
before fit
(b)
opposite sign
after fit
(c)
same sign
after fit
(d)
PTmin (GeV)
PTmin (GeV)
PTmin (GeV)
PTmin (GeV)

Fig. III-8

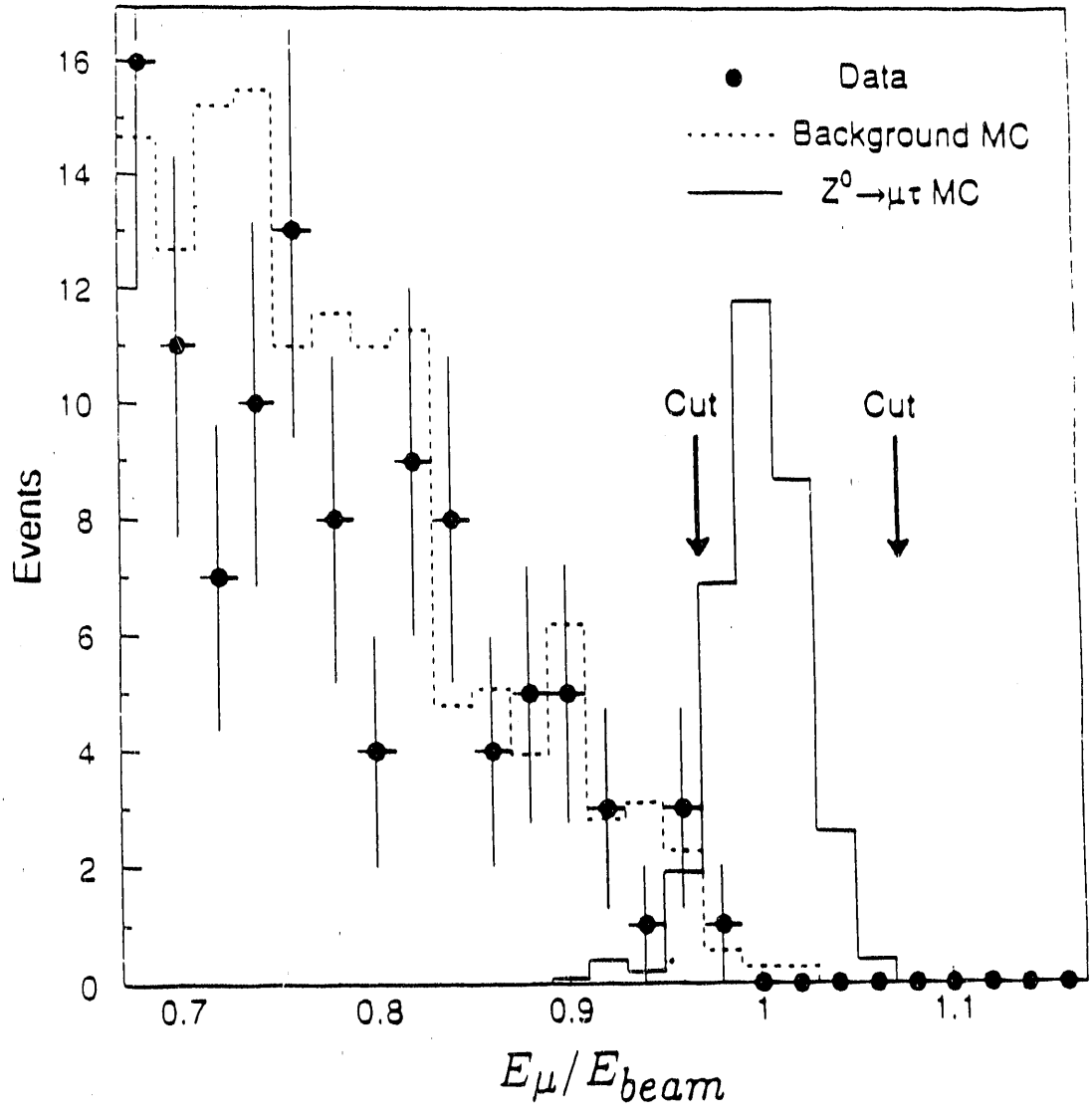
Data
Background MC
$Z^0 \rightarrow \mu\tau$ MC
Cut
Cut
Events
0
2
4
6
8
10
12
14
16
0.7
0.8
0.9
1
1.1
E_μ / E_{beam}

Fig. III-9

L3 Physics Papers

1. The Construction of the L3 Experiment.
2. A Determination of the Properties of the Neutral Intermediate Vector Boson Z°.
3. Mass Limits for Scaler Muons, Scalar Electrons, and Winos from e^+e^- Collisions near $\sqrt{s} = 91$ GeV.
4. Measurement of g_A and g_V, the Neutral Current Coupling Constants to Leptons.
5. Measurement of Z° Decays to Hadrons, and a Precise Determination of the Number of Neutrino Species.
6. A Measurement of the Z° Leptonic Partial Widths and the Vector and Axial Vector Couplings Constants.
7. Measurement of $Z^\circ \to b\bar{b}$ Decay Properties.
8. Mass Limits for Excited Electrons and Muons from Z° Decay.
9. A Determination of Electroweak Parameters from $Z^\circ \to \mu^+\mu^-(\gamma)$.
10. A Precision Measurement of the Number of Neutrino Species.
11. Search for the Neutral Higgs Boson in Z° Decay.
12. Determination of a_s from Jet Multiplicities Measured on the Z° Resonance.
13. A Test of QCD based on 4-Jet Events from Z° Decays.
14. Test of QCD in $e^+e^- \to \gamma\gamma$ at LEP.
15. Search for Excited Taus from Z° Decays.
16. Search for the Neutral Higgs Bosons of the Minimal Supersymmetric Standard Model from Z° Decays.
17. A Search for Heavy Charged and Neutral Leptons from Z° Decays.
18. A Determination of Electroweak Parameters from Z° Decays into Charged Leptons.
19. Search for the Charged Higgs Boson in Z° Decay.
20. Search for a Low Mass Neutral Higgs Boson in Z° Decay.
21. A Measurement of B°-$\bar{B}^\circ$ Mixing in Z° Decays.
22. Search for Excited Neutrinos from Z° Decays.
23. A Measurement of the $Z^\circ \to b\bar{b}$ Forward-Backward Asymmetry.

24. Determination of a_s from Energy-Energy Correlations Measured on the Z° Resonance.

25. Search for the Neutral Higgs Boson.

26. Measurement of the Inclusive Production of Neutral Pions and Charged Particles on the Z° Resonance.

27. Search for Leptoquarks in Z° Decays.

28. Measurement of $Z^\circ \rightarrow b\bar{b}$ Decays and the Semileptonic Branching Ratio $Br(b \rightarrow l + X)$.

29. Measurement of Electroweak Parameters from Hadronic and Leptonic Decays of the Z°.

30. Search for Narrow High-Mass Resonances in Radiative Decays of the Z°.

31. A Test of QCD Based on 3-Jet Events from Z°Decays.

32. Decay Properties of Tau Leptons Measured at the Z° Resonance.

33. Search for Lepton Flavour Violation in Z° Decays.

34. Measurement of the Lifetime of B-Hadrons and a Determination of $|V_{cb}|$.

35. Measurement of the Strong Coupling Constant α_s for Bottom Quarks at the Z° Resonance.

IV. The SDC Detector for pp Collisions at the SSCL (Calorimeters)

The personnel who have worked on this project are Professors Virgil Barnes and Arthur Garfinkel, project associate Alvin Laasanen and graduate students James Tonnison and James Ross, as well as several undergraduate students during summers and during the academic year. We are founding members of the Solenoidal Detector Collaboration (SDC). One of our long-range goals is to collaborate in building the calorimeters for the proposed Solenoidal Detector for the SSC. This initiative began in close collaboration with some of our Fermilab CDF colleagues, and is aimed not only at the SSC, but also at the upgrade of the CDF endplug calorimeter. A ray-tracing Monte Carlo program developed by Barnes and Tonnison gave the first indications that excellent light yield and uniformity of response were possible for tiles with small diameter waveshifting fiber readout. [See Fig. IV-1 for a typical ray trace output of a fiber tile.] This was the inception of the interest in this technology, which has led to its being the technology of choice for the CDF endplug upgrade proposed for 1994-95 to replace the gas readout calorimetry in the CDF plug and forward regions.

This technology has now also been chosen for all or most of the SDC calorimetery. Test beam studies of prototype EM and Hadron calorimeters at Fermilab in late 1991 gave very encouraging results. Purdue provided calibrations, using moving radioactive sources, of these prototypes, and also of CDF endplug upgrade EM and Hadron calorimeter prototypes which are directly relevant to SDC calorimeter design choices. Some detailed results will be shown below. Results obtained for an earlier spaghetti calorimeter during and after the August 1990 Fermilab test beam run were presented at the Fort Worth SSC Conference and the Fermilab International Calorimeter Conference, both in the fall of 1990, and are in the published proceedings of those conferences. Preliminary results of the fall, 1991, calibration of the CDF plug upgrade EM and Hadron calorimeter prototypes at the testbeam were reported at the October, 1991 Capri Calorimeter Conference and will appear in the published proceedings.

The CDF plug upgrade EM prototype was extensively instrumented with source tubes in every layer of every tower. It achieved good energy resolution, seen in Fig. IV-2 where the calorimeter energy response has a σ/E of 1.6% for 100 GeV electrons. Figure IV-3 shows the relation between beam energy and calorimeter resolution for a typical tower, with $\sigma/E = 15.2\%/\sqrt{E} + 0.7\%$. Figure IV-4 shows the equalization of the responses of tiles within a tower to the moving Cs137 calibration source, using grey-scale masking at the

phototube cookie, where Mask 0 = no mask, and Mask 2 gave nearly complete equalization. Other features of the sourcing will be shown below in the detailed discussion of the moving source technique and hardware.

We have had responsibility for the calibration and characterization of every one of the CDF and SDC scintillating tile calorimeter prototypes for the Fermilab beam tests. We are also helping with radiation hardness studies taking place at various foreign laboratories which have ~ 1 - 2 GeV intense electron beams. We constructed last year twenty small Radiation-Hardness-testing calorimeters ("Personal Calorimeters") in collaboration with Fermilab, some of which were shipped to Beijing, to Saclay and to KEK. Radiation hardness adequate for the SDC barrel calorimeter and much of the SDC endcap calorimeter has been seen in these modules, with scintillators and wavelength shifting fibers of the type used in the recent testbeam prototypes. Figure IV-5 shows a typical longitudinal scan of the source past the edges of the twenty tiles in an undamaged module. Figure IV-6 shows the depth profile of the radiation damage, that is the response of each tile relative to its undamaged response, as a function of depth in a Rad-Hardness-testing module exposed to various integrated doses (calculated at shower maximum) from the Beijing electron accelerator. The ~40% degradation at a dose of ~600 kiloRads (10 SSC years at 10**34 luminosity) could be corrected by differential grey-scale masking of the fibers from each tile. Even in the absence of masking, the damage profile, measured by the moving source, could be used in software correction of the response of the calorimeter as a function of electron energy. If a second EM calorimeter depth segment is available, software correction can also be made for shower-to-shower depth fluctuations, thereby recovering most of the energy resolution of an undamaged calorimeter.

We have also used a moving source calibration to obtain longitudinal response profiles of the tiles in a prototype module of the CDF Microplug, a calorimeter proposed for installation at very forward angles just outside the CDF beam pipe. The Microplug performed well in the 1991 testbeam, and we are hopeful that it will be approved for installation for phase 2 of the upcoming CDF run. One proposed use of the Microplug is as a radiation damage test bed for various promising new scintillating tiles and readout fibers in realistic radiation fields, where the moving source can monitor the development of the damage profile.

We have also been asked to provide moving source calibration of the Shower Maximum position detector within the CDF plug upgrade EM calorimeter,

which uses long scintillating tile "fingers" with wavelength shifting readout. These will need to have known responses for each channel and known optical attenuation lengths along each finger.

Description of the moving source calibration system

We have been involved since a very early stage in studies of scintillating tile calorimeters as well as early studies of scintillating fiber calorimeters, under SSC Generic Detector and Major Subsystem funding. For all of these projects we have designed and constructed systems using a remotely movable Cs137 gamma source to calibrate many places within each calorimeter tower. The system has the capability to select remotely one of a large number of possible channels within the calorimeter, and to drive a pointlike source at the end of a long fine wire at a constant speed into the calorimeter. The position of the source is measured to 0.1 mm least count. Either manual or computer control of the drive motors is possible.

The source response is a key way of carrying test beam calibrations forward in time; it is useful in setting the initial phototube gains; it can conceivably substitute for test beam exposures if the calorimeter towers are sufficiently uniformly built and well characterized; and the source response can permit a check on the uniformity of response of a tower during and after construction — a key to obtaining the excellent energy resolution desired. Based on the source measurements, every tile in a tower can be corrected to have the same response, if the fibers from each tile are in an orderly array at the phototube cookie, by applying a suitable grey-scale mask at each fiber. An example of such a grey-scale mask is shown in Fig. IV-7, and the results of masking a typical EM calorimeter tower were shown above in Fig. IV-4. The source response is taken to be the peak value of a current vs. time plot as the source is moved at constant speed past the calorimeter tiles. A plot of the responses of 8 towers in a row, traversed by one source tube, is shown in Fig. IV-8. The reproducibility of the peak values is better than one percent, and Fig. IV-9 shows the distribution for a set of EM calorimeter towers, of the RMS deviations between two source calibrations taken several weeks apart, calculated over the 23 tiles within a each tower. The typical RMS is less than 0.5%, indicating that this method should provide a very precise way of carrying forward testbeam calibrations through time for use during collider running.

We have constructed ten copies of the second generation Purdue source driver, which has a circular indexer to select from among up to 72 (more recently 216) source entry channels within a calorimeter. These drivers can

be flexibly coupled via 1/8-inch nylon tubing from the source driver to fine metal tubes running within the calorimeter. The source drivers have seen a lot of use, and while they have done their jobs well, they require some mechanical upgrades to improve their reliability under heavy use. We have designed the necessary improvements, had them produced at the Purdue Central Machine Shops, and have begun to retrofit them onto the existing driver units, which continue to be used extensively.

After an extensive R&D study we settled on a CAMAC-based DAQ system for the DC source current measurements, using the DSP 2032 autoranging scanning DVM, for use in most of the test areas. The CDF RABBIT front end electronics were used in the CDF testbeam and will be used in the final CDF plug upgrade. The SDC front end electronics will need to provide current measuring capabilities similar to the Rabbit system as well as considerably faster pulse DAQ for events.

Summary

It is worth noting that both the tile-with-fiber-readout and the scintillating-fiber calorimeters offer a number of improvements over conventional scintillator calorimeters with waveshifter bar or waveshifter plate readouts: (a) the potential for better radiation hardness (due to early shifting to longer wavelengths of light, where plastics suffer less degradation by radiation), (b) better light yield, (c) good compensation between EM and hadronic responses and hence better linearity of response and better energy resolution, (d) absence of "cracks" within or between towers, and (e) the possibility of finer tower segmentation. In comparison with non-scintillator calorimetery, the scintillators have the advantage of no fluid containment vessels and a fast signal output.

In summary, we have had a very productive, albeit exhausting, year working on the new scintillating tile technology for calorimetry, and the calibration thereof. We are delighted that the technology is proving so successful and has been chosen for both the SDC and CDF detectors.

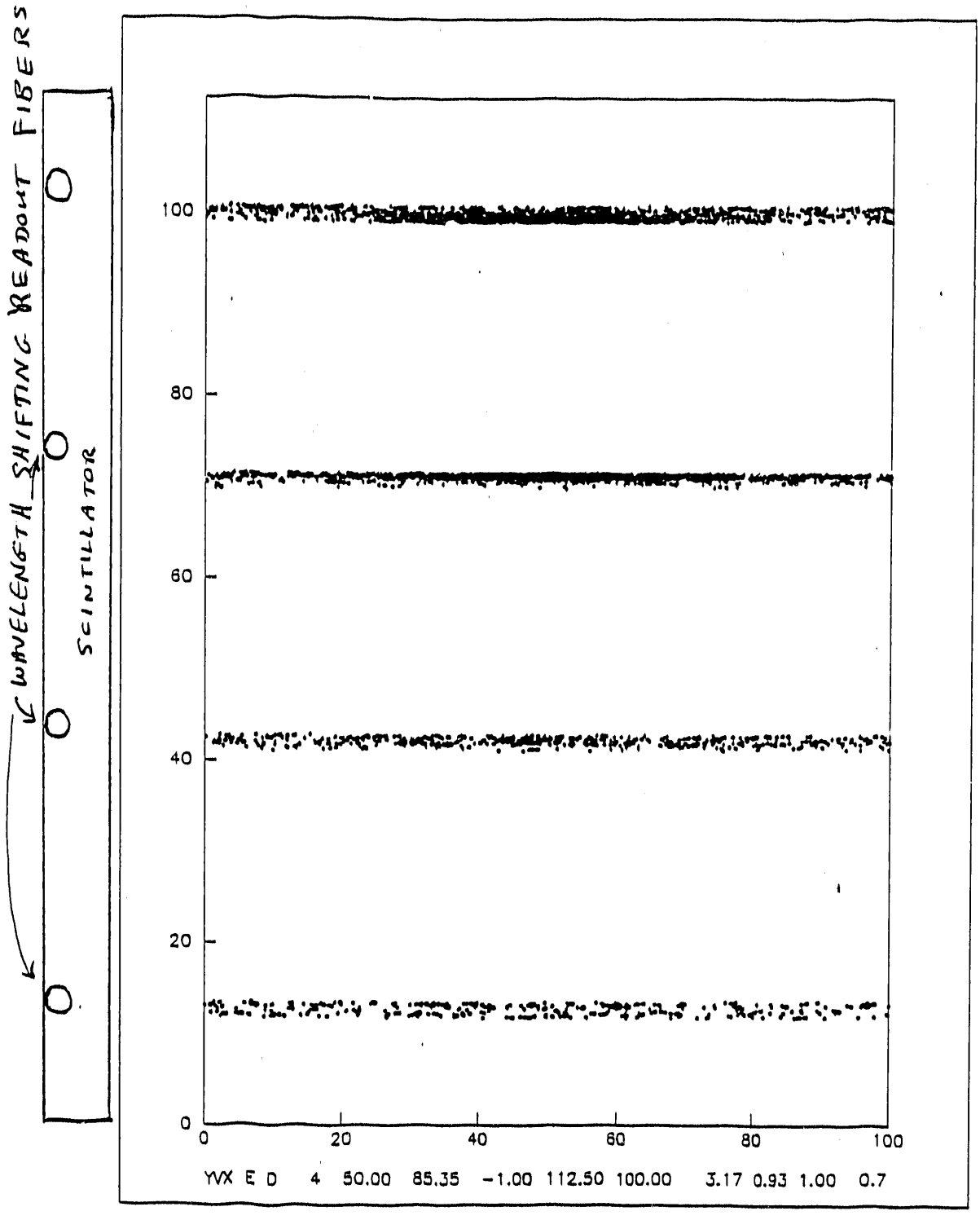

Fig. IV-1 Ray tracing simulation of a scintillating tile with four imbedded wavelength shifting readout fibers, and the source near one of the fibers. Schematic of the fiber layout is shown at the left of the plot. Dots show photons converted by a readout fiber. The summed response is uniform to a few percent as the source position is varied over the face of the tile.

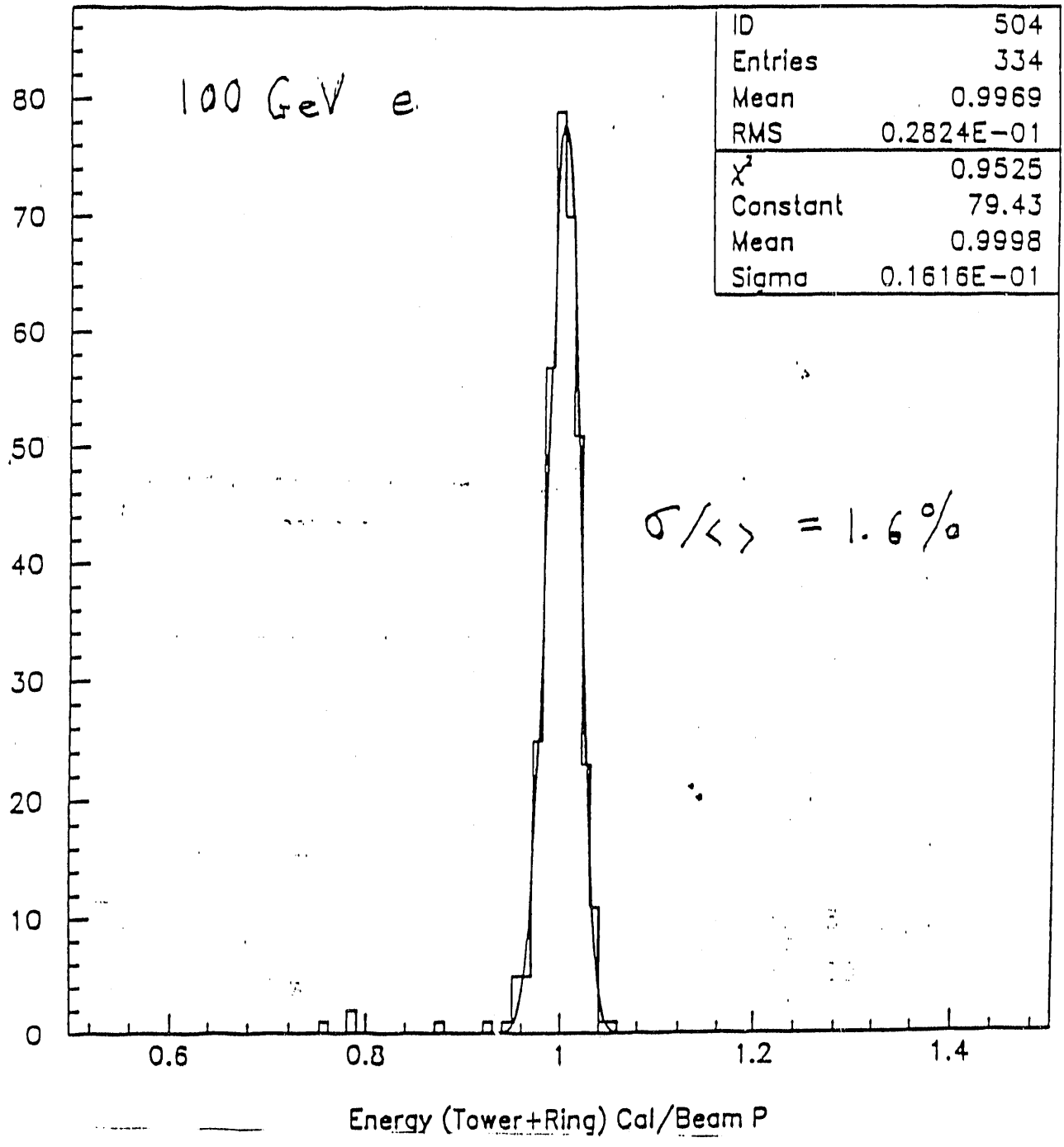

Fig. IV-2 Calorimeter energy divided by beam momentum, one tower of CDF Plug Upgrade EM prototype calorimeter exposed to 100 GeV electron beam.

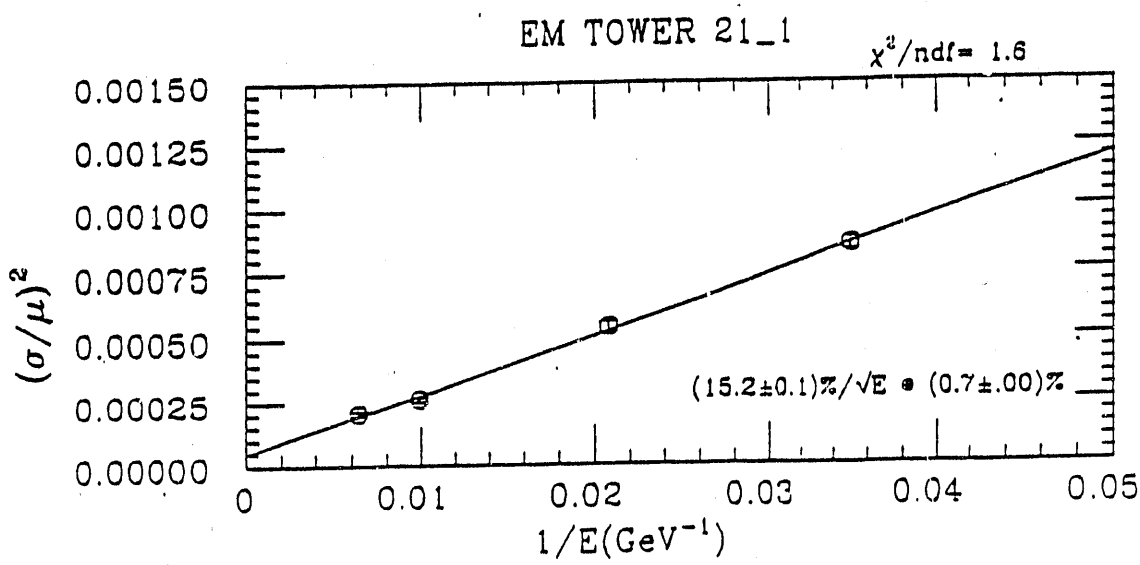

Fig. IV-3 Prototype tile EM calorimeter resolution as a function of energy. CDF Plug Upgrade.

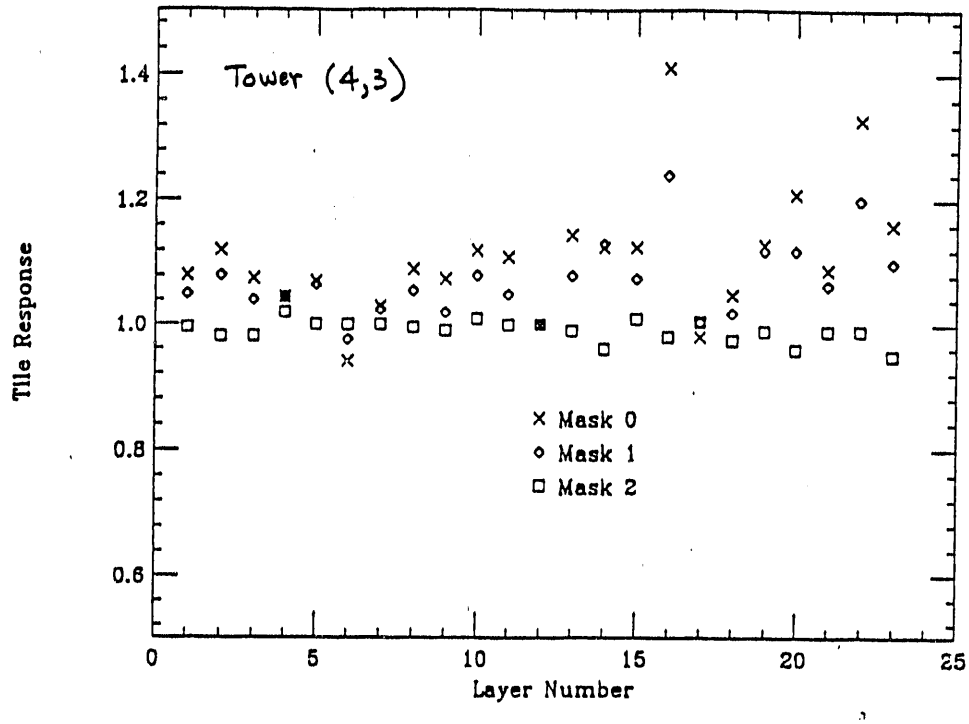

Fig. IV-4 Equalization of tile source responses in one calorimeter tower using grey scale masking. Mask 0 - no mask, mask 1 achieved partial and mask 2 achieved full equalization.

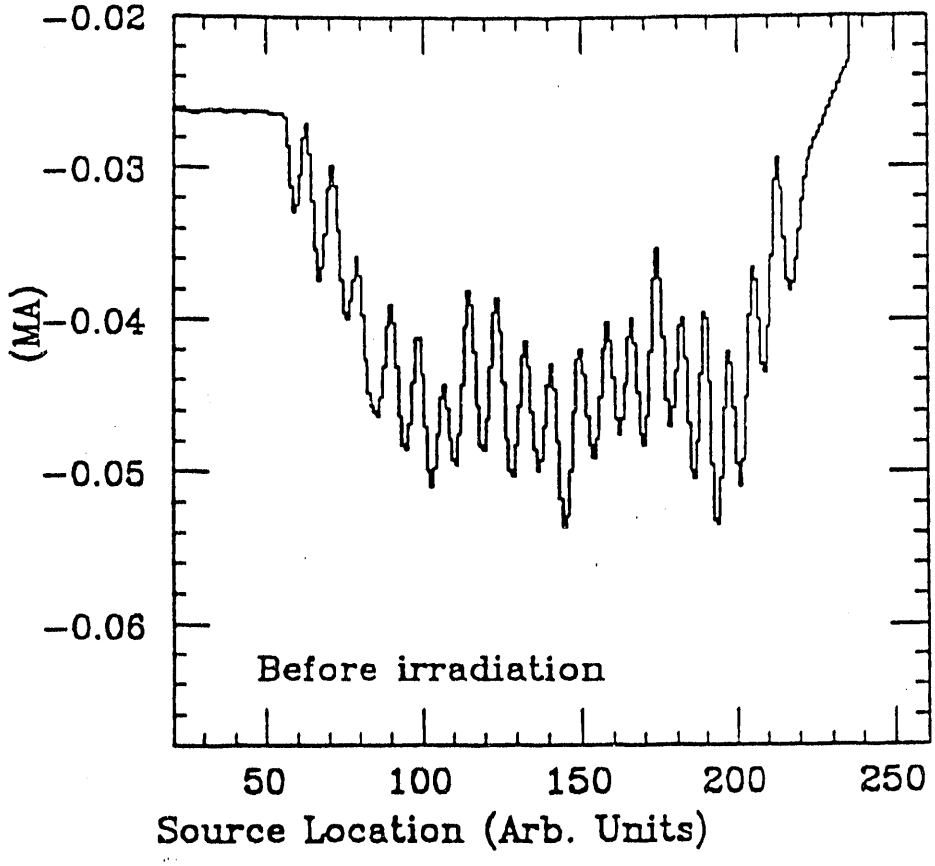

Fig. IV-5 Longitudinal source scan of undamaged Purdue/Fermilab Radiation Hardness Test Calorimeter Module, containing 20 layers of scintillating tile and lead.

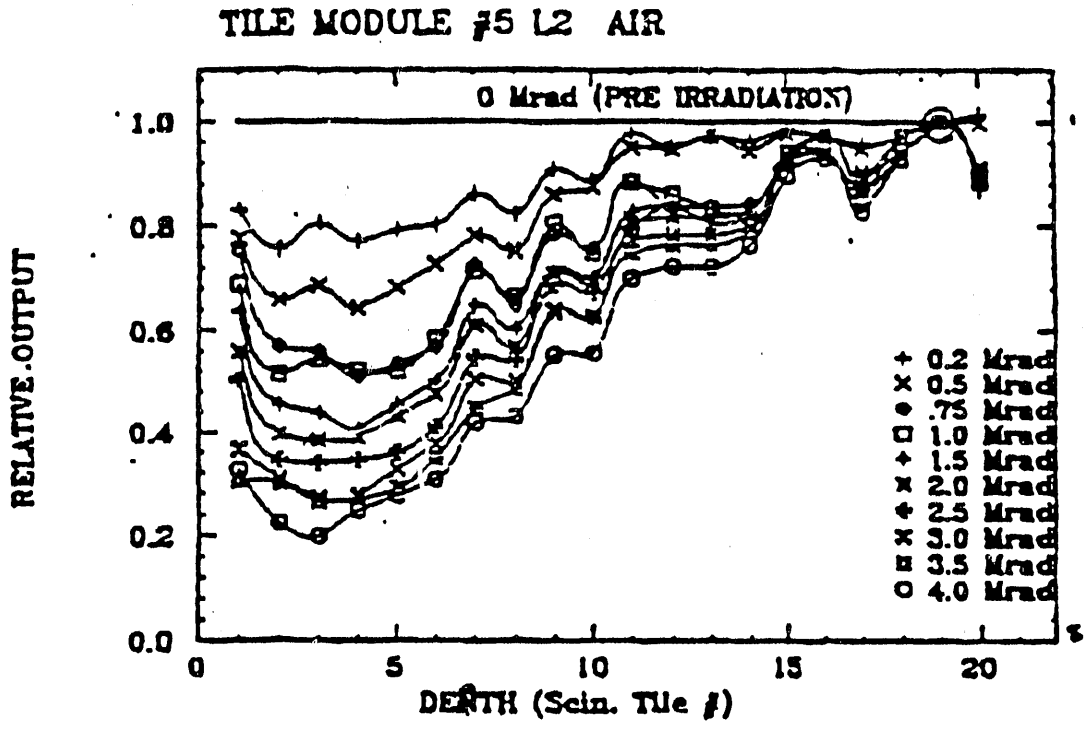

Fig. IV-6 Longitudinal source response of Radiation Hardness Test Calorimeter Module, relative to undamaged tiles, for various integrated radiation doses at shower maximum from the Beijing electron accelerator.

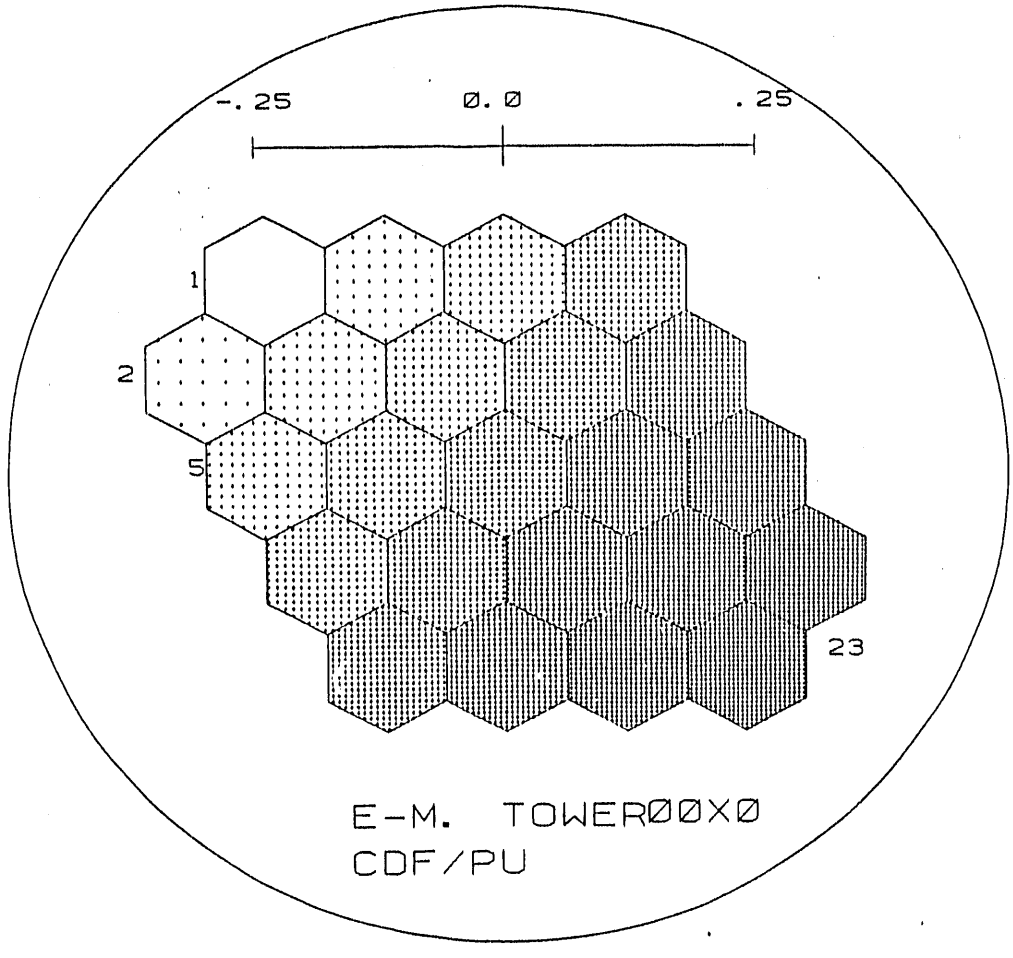

Fig. IV-7 A laser-printed grey scale mask for equalizing the source responses of the tiles in a calorimeter tower. The pattern is then demagnified onto photographic film placed between the fiber cookie and the light mixer which is attached to the phototube.

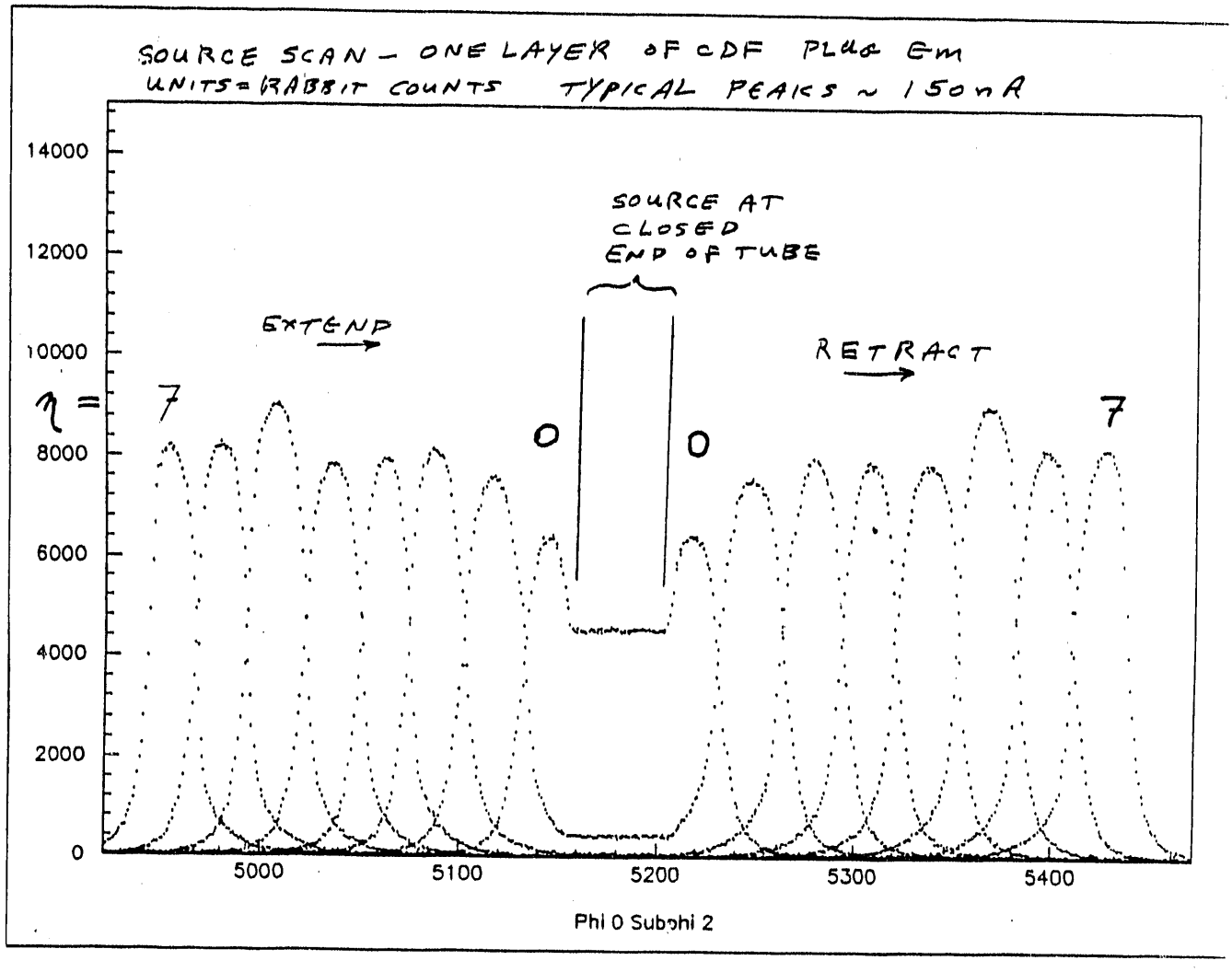

Fig. IV-8 DC currents from the phototubes of eight consecutive calorimeter towers traversed by one source tube, plotted vs. time as the source moves in and out of the calorimeter at constant speed.

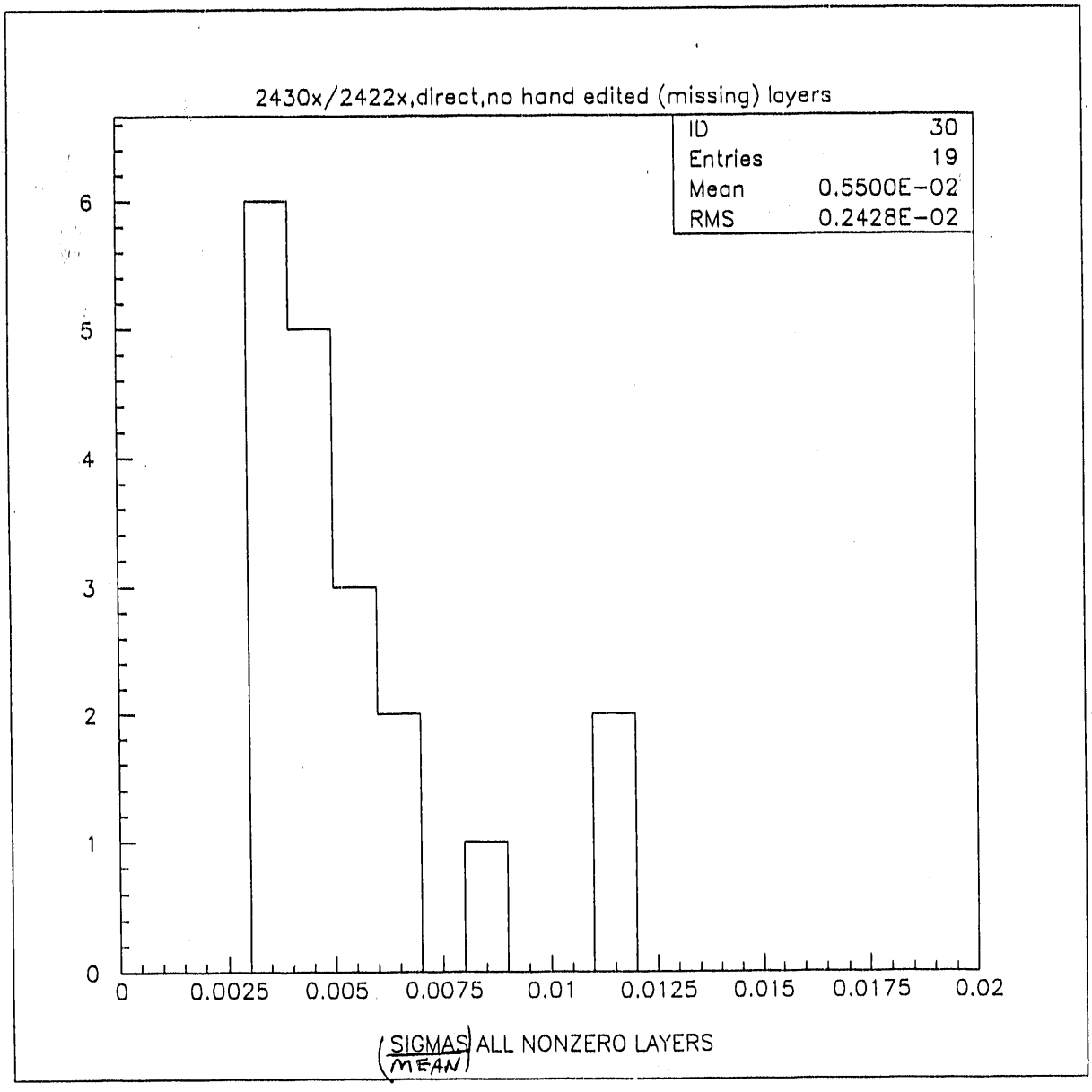

Fig. IV-9 Repeatability of source measurements: distribution of RMS deviations within a tower of the ratios of source responses of calorimeter tiles calibrated several weeks apart. Each RMS value is calculated for the 23 tiles in one tower.

V. The SDC Muon Detector for p-p Collisions at the SSCL

5.1 Introduction

The idea of building a high resolution muon detector to search for the Higgs particle via the reaction

$$H \rightarrow Z^{\circ} + Z^{\circ}$$
$$\mu^{+} + \mu^{-}$$
$$\mu^{+} + \mu^{-}$$

is described in the proceedings of the SSC workshop held at Berkeley in 1987. As discussed in earlier progress reports, we made important contributions to the muon chamber design of the L^{*} proposal. Immediately after the rejection of the L^{*} proposal we joined the muon chamber group of the SDC collaboration. Our interest was to participate in the design and construction of the "slow system" of the muon chamber system controls. By this we mean the setting and monitoring of the High Voltages on the sense wires and field shaping strips as well as monitoring the wire tension. The muon tracking system will be built of 7m long aluminum drift tubes with field shaping. The crossection of the tube and the electrode structure is shown in Figs. V-1a and V-1b. Our first contribution has been the measurement of the tension elongation curves for gold plated tungsten wires of 75 micron and 90 micron wires diameters, which are possible candidates for anode wires. The results are shown in Fig. V-2. The magnitude of the sagitta for the two wires as function of tension is given in Fig. V-3. In addition we will participate in the resolution studies of the superlayer using the same system we designed for the L3 octant resolution test.

As part of the long term R&D for the straw muon tubes we will also be studying the tension stability and the quality of the crimping.

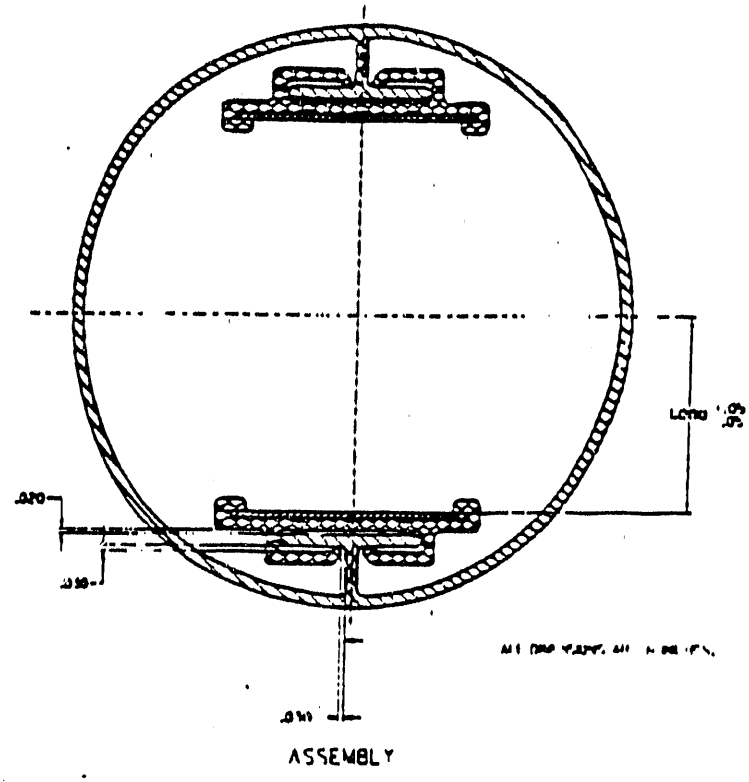

Fig. V-1a: Cross section of a drift tube.

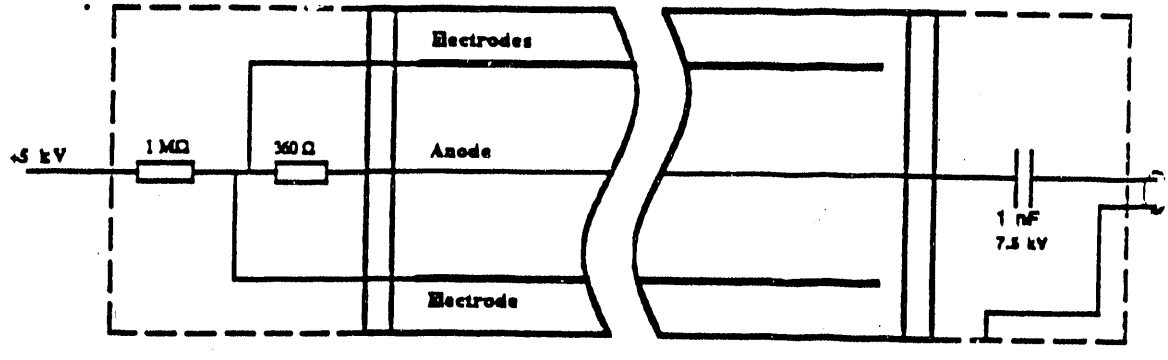

Fig. V-1b: **High voltage and signal connections. Field shaping electrodes and anode are both at +5 kV.**

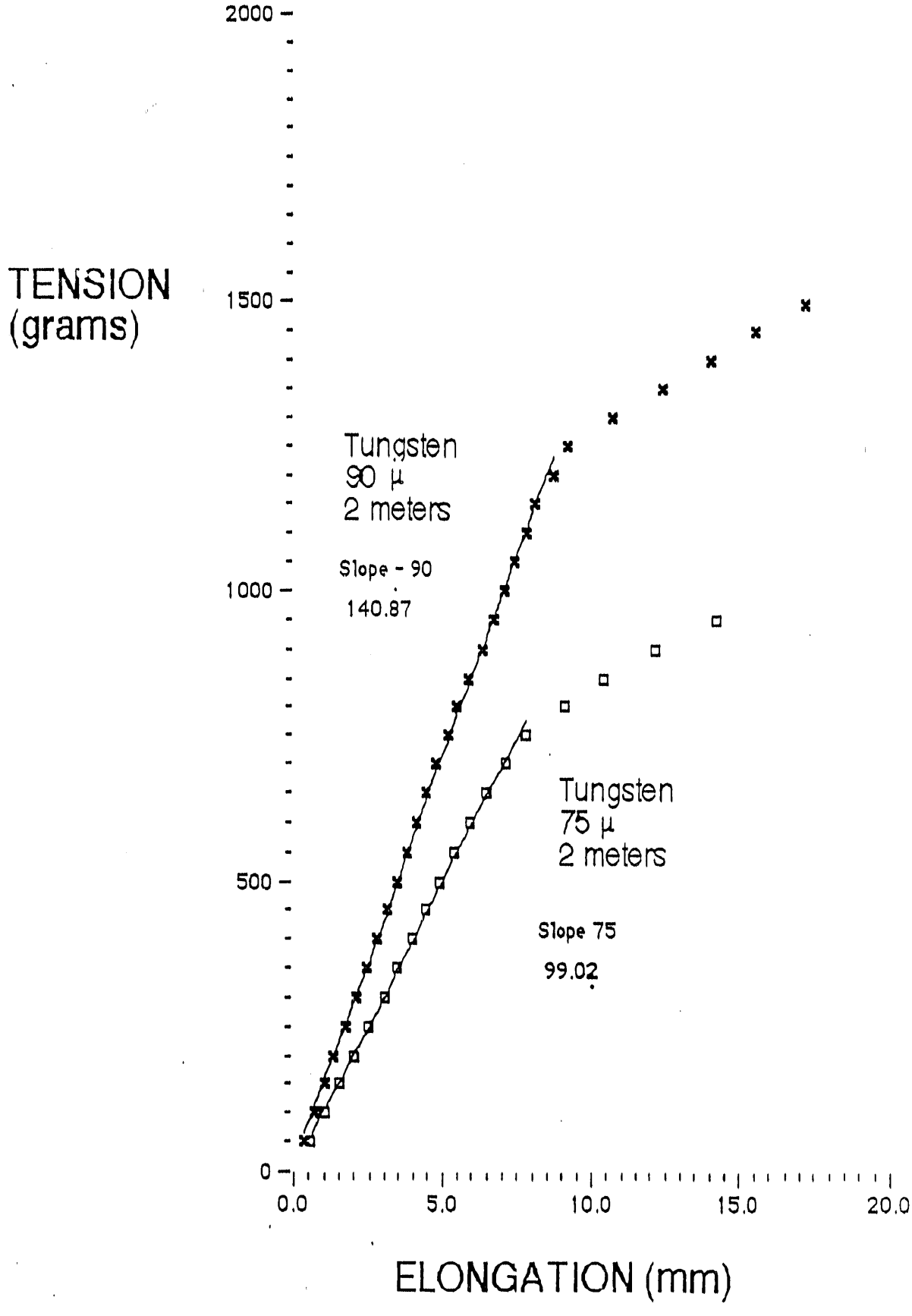
TENSION
(grams)
2000
1500
1000
500
0
Tungsten
90 μ
2 meters
Slope - 90
140.87
Tungsten
75 μ
2 meters
Slope 75
99.02
0.0
5.0
10.0
15.0
20.0
ELONGATION (mm)

Fig. V-2

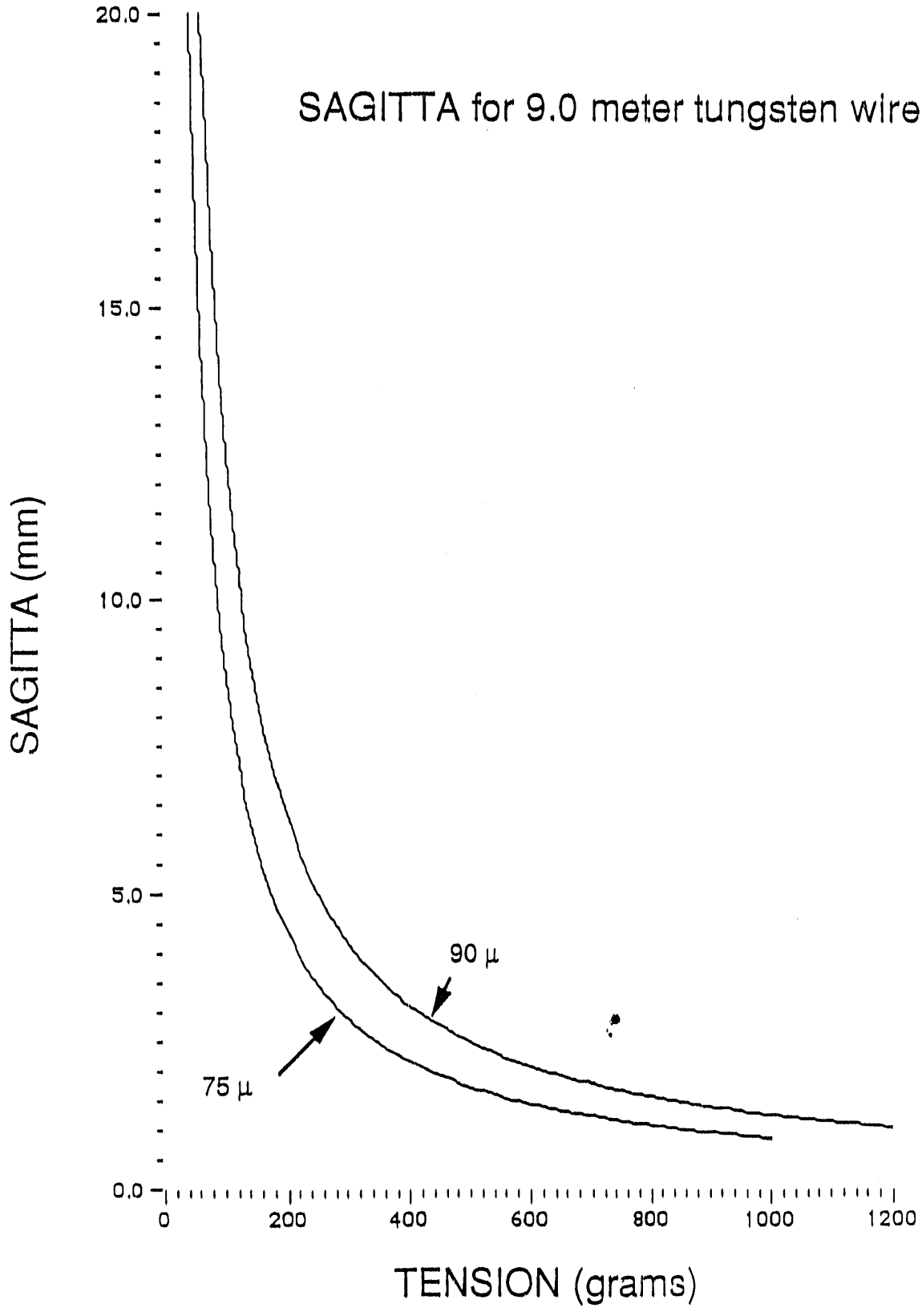
SAGITTA for 9.0 meter tungsten wire
SAGITTA (mm)
20.0
15.0
10.0
5.0
0.0
0
200
400
600
800
1000
1200
TENSION (grams)
90 μ
75 μ

Fig. V-3

VI. The CO Experiment for $\bar{p}p$ Collisions at FNAL

(A) Introduction

The members of Task D participating in E735 at the CO intersection area at Fermilab are Professors Duane Carmony and Laszlo Gutay, Research Assistant Professor Blair Stringfellow, Research Scientist Adam Bujak, Project Associate Robert de Bonte, and graduate student/post doc Tim McMahon.

By 1970, it had become clear that to understand highly inelastic (non jet) reactions, one had to turn to a statistical description because the number of particles continued to increase with bombarding energy. We attempted to fit the pion energy distributions to the Bose-Einstein (BE) equilibrium distribution. Plotting the energy distribution normal to the collision axis showed that it indeed resembled the equilibrium Bose-Einstein (BE) distribution in the central region. Further, the lifetime and size of the pion emitting system were also determined. This led to the concept of Centrally Produced Hadronic Matter (CPHM).

In subsequent studies at Fermilab and BNL the energy dependence ($1\ \mathrm{GeV/c} < P_{inc} < 400\ \mathrm{GeV/c}$) of fragment yield in p-nucleus interactions, we showed the existence of a liquid-gas phase transition and critical behavior in nuclear matter. This gave credence to thermodynamical description of hadronic matter and to the possibility of detecting a phase transition between normal matter and a new form of matter in high energy p-p or $\bar{p}$-p collisions. This new form of matter is termed the Quark-Gluon Plasma (QGP) and had been suggested by particle theorists, though at the time of the prediction the magnitude of the deconfinement temperature was not firmly predicted. In 1984, our proposal to search for QGP was accepted at the new Fermilab $\sqrt{s} = 1.8$ TeV $\bar{p}$-p collider as E-735.

The most general signature of a first order phase transition is the transfer of heat (latent heat) while the temperature and pressure remains constant. Since the temperature is related to the average transverse momentum of the emitted particles ($T \sim \langle p_t \rangle$), we expect that $\langle p_t \rangle$ is a function of entropy density (that is, the number of particles per unit of rapidity dn/dy) and exhibits the characteristic phase transition curve: rise-plateau-rise.

The second signature of QGP is strongly intertwined with the initial state of CPHM. It follows from QCD phenomenology that CPHM is saturated with gluons which collide with quarks and with each other. Since a priority, there are no strange quarks in the colliding $\bar{p}$-p system and thus, in CPHM, it is expected that the reversible reaction

$$g + g \rightleftarrows s + \bar{s}$$

will rapidly build up the strange quark provided the lifetime of the system is long enough for equilibrium to establish. With this provision and because of the high quark density in QGP, a profuse production of strange baryon production will set in.

Finally, it is important to measure the magnitude of transverse flow before the temperature of the system is determined from transverse momentum distribution. Large flow would both distort the exponential p_t distribution and would fake a high temperature.

(B) Experimental Results from the 1987 Collider Run

The goal of the first collider run was to test the trigger hodoscopes, the magnetic spectrometer, the TOF, and part of the data acquisition computer system. The central tracking chamber was not yet operational. The 1987 run showed that the C0 collider region, in spite of lower luminosity ($L_{CDF}/75$) and large beam halo, is a viable area for low p_t physics. The operation of the triggering system, timing and the spectrometer - TOF system was described in earlier progress reports.

The data reduction was done in 1987-1988, mainly on two Vax/780 computers at Purdue. It tied up our entire computer capacity for 6 months. The data analysis was equitably distributed among Duke, Notre Dame, and Purdue Universities. The results have been published in six papers (see publication list) with additional papers being completed and were the basis of the Ph.D. thesis of T. McMahon (directed jointly by Carmony and Gutay). Three of these papers were Physical Review letters with the following findings:

The main result of the first letter (PRL 60 1622 (1988)) is: The average transverse momentum $\langle p_t \rangle$ (done with negatives without particle identification) as a function of charged particle multiplicity (n_c) exhibits a behavior which is consistent with a first order phase transition, thus with the formation of quark gluon plasma (See Fig. VI-1).

In a second letter (PRL 62 12 (1989)), we showed evidence for $\Lambda - \bar{\Lambda}$ production and a dramatic rise of the Λ-$\bar{\Lambda}$ production cross section as function of energy. This indicates the expected strange particle enhancement (See Fig. VI-2).

A third letter published in 1990 (PRL 64 E991 (1990) shows that the K/π ratio rises as a function of both the charged multiplicity and increasing p_t. The $\bar{p}/\pi$ ratio, while rising even more rapidly with increasing charged multiplicity is nearly independent of p_t over the range from 0 to 1.5 GeV/c.

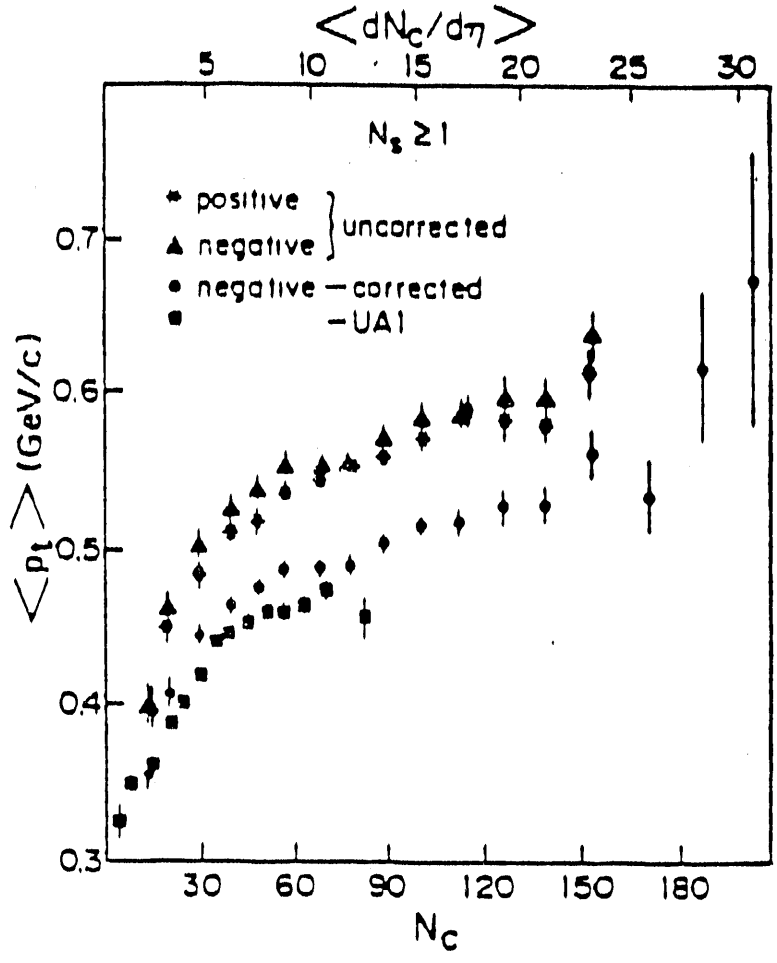

$\langle p_t \rangle$ as a function of N_c and $\langle dN_c/d\eta \rangle$ for all positive tracks and all negative tracks averaged over the interval 0.15 GeV/c $< p_t <$ 3.0 GeV/c. The corrected $\langle p_t \rangle$ of negative particles includes unobserved particles with $p_t <$ 0.15 GeV/c

Fig. VI-1 Variation of the average momentum transfer ($\langle p_t \rangle$) as a function of the charged particle density dN/dη for all particles.

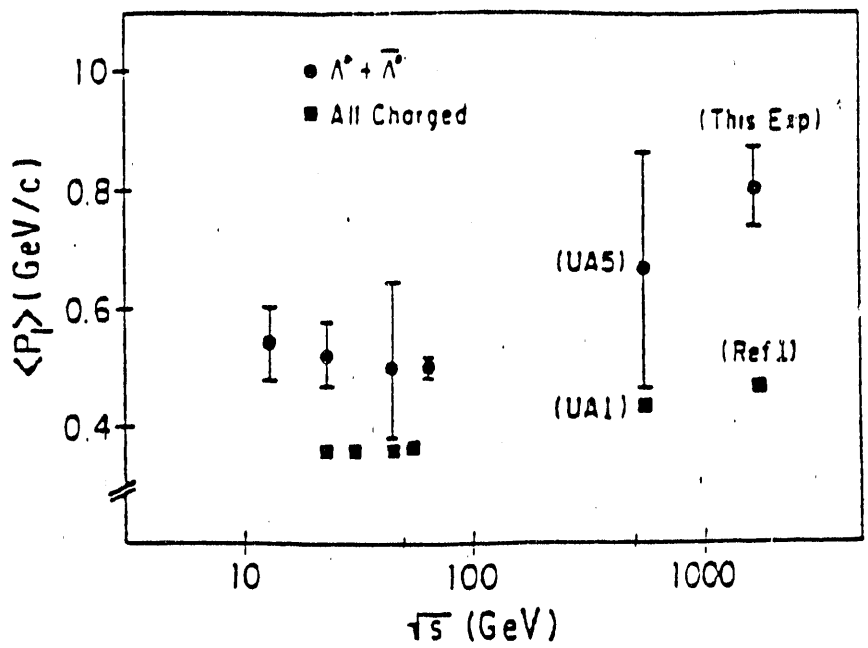

The $\langle p_t \rangle$ of $\Lambda^0 + \bar{\Lambda}^0$ as a function of the center-of-mass energy The $\langle p_t \rangle$ of charged particles is also plotted for comparison.

Fig. VI-2 Variation of the Lambda average tranverse momentum ($\langle p_t \rangle$) as a function of the centre of mass energy ($\sqrt{s}$).

(C) Activities During 1988-1989 Collider Operation

The Collider operated for 11 months ending about 1 June 1989. Prior to the run, the magnetic spectrometer arm-TOF system was upgraded with a set of beam halo counters. They were installed, debugged, timed, and integrated into our trigger logic. The collider operation changed from $3\bar{p}$ bunches on 3p bunches to $6\bar{p}$ on 6p bunches. Thus the trigger logic had to be upgraded accordingly.

Most of the Purdue effort was concentrated on bringing the CTC into operation; creating a VME based data acquisition and chamber monitoring system and tying together and synchronizing the two data taking systems. When the task was accomplished we found that the ratio of the Spectrometer to CTC rates was about 10. The rate of transfer from the VME to the PDP11/60 computer contributed 90% of the overall dead time. To speed up the CTC readout we have removed the PDP and established a direct VME-tape drive link. A Ciprico tape drive controller was installed on the VME bus and the system memory was increased by an additional 2 Mbytes.

The necessary VME based software for servicing a magnetic tape drive has been developed. A multievent buffering scheme within VME data acquisition was implemented. This increased the CTC/Spectrometer ratio by a factor of 3 to 5 (depending on trigger mode).

Finally, the CTC itself was brought into operation and stable operating conditions were determined. Even though the intensity of the background radiation (I) and background rates (R) were high at C0 (I = 1 Rad/hour, R = 20-60 KHz) the chamber has performed well for the entire eleven months. From time to time, various sectors have not held full voltage (possibly due to radiation induced damage) but these sectors have been brought back by applying opposite polarity voltage for a few hours. Programs for pattern recognition, tracking, and track matching with the spectrometer were written and debugged.

(D) Activities Since the 1988-89 Run

The Fermilab Amdahl computer has been used to produce a complete set of DST tapes with the CTC chamber data merged with the spectrometer arm, time of flight, and hodoscope data. Preliminary tracking of the combined data were finished during the summer of 1990. With the help of this data we improved: vertex finding algorithm, the interaction time, representation of magnetic field and track finding routines. The second round of improved tracking of the entire data sample were finished by summer 1991.

Depending on the multiplicity region being studied, the new data sample is 15-30 times as large as the engineering run. The next year should produce additional high statistics papers and a better understanding of the effects being observed. Although all results are still preliminary, we illustrate the new data with two figures using the approximately 7000 lambda events extracted from the 1989-90 run. Fig. VI-3 shows the ratio of lambdas to all charged secondaries as a function of p_t. The rapid increase with increasing p_t is similar to that observed for antiprotons in the engineering run. Fig. VI-4 shows the ratio of lambdas to p bars as a function of charged multiplicity (N_h is counts in the charged particle hodoscope). The ratio is constant.

In addition to extended running at $\sqrt{s}$ = 1800 GeV, we ran at the CERN energy of 540 GeV as well as at 300 and 1000 GeV. A long paper studying the average p_t and various particle production ratios as a function of $\sqrt{s}$ will be forth coming.

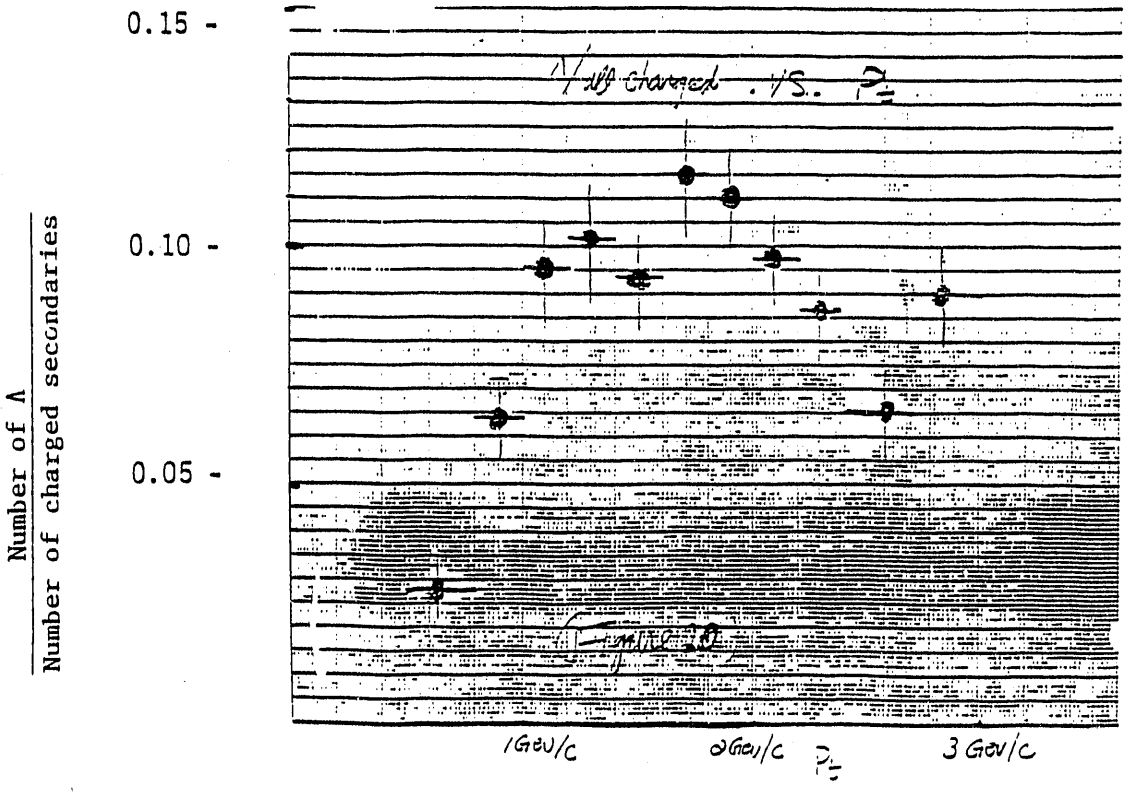

Fig. VI-3 The ratio of Lambdas to all charged particles as a function of p_t (1988 - 89 data).

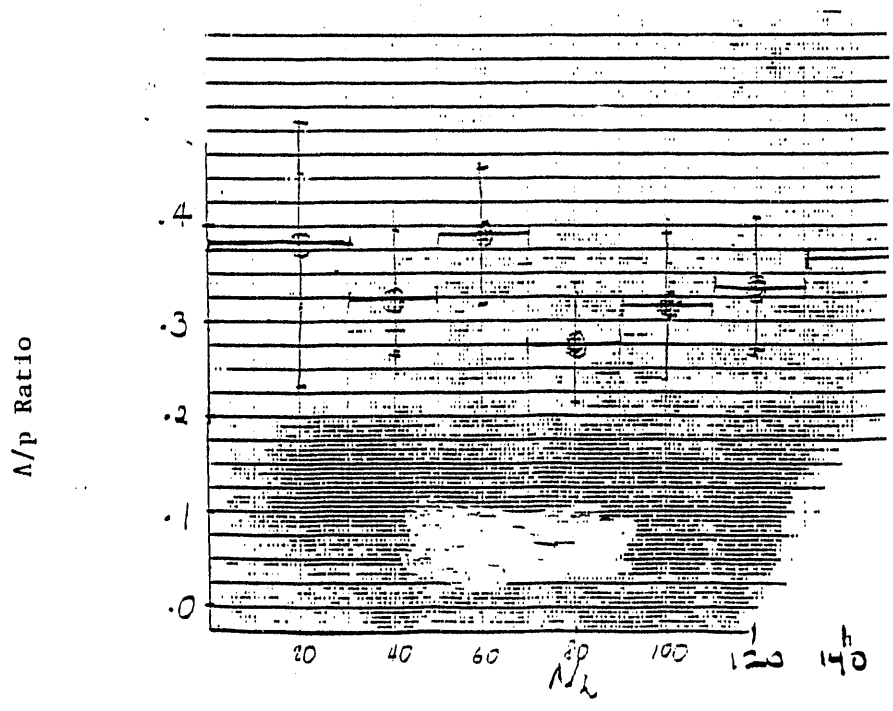

Fig. VI-4 Lambda to proton ratio as a function of multiplicity (1988 - 89 data).

VII. Accelerator Physics at Fermilab

Introduction

Strong coupled-bunch mode (CBM) oscillations and longitudinal emittance growth have long been observed in the Fermilab Booster synchrotron, which accelerates protons from 200 MeV to 8 GeV. The oscillations can lead to beam loss, especially during transfer to the Main Ring. This coupled-bunch instability has also been believed to cause emittance growth, i.e. bunch lengthening and momentum spread, limiting the beam brightness (intensity per unit phase space area.) The coupled-bunch oscillations and bunch lengthening are thus expected to critically limit the luminosity during upcoming collider operation in the Tevatron.

This report summarizes progress to date in thesis research under the Joint Purdue-Fermilab Doctoral Program in Accelerator Physics. The topic is the study of longitudinal beam instabilities and emittance growth in the Fermilab Booster. Numerous studies have been performed in the past to measure and damp the unstable motion and determine the driving source(s). The physics of the interaction has not been well understood. Through recent experiments and calculations we believe we can now characterize the longitudinal coupled-bunch instability. We are currently carrying out an experiment to damp what we have determined to be the source of the CBM oscillations.

RF Cavity HOM Damping and Transition Energy Studies

The present effort draws on the evidence of a strong correlation between the CBM instability and the influence of higher-order modes (HOM) in the RF accelerating cavities. The schematic of a Booster RF cavity is shown in Fig. VII-1. As the beam is accelerated by the RF field across the gaps in each cavity, it excites the HOMs which can then act back on the beam. The approach is to passively damp those HOMs in the cavities coupling most strongly to the beam. Detailed beam and cavity measurements indicate that three cavity modes, around 83, 165 and 220 MHz, correlate with the unstable beam modes (the fundamental cavity mode is around 53 MHz.) These data agree with linear CBM instability growth rate calculations. We designed and tested HOM dampers for the three cavity modes and installed them in four of the 17 Booster cavities. The damper for the 83 MHz modes is inductively coupled, and for the 165 and 220 MHz modes capacitively coupled inside the cavity. The modified cavity showing the HOM dampers is shown in Fig. VII-2. The external circuits essentially are bandpass filters with center frequencies at

83, 165, and 220 MHz, respectively. In this way, the energy coupled out is dissipated in a load.

Results

Preliminary beam measurements with four of the Booster cavities damped show a reduction in the CBM oscillations, but the bunch lengthening appears unaffected. The measurements were made using a resistive wall monitor, which measures the return current across a ceramic gap in the beampipe wall. Using an oscilloscope, one can thus record the spatial density distribution of the beam. In the Booster, the beam is bunched at a harmonic number 84. The longitudinal emittance is calculated from the bunch length. The CBM structure may be seen after performing a Fourier transform of the time-domain signal. The result is a spectrum rich in structure. A main feature is a line at the RF frequency (around 53 MHz) and at harmonics of this frequency. The unstable CBMs appear in between the RF periods, spaced at the synchrotron revolution frequency ($f_{RF} = 84\ f_0$). Fig. VII-3 and VII-4 show the beam spectrum with 15 cavities turned on, with all the cavities nominal (HOM dampers out) and with four cavities damped (HOM dampers in), respectively. These measurements were made with a beam intensity of 2×10^{10} protons per bunch (ppb.) One can see that the spectral lines are reduced between the RF harmonics in the case with four cavities damped. Fig. VII-5 shows the results of the emittance calculation under these same conditions. The emittance appears unaffected by the damped cavities. This result indicates that the dampers have to turn on all the cavities and that the manner the beam is accelerated through the transition energy region has to be studied also.

Summary

We will complete the RF cavity HOM damper study by modifying all the cavities and measuring the beam response. We will complete the analytical calculations to compare these data with the linear CBM theory. To try to determine potential causes for the emittance growth, we are investigating quasi-linear and non-linear models, which in turn will help to define experiments. We believe that in separating these two phenomena, i.e. coupled-bunch instability and longitudinal emittance growth and the dependence of their magnitudes on damping and the manner the beam passing through the transition energy region, we potentially have identified a new area of instability research in beam physics.

Fig. VII-1

NUMINAL BOOSTER CAVITY

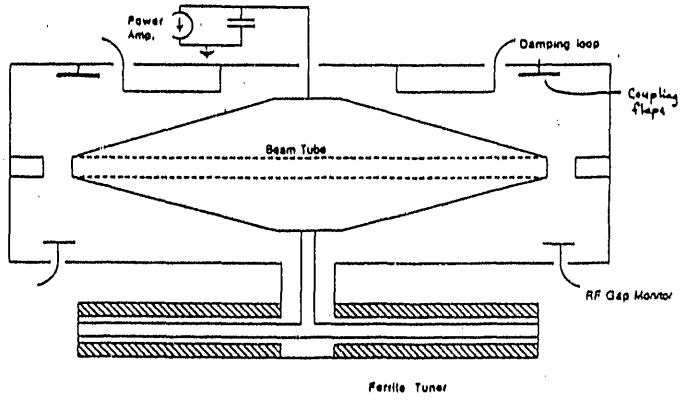

Fig. VII-2

MODIFIED BOOSTER CAVITY ⇒ HIGHER-ORDER MODE DAMPERS
(Dave Wildman, 1991 memo)

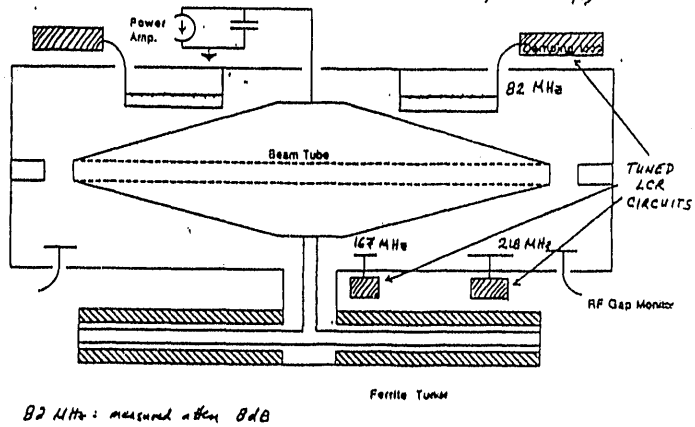

82 MHz: measured atten 8dB
or factor of 2.5

BASIC TUNED CIRCUIT:
SERIES RESONANT @ 60 MHz
PARALLEL RESONANT @ 140M

Fig. VII-3

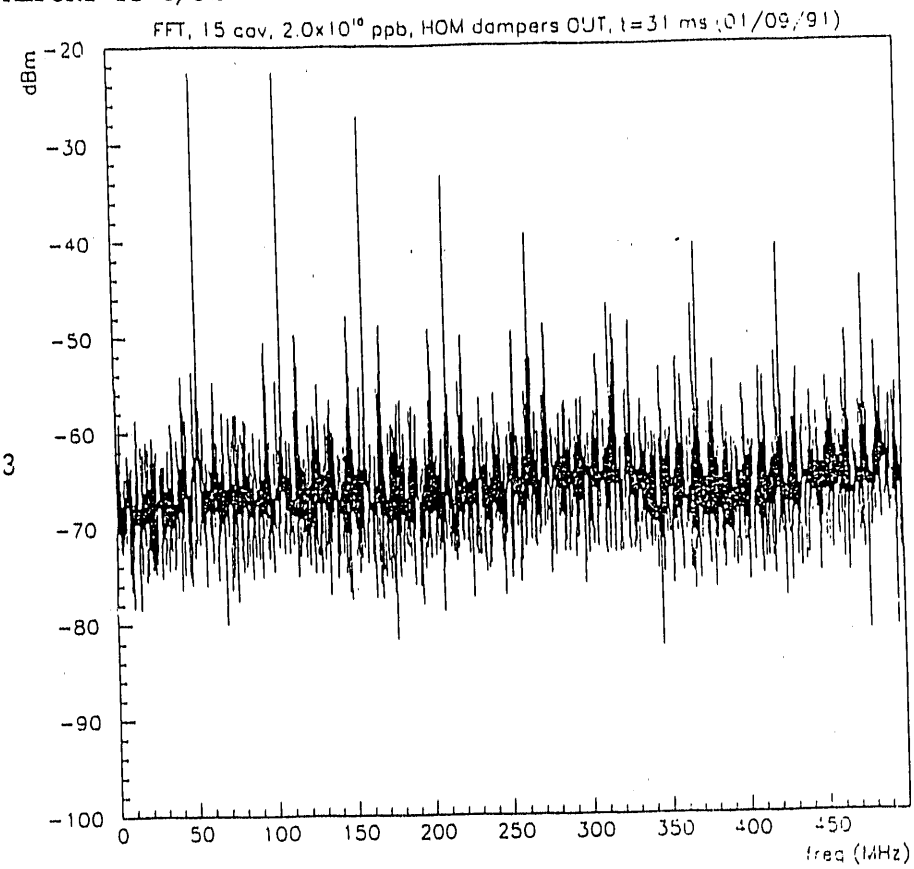

Fig. VII-4

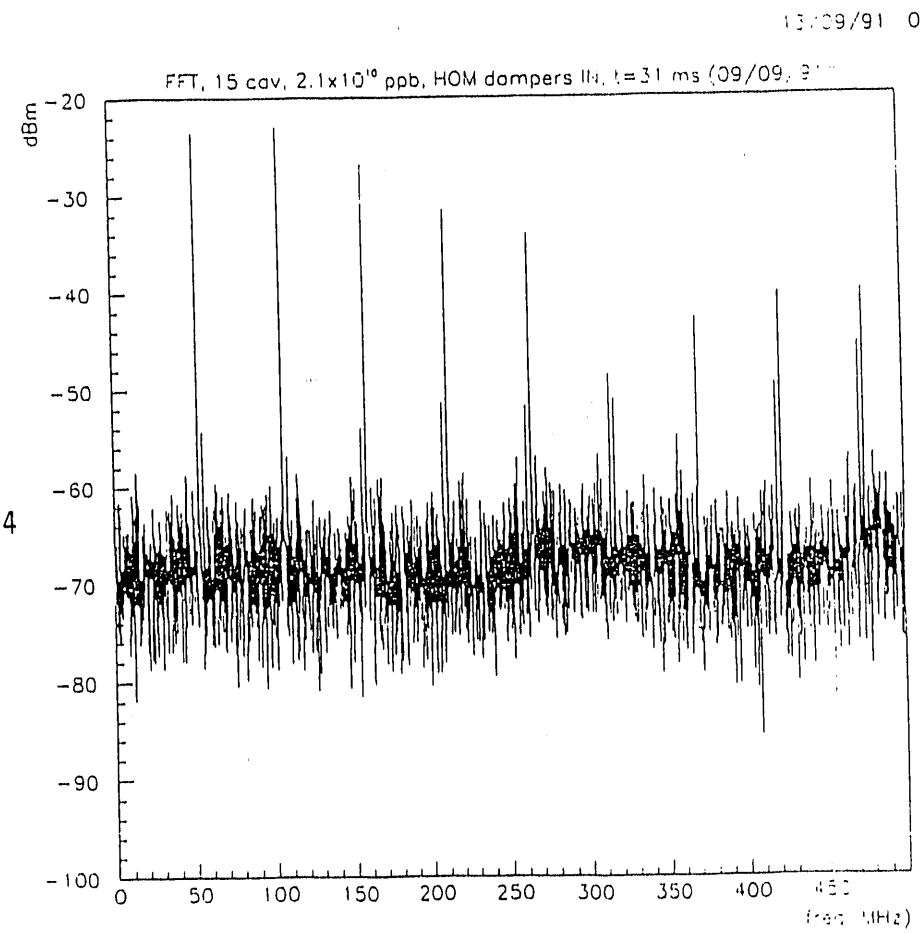

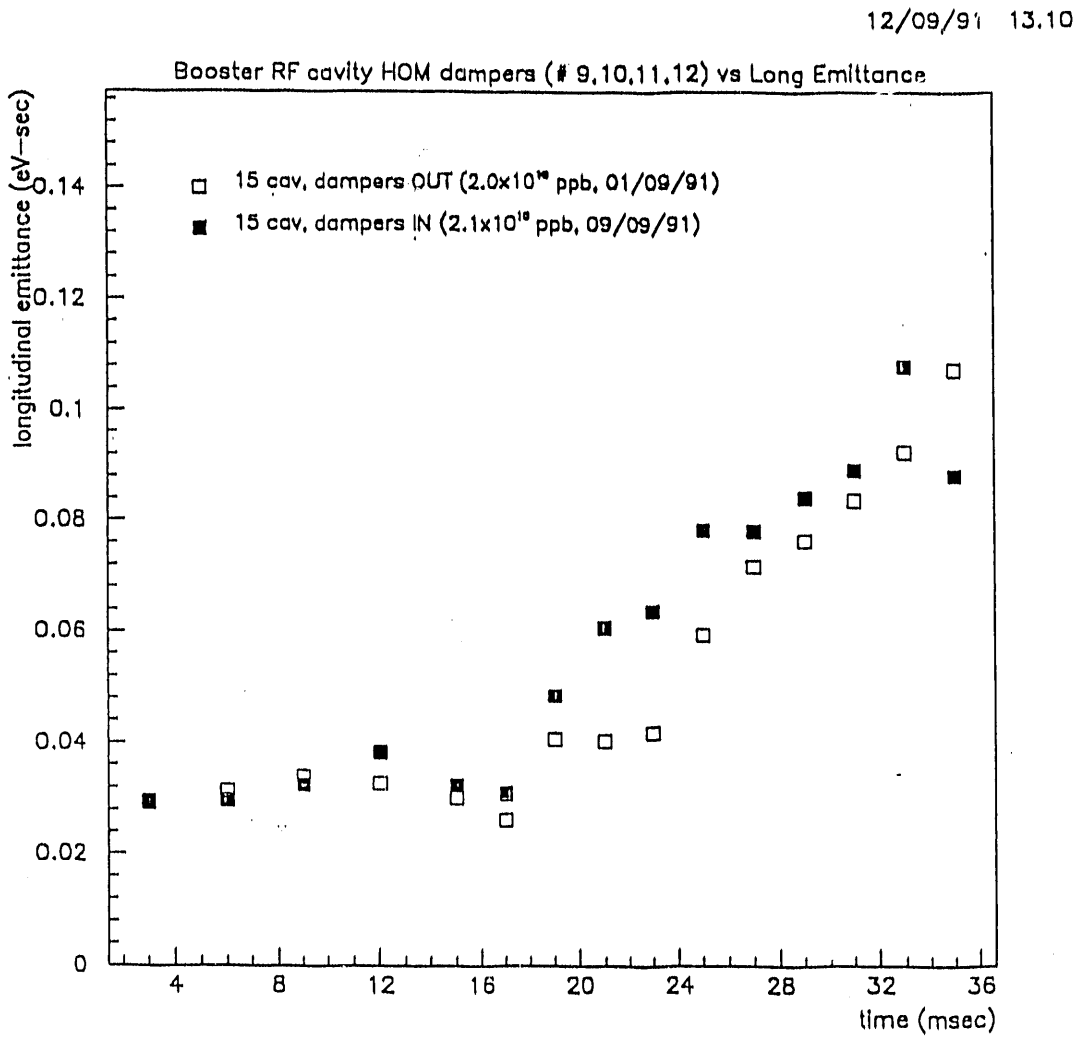
12/09/91 13.10
Booster RF cavity HOM dampers (# 9,10,11,12) vs Long Emittance
15 cav, dampers OUT (2.0x10^16 ppb, 01/09/91)
15 cav, dampers IN (2.1x10^16 ppb, 09/09/91)
longitudinal emittance (eV-sec)
0.14
0.12
0.1
0.08
0.06
0.04
0.02
0
4
8
12
16
20
24
28
32
36
time (msec)

Fig. VII-5

VII. Publications since 1985

Numbering of publications starts June 1, 1975, at the inception of Task D. For a full list of publications see the 1987 progress report.

93. Report of Working Group on Detectors for Hadrons and Event Parameters at Colliders, W. Carithers, D.D. Greiner, W. Meyers, L.S. Schroeder, H. Steiner, T.J.M. Symons, G. Young, D. Beavis, G. van Dalen, D.D. Carmony A.S. Goldhaber, G.D. Westfall, and H. Wieman, Proceedings of the Workshop on Detectors for Relativistic Nuclear Collisions, pp 75-83, Lawrence Berkeley Lab LBL-18225 (1984).

94. Charge Distributions of Hadrons Associated with Hadronic J/ψ Production, H.S. Budd, G.O. Alverson, T.L. Graff, S.R. Hahn, L.E. Holloway, L.J. Koester, U.E. Kruse, W.G. Li, P.T. Lukens, R.D. Sard, P. Schoessow, D.A. Bauer, D.J. Judd, T.B.W. Kirk, T. Lagerlund, S.H. Pordes, R. Raja, L.D. Spires, A.A. Wehmann, J.W. Cooper, V.E. Barnes, C. Davis, R.E. Davis, A.F. Garfinkel, A.T. Laasanen, S. Hossain, R.H. Milburn, and R.K. Thornton, Phys. Rev. D31, 1132 (1985).

95. Design and Fabrication of the CDF Large Angle Hadron Calorimetry, A.F. Garfinkel, V.E. Barnes, K. Chadwick, A. Di Virgilio, S. Kuhlmann, A.T. Laasanen, J.K. Simmons, S. Bartalucci, S. Bertolucci, M. Cordelli, M. Curatolo, B. Exposito, P. Giromini, S. Miozzi, A. Sansoni, F. Bedeschi, G. Bellettini, L. Bosisio, F. Cervelli, R. Del Fabbro, E. Focardi, S. Galeotti, P. Giannetti, M.A. Giorgi, A. Menzione, D. Passuello, L. Ristori, A. Scribano, P. Sestini, A. Stefanini, G. Tonelli, H. Jensen, and H. Kautzky, Proceedings of the Annual DPF Meeting, Santa Fe, NM (1984), p368.

96. Performance of the CDF Central Electromagnetic Calorimetry, P. Schoessow, V. Barnes, S. Bertolucci, W. Burley, K. Chadwick, S. Cihangir, D. Connor, J. Cooper, R. Diebold, J. Elias, A. Garfinkel, S. Hahn H. Jensen, T. Kamon, H. Kautzky, S. Kobayashi, K. Kondo, A. Laasanen, S.Mikamo, M. Miller, A. Murakami, L. Nodulman, J. Proudfoot, D. Quarrie, A. Sansoni, J. Simmons, No. Solomey, K. Takikawa, D. Underwood, R. Wagner, V. White, A. Wicklund, H. Williams, A. Ymashita, and K. Yasuoka, Proceedings of the Annual DPF Meeting, Santa Fe, NM (Oct. 31 - Nov. 3, 1984), p366.

97. Performance of a Lead Glass Spectrometer at High Energies, A.T. Laasanen, V.E. Barnes, C. Davis, A.F. Garfinkel, J.K. Simmons, J.R. Wilson, A.A. Wehmann, G.O. Alverson, J.N. Bellinger, N.S. Budd, S. Cihangir, T.L. Graff, S.R. Hahn, I. Karlinger, L.J. Koester, W.G. Li, P.T. Lukens,

R.D. Sard, M.A. Shupe, D.A. Bauer, J.W. Cooper, S. Hossain, R.H. Milburn, W.P.B Oliver, and R.K. Thornton, Nucl. Inst. & Methods, A236 307 (1985).

98. Differences Between Proton and π^- Induced Production of the Charmonium χ States, D.A. Bauer, T.L. Graff, P.T. Lukens, J.R. Wilson, GO. Alverson, G. Ascoli, V.E. Barnes, J.N. Bellinger, S. Cihangir, J.W. Cooper, C. Davis, A.F. Garfinkel, L.E. Holloway, I. Karliner, T.B.W. Kirk, L.J. Koester, A.T. Laasanen, W.G. Li, W.P. Oliver, S.H. Pordes, R.D. Sard, J.K. Simmons, R.K. Thornton, and A.A. Wehmann, Phys. Rev. Lett. 54, 753 (1985).

99. Calibration of the CDF Central Electromagnetic Calorimetry, S. Hahn, V. Barnes, S. Bertolucci, W. Burley, K. Chadwick, S. Cihangir, D. Connor, J. Cooper, R. Diebold, J. Elias, A. Garfinkel, H. Jensen, T. Kamon, H. Kautzky, S. Kobayashi, K. Kondo, A. Laasanen, S. Mikamo, M. Miller, A. Murakami, L. Nodulman, J. Proudfoot, D. Quarrie, A. Sansoni, P. Schoessow, J. Simmons, N. Solomey, K. Takikawa, D. Underwood, R. Wagner, V. White, A. Wicklund, H. Williams, A. Yamashita, and K. Yasuoka, Proceedings of the Annual DPF Meeting, Santa Fe, NM (Oct. 31 - Nov. 3, 1984), p365.

100. The Description of Fragmentation as a Critical Phenomenon in High Energy P-Nucleus Collisions, A.S. Hirsch, A. Bujak, J.E. Finn, L.J. Gutay, R.W. Minich, N.T. Porile, R.P. Scharenberg, B.C. Stringfellow, and R. Turkot, Nucl. Phys. A418, 267c (1984).

101. Nuclear Charge Dispersion in the Fragmentation Mass Region and the Thermal Liquid Drop Model, N.T. Porile, A. Bujak, J.E. Finn, L.J. Gutay, A.S. Hirsch, R.W. Minich, G. Paderewski, R.P. Scharenberg, B.C. Stringfellow, and F. Turkot, Phys. Lett. 156B 177 (1985).

102. Mass Yield Distribution for the Interaction of Silver with 300 GeV Protons, A. Bujak, J.E. Finn, L.J. Gutay, A.S. Hirsch, R.W. Minich, G. Paderewski, N.T. Porile, R.P. Scharenberg, B.C. Stringfellow, and F. Turkot, Phys. Rev. C 32 620 (1985).

103. Accelerator Internal Target Experiments Using a Supersonic Gas Jet, B.C. Stringfellow, A.T. Bujak, Y.H. Chung, J.E. Finn, L.J. Gutay, A.S. Hirsch, M. Mahi, G.L. Paderewski, N.T. Porile, T.C. Sangster, R.P. Scharenberg, and F. Turkot, Nuclear Instruments and Methods in Phys. Rev. A251, 242-253, (1986).

104. Fragment Emission in Proton Xenon Interactions at Near Threshold Energies. N.T. Porile, A. Bujak, D.D. Carmony, Y.H. Chung, L.J. Gutay, A.S. Hirsch, M. Mahi, G.L. Paderewski, T.C. Sangster, R.P. Scharenberg, B.C. Stringfellow Proceedings, Nuclear Dynamics 113-115. (Copper Mountain, 1986).

105. FNAL E-735, A Search for A Deconfined Quark Gluon Phase of Strongly Interacting Matter in $\bar{p}$-p Interactions at $\sqrt{s}$ = 2 TeV, L.R Fortney, A.T. Goshaw, S. Oh, W.J. Robertson, W.D. Walker, V.H. Areti, C. Hojvat, D. Reeves, F. Turkot, E.W. Anderson, C. Lindsey, M. Duong-Van, J.M. Bishop, N.N. Biswas, J. LoSecco, P. Kenney, J. Piekarz, A. Bujak, D.D. Carmony, R.J. De Bonte, L.J. Gutay, A.S. Hirsch, D.S. Koltick, N. Morgan, N.T. Porile, R.P. Scharenberg, B.C. Stringfellow, A. Erwin, C. Findeisen, K. Nelson, and M. Thompson, Proceedings of XVII International Symposium on Multiparticle dynamics (Seewinkel, Austria, June 1986), World Scientific Press pp 839-842.

106. FNAL Experiment E-735 at the C0 Collider Intersection, L.R. Fortney, A.T. Goshaw, S. Oh, W.J. Robertson, W.D. Walker, V.H. Areti, C. Hojvat, D. Reeves, F. Turkot, E.W. Anderson, C. Lindsey, M. Duong-Van, J.M. Bishop, N.N. Biswas, J. LoSecco, V.P. Kenney, J. Piekarz, A. Bujak, D.D. Carmony, R.J. De Bonte, L.J. Gutay, A.S. Hirsch, D.S. Koltick, N. Morgan, N.T. Porile, R.P. Scharenberg, B.C. Stringfellow, A. Erwin, C. Findeisen, K. Nelson, and M. Thompson, Proceedings of the International conference on antiproton-proton Interactions, Aachen (1986).

107. Light-Fragment Production in Proton-Xenon Interactions between 1 and 19 GeV, T.C. Sangster, A.T. Bujak, D.D. Carmony, Y.H. Chung, L.J. Gutay, A.S. Hirsch, M. Mahi, G.L. Paderewski, N.T. Porile, R.P. Scharenberg, B.C. Stringfellow, Phys. Lett. B 188 29-32 (1987).

108. Fragment Production from 1-GeV to 20-GeV P + Xe Reactions. T.C. Sangster, A. Bujak, D.D. Carmony, Y.H. Chung, L.J. Gutay, A.S. Hirsch, M. Mahi, G.L. Paderewski, N.T. Porile, R.P. Scharenberg, B.C. Stringfellow. Proceedings, High Energy Heavy Ion Study 363-371. (Berkeley, 1987).

109. Energy dependence of Proton Induced Xenon Fragmentation and the Approach to Liquid-gas Criticality in Nuclear Matter, A.S. Hirsch, A.T. Bujak, D.D. Carmony, Y.H. Chung, L.J. Gutay, M. Mahi, G.L. Paderewski, N.T. Porile, T.C. Sangster, R.P. Scharenberg, and B.C. Stringfellow, Phys. Rev. Letters. 60 1936-1939 (1988).

110. Fragment Emission in Proton-Xenon Interactions in the Near-Threshold Regime, N.T. Porile, A.T. Bujak, D.D. Carmony, Y.H. Chung, L.J. Gutay,

A.S. Hirsch, M. Mahi, G.L. Paderewski, T.C. Sangster, R.P. Scharenberg, and B.C. Stringfellow, Nuclear Physics A 471 149c-169c (1987).

111. Degradation of Plastic Scintillator Exposed to Tevatron Tunnel Background Radiation, C.S. Lindsey, E.W.Anderson, C. Hojvat, F. Turkot, A. Bujak, Nuclear Instruments and Methods in Physics A254 212-214 (1987).

112. Central Jets in the CDF Experiment, Arthur F. Garfinkel, Proceedings of the International Europhysics Conference on High Energy Physics, ed. by O. Botner, Uppsala University (1987).

113. Compositeness and QCD at the SSC, V. Barnes, B. Blumenfeld, R. Cahn, S. Chivukula, S. Ellis, J. Freeman, C. Heusch, J. Huston, K. Kondo, J. Morfin, L. Randall, and D. Soper, 45pp., Proceedings of the Workshop on Experiments, Detectors, and Experimental Areas for the Superconducting Supercollider, July 1987, Berkeley, CA. (World Scientific)

114. Report of the Large Solenoid Detector Group, V. E. Barnes with G. G. Hanson et al., 46pp., Ibid.

115. Status and Prospects of the Fermilab Collider Detector, TeVatron Collider and Antiproton Source, Virgil E. Barnes for the CDF Collaboration, Proceedings of the Eighth Vanderbilt Conference - Collider Physics: Current Status and Future Prospects; October, 1987 (World Scientific).

116. Multiplicity dependence of the transverse-momentum spectrum for centrally produced hadrons in antiproton-proton collisions at $\sqrt{s} = 1.8$ TeV, T. Alexopoulos, C. Allen, E.W. Anderson, H. Areti, S. Banerjee, P.D. Berry, N.N. Biswas, A. Bujak, D.D. Carmony, T. Carter, P. Cole, Y. Choi, R. De Bonte, A. Erwin, C. Findeisen, A.T. Goshaw, L.J. Gutay, A.S. Hirsch, C. Hojvat, V.P. Kenney, D. Koltick, C.S. Lindsey, J.M. Losecco, T. McMahon, A.P. McManus, N. Morgan, K. Nelson, S.H. Oh, J. Piekarz, N.T. Porile, D. Reeves, R.P. Scharenberg, B.C. Stringfellow, S.R. Stampke, M. Thompson, F. Turkot, W.D. Walker, C.H. Wang, and D.K. Wesson. Phys. Rev Lett. 60 1622-1625 (1988).

117. Approach to Criticality in the Fragmentation of Xenon, N.T. Porile, A.J. Bujak, D.D. Carmony, Y.H. Chung, L.J. Gutay, A.S. Hirsch, M. Mahi, G.L. Pawerewski, T.C. Sangster, R.P. Scharenberg, and B.C. Stringfellow). Phys. Rev. C39, 1914 - 1928 (1989).

118. The CDF Central and Endwall Hadron Calorimeter, V. E. Barnes, A. Di Virgilio, A. F. Garfinkel, S. E. Kuhlmann, and A. T. Laasanen, with authors from Frascati, Pisa and FNAL, Nucl. Inst. & Methods A267, 301-314 (1988).

119. The CDF Front End Electronics: The Rabbit System, S. E. Kuhlmann with

authors from FNAL, Nucl. Inst. & Methods A267,68-81 (1988).

120. Cosmic Ray Test of the CDF Central Calorimeters, A. Di Virgilio with authors from ANL, KEK, Tsukuba, Saga, U. of Penn., FNAL, and U. of Illinois, Nucl. Inst. & Methods A267, 330-350 (1988).

121. Design and Construction of the CDF Central Tracking Chamber, A. Byon with authors from FNAL, and Pisa, Nucl. Inst. & Methods A268, 50-74 (1988).

122. The CDF Vertex Time Projection Chamber System, M. H. Schub with authors from U. of Chicago, FNAL, and Tsukuba, Nucl. Inst. & Methods A268, 75-91 (1988).

123. Transverse Momentum Distributions of Charged Particle Produced in $\bar{p}p$ Interactions at $\sqrt{s}$ = 630 and 1800 GeV, V. E. Barnes, A. Byon, A. F. Garfinkel, S. E. Kuhlmann, A. T. Laasanen, M. Schub et al., Phys. Rev. Lett. 61, 1819-1822 (1988).

124. The Transverse Momentum Spectrum of Charged Particles Produced in $\bar{p}p$ Collisions at $\sqrt{s}$ = 1.8 TeV, T. Alexopoulos, C. Allen, E. W. Anderson, H. Areti, S. Banerjee, P. D. Berry, N. N. Biswas, A. Bujak, D. D. Carmony, T. Carter, P. Cole, Y. Choi, R. De Bonte, A. Erwin, C. Findeisen, A. T. Goshaw, L. J. Gutay, A. S. Hirsch, C. Hojvat, V. P. Kenney, D. Koltick, C. S. Lindsey, J. M. LoSecco, T. McMahon, A. P. McManus, N. Morgan, K. Nelson, S. H. Oh, J. Piekarz, N. T. Porile, D. Reeves, R. P. Scharenberg, B. C. Stringfellow, S. R. Stampke, M. Thompson, F. Turkot, W. D. Walker, C. H. Wang, and D. K. Wesson, Proceedings of the Rencontres de Moriond, Les Arcs, France (1988).

125. A Study of 1.8 TeV Proton-Antiproton Collisions at the C0 region of the Fermilab Tevatron Collider, T. Alexopoulos, C. Allen, E. W. Anderson, H. Areti, S. Banerjee, P. D. Berry, N. N. Biswas, A. Bujak, D. D. Carmony, T. Carter, P. Cole, Y. Choi, R. De Bonte, A. Erwin, C. Findeisen, A. T. Goshaw, L. J. Gutay, A. S. Hirsch, C. Hojvat, V. P. Kenney, D. Koltick, C. S. Lindsey, J. M. LoSecco, T. McMahon, A. P. McManus, N. Morgan, K. Nelson, S. H. Oh, J. Piekarz, N. T. Porile, D. Reeves, R. P. Scharenberg, B. C. Stringfellow, S. R. Stampke, M. Thompson, F. Turkot, W. D. Walker, C. H. Wang, and D. K. Wesson, Proceedings of the Division of Particles and Fields Meeting, Storrs, CT (1988).

126. The CDF Central and Endwall Hadron Calorimeter, V. E. Barnes, A. Di Virgilio, A. F. Garfinkel, S. E. Kuhlmann, A. T. Laasanen, et al.,

Nucl. Instr. & Methods A267, 301-304 (1988).

127. Response Maps of the CDF Central Electromagnetic Calorimeter with Electrons, V. E. Barnes, K. Chadwick, A. F. Garfinkel, S. E. Kuhlmann, A. T. Laasanen, J. Simmons, et al., Nucl. Instr. & Methods A267, 315-329 (1988).

128. The CDF Detector: An Overview, V. E. Barnes, A. Byon, A. F. Garfinkel, S. E. Kuhlmann, A. T. Laasanen, M. Schub et al., Nucl. Instr. & Methods A271, 387-403 (1988).

129. Inclusive Central Jets at the Tevatron $\bar{P}P$ Collider, Proceedings of Seventh Topical Workshop on Proton Antiproton Colliders Physics, (A. F. Garfinkel), ed. R. Raja and J. Yoh (FNAL, Batavia) 1988.

130. Preliminary Results on p(t) Distributions for TOF Identified Hadrons from Anti-P P Collisions at $\sqrt{s}$ = 1.8-TeV. E-735 Collaboration. FNAL-E735 experiment. V.P. Kenney, T. Alexopoulos, C. Allen, E.W. Anderson, H. Areti, S. Banerjee, P.D. Beery, N.N. Biswas, A. Bujak, D.D. Carmony, T. Carter, P. Cole, Y. Choi, R. De Bonte, A. Erwin, C. Findeisen, A.T. Goshaw, L.J. Gutay, A.S. Hirsch, C. Hojvat, D. Koltick, C.S. Lindsey, J.M. LoSecco, T. McMahon, A.P. McManus, N. Morgan, K. Nelson, S.H. Oh, K. Piekarz, N.T. Porile, D. Reeves, R.P. Scharenberg, B.C. Stringfellow, S.R. Stampke,M. Thompson, F. Turkot, W.D. Walker, C.H. Wang, D.K. Wesson, 1988. Proceedings, Current Issues in Hadron Physics 193-196. (Les Arcs, 1988).

131. Lambda and Anti-lambda Production from Anti-P P Collisions at 1.8-TeV Center of Mass Energy. E735 collaboration. Fnal-735 experiment. S.H. Oh, S. Banerjee, P.D. Beery, N.N. Biswas, A. Bujak, D.D. Carmony, T. Carter, Y. Choi, C. Findeisen, A.T. Goshaw, C. Hojvat, C.S. Lindsey, J.M. LoSecco, A.P. McManus, N. Morgan, K. Nelson, J. Piekarz, D. Reeves, S.R. Stampke, M. Thompson, F. Turkot, W.D. Walker, C.H. Wang, D.K. Wesson Proceedings, Hadronic matter in collision 594-606. (Tucson, 1988).

132. Measurement of p_t as a function of N_c at the FNAL $p\bar{p}$ Collider. S.R. Stampke, T. Alexopoulos, C. Allen, E.W. Anderson, H. Areti, S. Banerjee, P.D. Beery, N.N. Biswas, A. Bujak, D.D. Carmony, T. Carter, P. Cole, Y. Choi, R. DeBonte, A. Erwin, C. Findeisen, A.T. Goshaw, L.J. Gutay, A.S. Hirsch, C. Hojvat, V.P. Kenney, D. Koltick, C.S. Lindsey, J.M. LoSecco, T. McMahon, A.P. McManus, N. Morgan, K. Nelson, S.H. Oh, J. Piekarz, N.T. Porile, D. Reeves, R.P. Scharenberg, B.C. Stringfellow, M. Thompson, F. Turkot, W.D. Walker, C.H. Wang, D.K. Wesson (Duke U. & Fermilab & Iowa State U. & Notre Dame U. & Purdue U. & Wisconsin U.,

Madison), 1988. Proceedings, Hadronic matter in collision 1988 67-77. (Tucson, 1988).

133. Recent results from E735 at the Fermilab Tevatron Proton Anti-proton Collider with $\sqrt{s}$ = 1.8-TEV. C.S. Lindsey, T. Alexopoulos, C. Allen, E.W. Anderson, H. Areti, S. Banerjee, P.D. Beery, N.N. Biswas, A. Bujak, D.D. Carmony, T. Carter, P. Cole, Y. Choi, R. Debonte, A. Erwin, C. Findeisen, A.T. Goshaw, L.J. Gutay, A.S. Hirsch, C. Hojvat,V.P. Kenney, D. Koltick, J.M. Losecco, T. Mcmahon, A.P. Mcmanus, N. Morgan, K. Nelson, S.H. Oh, J. Piekarz, N.T. Porile, D. Reeves, R.P. Scharenberg, S.R. Stampke, B.C. Stringfellow, M. Thompson, F. Turkot, W.D. Walker, C.H. Wang, D.K. Wesson. Nucl. Phys. A498 181C-192C (1989).

134. Λ° and $\bar{\Lambda}^\circ$ Production from Proton-Antiproton Collisions at $\sqrt{s}$ = 1.8 TeV, S. Banerjee, P. D. Berry, N. N. Biswas, A. Bujak, D. D. Carmony, T. Carter, Y. Choi, C. Findeisen, A. T. Goshaw, C. Hojvat, C. S. Lindsey, J. M. LoSecco, A. P. McManus, N. Morgan, K. Nelson, S. H. Oh, J. Piekarz, D. Reeves, S. R. Stampke, M. Thompson, F. Turkot, W. D. Walker, C. H. Wang, and D. K. Wesson, Phys. Rev. Lett. 62, 12-15 (1989).

135. Measurement of the Inclusive Jet Cross Section in $\bar{p}p$ Collisions at $\sqrt{s}$ = 1.8 TeV, V. E. Barnes, A. Byon, S. Behrends, A. F. Garfinkel, S. Kuhlmann, A. T. Laasanen, M. Schub et al., Phys. Rev. Lett. 62, 613-616 (1989).

136. Measurement of W Boson Production in 1.8 TeV $\bar{p}p$ Collisions, V. E. Barnes, A. Byon, A. F. Garfinkel, A. T. Laasanen, M. H. Schub et al., Phys. Rev. Lett. 62, 1005-1008 (1989).

137. Recent Results: Collider Detector at Fermilab, V. E. Barnes, Proceedings of the Quark Matter '88 conference, Nucl. Physics A498, 193C-204C (1989).

138. Limits on the Masses of Supersymmetric Particles from 1.8 TeV $\bar{p}p$ Collision, V. E. Barnes, A. Byon, S. Behrends, A. F. Garfinkel, A. T. Laasanen, M. H. Schub, et al., Phys. Rev. Letters. 62, 1825-1828 (1989).

139. Soft Hadron Production at CDF, V. E. Barnes, Proceedings of the XXIVth Rencontres de Moriond (1989).

140. Dijet Angular Distributions from pbar p Collisions at $\sqrt{s}$ = 1.8 TeV, V. E. Barnes, A. Byon, S. Behrends, A. F. Garfinkel, A. T. Laasanen, M. H. Schub, et al., Phys. Rev. Letters 62, 3020-3023 (1989).

141. Measurement of the Mass and Width of the Z° Boson at the Fermilab Tevatron, V. E. Barnes, A. Byon, S. Behrends, A. F. Garfinkel,

A. T. Laasanen, M. H. Schub, et al., Phys. Rev. Letters 62, 720-723 (1989).

142. Search for Heavy Charged Particles in 1.8-TeV $P\bar{P}$ Collisions at the Fermilab Collider, (CDF Collaboration w/F. Abe, V. E. Barnes, A. Byon, A. F. Garfinkel, S. E. Kuhlmann, A. T. Laasanen, M. H. Schub, et. al.,) Phys. Rev. Letters 63, 1447-1450, (1989).

143. K_S^0 production in $\bar{P}P$ interactions at $\sqrt{s}$ = 630 and 1800 GeV, (CDF Collaboration w/F. Abe, V. E. Barnes, A. Byon, A. F. Garfinkel, S. E. Kuhlmann, A. T. Laasanen, M. H. Schub, et. al.,) Phys. Rev. D, Rapid Comm., 40, 3791-3794, (1989).

144. Search for the Top Quark in the Reaction $\bar{p}p \rightarrow$ Electron + Jets at $\sqrt{s}$ = 1.8 TeV, V. E. Barnes, S. Behrends, A. Byon, A. F. Garfinkel, B. T. Huffman, A. T. Laasanen, M. H. Schub J. Tonnison et al., Phys. Rev. Letters 64, 142-146 (1990).

145. Search for New Heavy Quarks in Electron-Muon Events at the Fermilab Tevatron Collider, V. E. Barnes, S. Behrends, A. Byon, A. F. Garfinkel, B. T. Huffman, A. T. Laasanen, M. H. Schub J. Tonnison et al., Phys. Rev. Letters 64, 147-151 (1990).

146. Measurement of the Ratio $\sigma(W \rightarrow e\nu)/\sigma(Z \rightarrow ee)$ in $\bar{p}p$ Collisions at $\sqrt{s}$ = 1.8 TeV, V. E. Barnes, A. Byon, A. F. Garfinkel, B. T. Huffman, A. T. Laasanen, M. H. Schub J. Tonnison et al., Phys. Rev. Letters 64, 152-156 (1990).

147. Two-Jet Differential Cross Section in $\bar{P}P$ Collisions at $\sqrt{s}$ = 1.8 TeV, (CDF Collaboration w/F. Abe, V. E. Barnes, S. Behrends, A. Byon, A. F. Garfinkel, S. E. Kuhlmann, A. T. Laasanen, M. H. Schub, et. al.,) Phys. Rev. Letters, 64, 157-160, January 1990.

148. Measurement of D^* Production in Jets from $\bar{P}P$ Collisions at $\sqrt{s}$ = 1.8 TeV, (CDF Collaboration w/F. Abe, V. E. Barnes, A. Byon, A. F. Garfinkel, S. E. Kuhlmann, A. T. Laasanen, M. H. Schub, et. al.,) Phys. Rev. Letters 64, 348-352, January 1990.

149. Search for a Light Higgs Boson at the Fermilab Tevatron Proton-Antiproton Collider, (CDF Collaboration/V. E. Barnes, S. Behrends, A. Byon, A. F. Garfinkel, B. T. Huffman, A. T. Laasanen, M. H. Schub, J. Tonnison, Phys. Rev. D41, 1717-1721, March 1990.

150. Two-Jet Invariant-Mass Distribution at $\sqrt{s}$ = 1.8 TeV, (CDF Collaboration/V. E. Barnes, S. Behrends, A. Byon, K. Chadwick, A. F. Garfinkel, S. E. Kuhlmann, A. T. Laasanen, M. H. Schub, Phys. Rev. D41, 1722-1725, March 1990.

151. Mass Identified Particle Yields in Antiproton-Proton Collisions at $\sqrt{s}$ = 1.8 TeV, T. Alexopoulos, C. Allen, E. W. Anderson, H. Areti, S. Banerjee, P. D. Berry, N. N. Biswas, A. Bujak, D. Carmony, T. Carter, P. Cole, Y. Choi, R. De Bonte, A. Erwin, C. Findeisen, A. T. Goshaw, L. J. Gutay, A. S. Hirsch, C. Hojvat, V. P. Kenney, C. S. Lindsey, J. M. LoSecco, T. McMahon, A. P. McManus, N. Morgan, K. Nelson, S. H. Oh, J. Piekarz, N. T. Porile, D. Reeves, R. P. Scharenberg, B. C. Stringfellow, S. R. Stampke, M. Thompson, F. Turkot, W. D. Walker, C. H. Wang, and D. K. Wesson, Phys. Rev. Lett. 64, 991-994 (1990).
152. Recent Results from E-735 at the Fermilab Tevatron Proton-Antiproton Collider at $\sqrt{s}$ = 1.8 TeV, C. Allen, A. Bujak, D. D. Carmony, P. Cole, Y. Choi, R. De Bonte, L. J. Gutay, A. S. Hirsch, D. Koltick, T. McMahon, N. K. Morgan, N. T. Porile, R. P. Scharenberg, B. C. Stringfellow et al., Nuclear Physics B12, 267-276 (1990).
153. A Cylindrical Drift Chamber for the Measurement of High Charged Particle Multiplicities in Hadronic Events, (C. Allen, A. Bujak, P. Cole, Y. Choi, R. De Bonte, J.E. Finn, L.J. Gutay, A.S. Hirsch, D. Koltick, T. McMahon, N.K. Morgan, N.T. Porile, R.P. Scharenberg, and B.C. Stringfellow). Nucl. Instr. and Methods A294 108-116(1990).
154. Search for Quark-Gluon Plasma in $\bar{p}p$ Collisions at $\sqrt{s}$ = 1.8 TeV, (with T. Alexopoulos, C. Allen, E.W. Anderson, H. Areti, S. Banerjee, J. Bishop, N.N. Biswas, A. Bujak, T. Carter, P. Cole, Y. Choi, R. De Bonte, A. Erwin, C. Findeisen, A.T. Goshaw, L.J. Gutay, A.S. Hirsch, C. Hojvat, V.P. Kenney, C.S. Lindsey, J.M. Losecco, T. McMahon, A.P. McManus, N. Morgan, K. Nelson, S.H. Oh, J. Piekarz, N.T. Porile, D. Reeves, R.P. Scharenberg, S.R. Stampke, B.C. Stringfellow, M. Thompson, F. Turkot, W.D. Walker, C.H. Wang, and D.K. Wesson). Proceedings of the Rio de Janeiro International Workshop on Relativistic aspects of nuclear physics, pp. 3-16 (World Scientific Publishing Co., 1990).
155. Deconfinement Signature, Mass Dependence of the Transverse Flow and Time Evolution in Antiproton-Proton Collisions at $\sqrt{s}$ = 1.8 TeV, (with T. Alexopoulos, C. Allen, E.W. Anderson, H. Areti, S. Banerjee, P. Bhat, J. Bishop, N.N. Biswas, A. Bujak, T. Carter, P. Cole, Y. Choi, R. De Bonte, A. Erwin, C. Findeisen, A.T. Goshaw, L.J. Gutay, A.S. Hirsch, C. Hojvat, V.P. Kenney, D. Koltick, C.S. Lindsey, C. Loomis, J.M. Losecco, T. McMahon, A.P. McManus, N. K. Morgan, K. Nelson, S.H. Oh, J. Piekarz, N.T. Porile, D. Reeves, W.R. Roberston, R.P. Scharenberg, S.R. Stampke, B.C. Stringfellow,

M. Thompson, F. Turkot, W.D. Walker, C.H. Wang, D.K. Wesson, and H. Zuong). Physica Scripta T32 122-125 (1990).

156. Pseudorapidity Distributions of Charged Particles Produced in $\bar{p}p$ Interactions at $\sqrt{s}$ = 630 and 1800 GeV, V. E. Barnes, A. Byon, K. Chadwick, A. G. Garfinkel, S. E. Kuhlmann, A. T. Laasanen, M. H. Schub, Phys. Rev. D, Rapid Comm. 41, 2330-2338, April 1990.
157. Jet-Fragmentation Properties in $\bar{p}p$ Collisions at $\sqrt{s}$ = 1.8 TeV, V. E. Barnes, S. Behrends, A. Byon, K. Chadwick, A. F. Garfinkel, S. E. Kuhlmann, A. T. Laasanen, M. H. Schub, Phys. Rev. Letters 65, 968-971, August 1990.
158. Mass Limits for Excited Electrons and Muons from Z° Decay, L3 Collaboration/A. Bujak, L. Gutay, T. McMahon, B. Stringfellow, Phys. Lett. B247, 117-184, September 6, 1990.
159. A Determination of Electroweak Parameters from $Z^\circ \rightarrow \mu^+\mu^-(\gamma)$, L3 collabortion/A. Bujak, L. Gutay, T. McMahon, B. Stringfellow, Phys. Lett. B247, 473-480, September 13, 1990.
160. A Test of QCD Based on 4-Jet Events from Z° Decays, L3 collaboration/A. Bujak, L. Gutay, T. McMahon, B. Stringfellow, Phys. Lett. B248, 227-234, September 27, 1990.
161. Determination of α_s from Jet Multiplicities Measured on the Z° Resonance, L3 collaboration/A. Bujak, L. Gutay, T. McMahon, B. Stringfellow, Phys. Lett. B248, 464-472, October 4, 1990.
162. Calibration of a Scintillating Fiber Calorimeter Prototype Using a Moving Radioactive Source, V. E. Barnes and A. T. Laasanen, Proceedings of the SSC Detector Conference, Ft. Worth, Texas, October 15 - 17, 1990.
163. A Precision Measurement of the Number of Neutrino Species, L3 collaboration/A. Bujak, L. Gutay, T. McMahon, B. Stringfellow, Phys. Lett. B249, 341-352, October 18, 1990.
164. Measurement of the W-Boson Mass, V. E. Barnes, A. Byon, A. F. Garfinkel, B. T. Huffman, A. T. Laasanen, M. H. Schub, J. Tonnison, Phys. Rev. Lett. 65, 2243-2246, October 1990.
165. Calibration of Scintillating Calorimeters Using a Moving Radioactive Source, V. E. Barnes and A. T. Laasanen, Proceedings of the International Conference on Calorimetry in High Energy Physics, Fermilab, October 29 - November 1, 1990.
166. A Determination of Electroweak Parameters from Z° Decays into Charged Leptons, L3 collaboration/A. Bujak, L. Gutay, T. McMahon, and B. Stringfellow, Phys. Lett. B250, 183-192, November 1, 1990.

167. Test of QCD in $e^+e^- \rightarrow \gamma\gamma$ at LEP, L3 collaboration/A. Bujak, L. Gutay, T. McMahon, and B. Stringfellow. Phys. Lett. B250, 199-204, November 1, 1990.
168. Search for Excited Taus, L3 collaboration/A. Bujak, L. Gutay, T. McMahon, and B. Stringfellow, Phys. Lett. B250, 205-211, November 1, 1990.
169. Search for the Neutral Higgs Bosons of the Minimal Supersymmetric Standard Model from Z° Decays, L3 collaboration/A. Bujak, L. Gutay, T. McMahon, and B. Stringfellow, Phys. Lett. B251, 311-320, November 15, 1990.
170. A Search for Heavy Charged and Neutral Leptons from Z° Decays, L3 collaboration/A. Bujak, L. Gutay, T. McMahon, and B. Stringfellow, Phys. Lett. B251, 321-330, November 15, 1990.
171. Search for the Charged Higgs Boson in Z° Decay, L3 collaboration/A. Bujak, L. Gutay, T. McMahon, and B. Stringfellow, Phys. Lett. B252, 511-517, December 20, 1990.
172. Search for a Low Mass Neutral Higgs Boson in Z° Decay, L3 collaboration/A. Bujak, L. Gutay, T. McMahon, and B. Stringfellow, Phys. Lett. B252, 518-524, December 20, 1990.
173. Search for Excited Neutrinos from Z° Decays, L3 collaboration/A. Bujak, L. Gutay, T. McMahon, and B. Stringfellow, Phys. Lett. B252, 525-532, December 20, 1990.
174. A Measurement of B°-$\bar{B}^\circ$ Mixing in Z° Decays, L3 collaboration/A. Bujak, L. Gutay, T. McMahon, and B. Stringfellow, Phys. Lett. B252, 703-712, December 20, 1990.
175. A Measurement of the $Z^\circ \rightarrow b\bar{b}$ Forward-Backward Asymmetry, L3 collaboration/A. Bujak, L. Gutay, T. McMahon, and B. Stringfellow, Phys. Lett. B252, 713-721, December 27, 1990.
176. A Quark - Gluon Plasma Search in Anti-P P at $\sqrt{s}$ = 1.8 TeV. By E735 Collaboration. T. Alexopoulos, C. Allen, E.W. Anderson, H. Areti, S. Banerjee, P.D. Beery, N.N. Biswas, A. Bujak, D.D. Carmony, T. Carter, P. Cole, Y. Choi, R. De Bonte, A. Erwin, C. Findeisen, A.T. Goshaw, L.J. Gutay, A.S. Hirsch, C. Hojvat, V.P. Kenney, C.S. Lindsey, L.M. LoSecco, T. McMahon, A.P. McManus, N. Morgan, K. Nelson, S.H. Oh, J. Piekarz, N.T. Porile, D. Reeves, R.P. Scharenberg, S.R. Stampke, B.C. Stringfellow, M. Thompson, F. Turkot, W.D. Walker, C.H. Wang, D.K. Wesson. Nucl.Phys. A525:165-170 (1991).
177. Hyperon Production from Proton-Antiproton Collisions at $\sqrt{s}$ = 1.8 TeV, T. Alexopoulos, C. Allen, H. Areti, S. Banerjee, Bhat, J. Bishop, N.N. Biswas, A. Bujak, D.D. Carmony, T. Carter, P. Cole, Y. Choi, R. De Bonte, A. Erwin, C. Findeisen, A.T. Goshaw, L.J. Gutay, A.S. Hirsch,

C. Hojvat, V.P. Kenney, D. Koltick, C.S. Lindsey, C. Loomis, J. LoSecco, T. McMahon, A.P. McManus, N. Morgan, K. Nelson, S.H. Oh, K. Piekarz, N.T. Porile, D. Reeves, R.P. Scharenberg, R. Stampke, B.C. Stringfellow, M. Thompson, F. Turkot, W.D. Walker, C.H. Wang, D.K. Wesson, and H. Zuong. Submitted to Physical Review D (1991).

178. Top-Quark Search in the Electron + Jets Channel in Proton-Antiproton Collisions at $\sqrt{s}$ = 1.8 TeV, V. E. Barnes, S. Behrends, A. Byon, A. F. Garfinkel, B. T. Huffman, A. T. Laasanen, M. H. Schub, J. Tonnison, Phys. Rev. D43, 664-686, February 1991.
179. Search for the Neutral Higgs Boson, L3 collaboration/A. Bujak, L. Gutay, T. McMahon, and B. Stringfellow, Phys. Lett. B257, 450, March 28, 1991.
180. Determination of α_s from Energy-Energy Correlations Measured on the Z° Resonance, L3 collaboration/A. Bujak, L. Gutay, T. McMahon, and B. Stringfellow, Phys. Lett. B257, 469, March 28, 1991.
181. Recent Results From E735 — Search For QGP in $\sqrt{s}$ = 1.8 TeV pbar-p Collisions, (with T. Alexopoulos, C. Allen, E.W. Anderson, H. Areti, S. Banerjee, P. Bhat, J. Bishop, N.N. Biswas, A. Bujak, T. Carter, P. Cole, Y. Choi, R. De Bonte, A. Erwin, C. Findeisen, A.T. Goshaw, L.J. Gutay, A.S. Hirsch, C. Hojvat, V.P. Kenney, D. Koltick, C.S. Lindsey, C. Loomis, J.M. Losecco, T. McMahon, A.P. McManus, N. K. Morgan, K. Nelson, S.H. Oh, J. Piekarz, N.T. Porile, D. Reeves, W.R. Roberston, R.P. Scharenberg, S.R. Stampke, B.C. Stringfellow, M. Thompson, F. Turkot, W.D. Walker, C.H. Wang, D.K. Wesson, and H. Zuong). Proceedings of the 7th Winter Workshop on Nuclear Dynamics, Key West, January 27 - February 1 1991. (to be published).
182. Measurement of the W-boson Mass in 1.8 TeV $\bar{p}p$ Collisions, (CDF Collaboration/V. E. Barnes, A. Byon, A. F. Garfinkel, B. T. Huffman, A. T. Laasanen, M. H. Schub, J. Tonnison et al., Phys. Rev. D43, 2070-2093, April 1, 1991.
183. Measurement of the Inclusive Production of Neutral Pions and Charged Particles on the Z° Resonance, L3 Collaboration/A. Bujak, L. Gutay, T. McMahon, and B. Stringfellow, To be published in Physics Letters B.
184. Search for Leptoquarks in Z° Decays, L3 Collaboration/A. Bujak, L. Gutay, T. McMahon, and B. Stringfellow, To be published in Physics Letters B.
185. Measurement of $Z^\circ \to b\bar{b}$ Decays and the Semileptonic Branching Ratio Br($b \to L + X$), L3 Collaboration/A. Bujak, L. Gutay, T. McMahon, and B. Stringfellow, To be published in Physics Letters B.

186. Measurement of Electroweak Parameters from Hadronic and Leptonic Decays of the Z°, L3 Collaboration/A. Bujak, L. Gutay, T. McMahon, and B. Stringfellow, To be published in Zeitschrift fur Physik G.
187. Search for Narrow High-Mass Resonances in Radiative Decays of the Z°, L3 Collaboration/A. Bujak, L. Gutay, T. McMahon, and B. Stringfellow, To be published in Physics Letters B.
188. Measurement of the W-Boson P_T Distribution in $\bar{p}p$ Collisions at $\sqrt{s} = 1.8$ TeV, V. E. Barnes, A. Byon, A. F. Garfinkel, B. T. Huffman, A. T. Laasanen, M. H. Schub et al., Phys. Rev. Lett. 66, 2951-2955, June 1991.
189. Measurement of $\sigma B(W \to e\nu)$ and $\sigma B(Z^\circ \to e^+e^-)$ in $\bar{p}p$ Collisions at $\sqrt{s}$=1800 GeV, V. E. Barnes, S. Behrends, A. Byon, A. F. Garfinkel, B. T. Huffman, A. T. Laasanen et al., M. H. Schub, J. Tonnison, Phys. Rev. D44, 29-52, July 1, 1991.
190. Measurement of QCD Jet Broadening in $p\bar{p}$ Collisions at $\sqrt{s}$=1.8 TeV, V. E. Barnes, S. Behrends, A. Byon, A. F. Garfinkel, A. T. Laasanen, M. H. Schub, J. Tonnison et al., Phys. Rev. D44, 601-616, August 1, 1991.
191. Measurement of the e^+e^- Invariant-Mass Distribution in $\bar{p}p$ Collisions at $\sqrt{s}$=1.8 TeV, V. E. Barnes, S. Behrends, A. Byon, A. F. Garfinkel, B. T. Huffman, A. T. Laasanen, M. H. Schub, J. Tonnison et al., Phys. Rev. Lett. 67, 2418-2422, October 1991.
192. Search for $W' \to e\nu$ and $W' \to \mu\nu$ in $\bar{p}p$ Collisions at $\sqrt{s}$=1.8 TeV, V. E. Barnes, A. Byon, A. F. Garfinkel, B. T. Huffman, A. T. Laasanen, M. H. Schub, J. Tonison et al., Phys. Rev. Lett. 67, 2609-2613, November 1991.
193. Measurement of $B^\circ\bar{B}^\circ$ Mixing at the Fermilab Tevatron Collider, V. E. Barnes, A. Byon, A. F. Garfinkel, B. T. Huffman, A. T. Laasanen, M. H. Schub, J. Tonnison et al., Phys. Rev. Lett. 67, 3351-3355, December 1991.
194. Measurement of the W-Boson Mass in 1.8 TeV $\bar{p}p$ Collisions, V. E. Barnes, A. Byon, A. F. Garfinkel, B. T. Huffman, A. T. Laasanen, M. H. Schub, J. Tonnison et al., Phys. Rev. D43, 2070-2093, April 1991.
195. Determination of $\sin^2\bar{\theta}_W$ from the Forward-Backward Asymmetry in $p\bar{p} \to Z^\circ X \to e^+e^- X$ Interactions at $\sqrt{s} = 1.8$ TeV, V. E. Barnes, A. Byon, A. F. Garfinkel, B. T. Huffman, A. T. Laasanen, M. H. Schub, N. M. Shaw, J. Tonnison et al., Phys. Rev. Lett. 67, 1502-1506, September 1991.
196. Measurement of the Z-Boson p_T Distribution in $\bar{p}p$ Collisions at $\sqrt{s}$=1.8 TeV, M. Bailey, V. E. Barnes, A. Byon, A. F. Garfinkel, B. T. Huffman, A. T. Laasanen, M. H. Schub, N. M. Shaw, J. Tonnison et al., Phys. Rev. Lett. 67, 2937-2941, November 1991.

197. Inclusive Jet Cross Section in $\bar{p}p$ Collisions at $\sqrt{s}$=1.8 TeV, M. W. Bailey, V. E. Barnes, A. F. Garfinkel, B. T. Huffman, A. T. Laasanen, M . H. Schub, N. M. Shaw, J. Tonnison, et. al., Phys. Rev. Lett. 68, 1104-1108, February 1992.

198. Lepton Asymmetry in W-Boson Decays from $\bar{p}p$ Collisions at $\sqrt{s}$=1.8 TeV, M. Bailey, V. E. Barnes, A. F. Garfinkel, B. T. Huffman, A. T. Laasanen, M. H. Schub, N. M. Shaw, J. Tonnison et al., Phys. Rev. Lett. 68, 1458-1462, March 1992.

199. A Lower Limit on the Top Quark Mass from Events with Two Leptons in $p\bar{p}$ Collisions at $\sqrt{s}$=1.8 TeV, M. W. Bailey, V. E. Barnes, A. F. Garfinkel, B. T. Huffman, A. T. Laasanaen, M. H. Schub, N. M. Shaw, J. Tonnison, et al., Phys. Rev. Lett 68, 447, 1992.

200. Topology of Three-Jet Events in $\bar{p}p$ Collisions at $\sqrt{s}$ = 1.8 TeV, M. W. Baily, V. E. Barnes, A. F. Garfinkel, B. T. Huffman, A. T. Laasanen, M. H. Schub, N. M. Shaw, J. Tonnison, et al., Phys. Rev. 45D, 1448, 1992.

201. Progress in the Construction of the CDF Silicon Vertex Detector, M. Bailey, A. F. Garfinkel, N. M. Shaw, To be published in Nuclear Instrument and Methods.

VI. Ph.D. Theses

1. A Study of π^+p, K^+p, and pp Interactions at 100 GeV/c Using a Hybrid Bubble Chamber-Spark Chamber System, W.M. Morse (1975).
2. Measurement of π^-p Backward Elastic Scattering Between 3.0 GeV/c and 5.5 GeV/c, R.L. Dixon (1975).
3. Some Aspects of Proton-Proton Interactions at 28.5 GeV/c as Viewed From the Statistical-Hydrodynamical Theory, C.R. Ezell (1977).
4. A Measurement of (p,n) Cross Sections on Li-6, C-12, and N-14 and Their Comparison to Calculations Using One-Pion Exchange, PCAC, and the Elementary Particle Model, G.L. Moake (1979).
5. Study of Quark Momentum Distributions in the Proton Using the Fermilab Broad Band Antineutrino Beam, E. Fernandez, (1979).
6. Study of Single-Pion Production by the Weak Charged-Current, G.M. Radecky (1980).
7. Particle Production in Pi-Minus Proton Interactions at 50 GeV/c, L.J. Dauwe (1980).
8. Experimental Study of $\bar{p}p$ collisions at 50 GeV/c Using the Fermilab 30-inch Bubble Chamber-Proportional Wire Chamber Hybrid System, D.E. Zissa (1980).
9. Nuclear Matter at Finite Temperature and Density: Theory and Experiment, R.W. Minich (1981).
10. Study of Neutral Current Distributions in Antineutrino-Proton, Neutrino-Proton Interactions Using the Fermilab Broad Band Antineutrino Beam, T.S. Carman (1981).
11. Experimental Evidence for Critical Phenomena in Hadronic Matter from Nuclear Fragmentation Induced by High Energy Protons, J.E. Finn (1982).
12. Study of Charmonium Chi States Produced in Proton and Negative Pion Interactions with a Beryllium Target, J. R. Wilson (1985)
13. (χ-states) Measurements of Chi(3510, Chi(3555) and Neutral Strange Particles in 190 GeV/c Pi^- Beryllium Interactions, James Simmons (1988).
14. Central Jet Transverse Momentum Distribution and Test of QCD for 1.8 TeV $\bar{p}p$ Collisions, Stephen Kuhlman (CDF), (1988).
15. Central Production of Charged Particles at CDF, AeSook Byon (CDF) (1989).
16. K_s^0 Production in Minimum Bias Events at the FNAL TeVatron Collider, Martin Schub (CDF) (1989).
17. Central $\langle n_c \rangle$ vs. $\langle p_T \rangle$ for 1.8 TeV $\bar{p}p$ Collisions, Timothy McMahon (CO) (1989).

Current Thesis Students:

Mark Bailey
Brian Huffman
Jim Tonnison
Bill Riemers
Atilla Rimai

END

DATE
FILMED
6/26/92